

Enabling end-to-end continuous manufacturing by API suspension feed and instantaneous drying in twin-screw wet granulation

Inaugural-Dissertation

zur Erlangung des Doktorgrades
der Mathematisch-Naturwissenschaftlichen Fakultät
der Heinrich-Heine-Universität Düsseldorf

vorgelegt von

Adrian Schmidt
aus Frankfurt (Oder)

Düsseldorf, Dezember 2017

aus dem Institut für
der Heinrich-Heine-Universität Düsseldorf

Gedruckt mit der Genehmigung der
Mathematisch-Naturwissenschaftlichen Fakultät der
Heinrich-Heine-Universität Düsseldorf

Berichterstatter:

1. Prof. Dr. Dr. h.c. Peter Kleinebudde

2. Prof. Dr. Jörg Breitkreutz

Tag der mündlichen Prüfung: 20. Februar 2018

Table of Contents

List of abbreviations	IV
List of publications	V
1 Introduction	1
1.1 Continuous manufacturing in pharmaceutical industries	1
1.1.1 Motivation	1
1.1.2 Advantages	2
1.1.3 Challenges	5
1.2 Integration of continuous manufacturing in pharmaceutical industry	6
1.2.1 Batch	6
1.2.1.1 Blending	6
1.2.1.2 Wet granulation	7
1.2.1.3 Drying	8
1.2.2 Bin-to-bin	9
1.2.2.1 Milling	9
1.2.2.2 Tableting	10
1.2.3 Partial integration	11
1.2.4 Chain integration of chemical/pharmaceutical processes	12
1.2.4.1 Chain integration of pharmaceutical processes	12
1.2.4.2 Chain integration of chemical processes	13
1.2.5 End-to-end integration	14
1.3 Vision and aims of the thesis	15
1.3.1 Vision	15
1.3.2 Continuous twin-screw wet granulation	15
1.3.2.1 Process setup of a twin-screw granulator	15
1.3.2.2 Process parameter in twin-screw wet granulation	17

1.3.3 Aims	19
1.4 Outline of the thesis	20
2 Materials and Methods	23
2.1 Materials	23
2.2 Methods	23
2.2.1 Manufacturing methods	23
2.2.1.1 Preparation of granulation powder blends	23
2.2.1.2 Screening of API suspensions and preparation of the granulation liquid	25
2.2.1.3 Twin-screw wet granulation	26
2.2.1.4 Fluidised-bed drying	31
2.2.1.5 Compaction	31
2.2.2 Analytical methods	32
2.2.2.1 Particle size distribution of powders and granules	32
2.2.2.2 Helium density of granules (true density)	32
2.2.2.3 Bulk and tapped density	32
2.2.2.4 Scanning electron microscopy	33
2.2.2.5 Compact porosity	33
2.2.2.6 Tensile strength	33
2.2.2.7 Friability	34
2.2.2.8 Disintegration time	34
2.2.2.9 Dissolution rate of ibuprofen compacts	34
2.2.2.10 Wettability of ibuprofen powder blends	34
2.2.2.11 Dissolved amount of Ibuprofen	35
2.2.2.12 Design of experiments	35

3 Results and discussion	39
3.1 Considerations to enable API suspension feed in twin-screw wet granulation	39
3.1.1 Background and objectives	39
3.1.2 Screening of API suspensions	40
3.1.3 Analytical method development for L/S ratio-dependent formulation screening	46
3.1.4 Formulation screening and selection	51
3.1.5 Summary	57
3.2 Comparison of API suspension feed and traditional API blend feed	58
3.2.1 Background and objectives	58
3.2.2 Comparison of granulation behaviour in twin-screw wet granulation	58
3.2.3 Comparison of granule and compact properties	69
3.2.4 Summary	76
3.3 In-barrel-drying	77
3.3.1 Background and objectives	77
3.3.2 Evaluation of the in-barrel-drying process setup	78
3.3.3 Characterising the in-barrel-drying process	82
3.3.4 Application of in-barrel-drying for API suspension feed	107
3.3.5 Summary	112
4 Summary and Outlook	113
5 Zusammenfassung und Ausblick	116
6 References	120
7 Danksagung	130
8 Appendix	132

List of abbreviations

API	Active pharmaceutical ingredient
BU	Blend uniformity
CDER	Center for Drug Evaluation and Research
CE	Conveying element
CMAC	Continuous manufacturing and crystallisation
CPP	Critical process parameter
CQA	Critical quality attribute
CU	Content uniformity
C-SOPS	Engineering Research Center for Structured Organic Particulate Systems
DOE	Design of experiments
HPLC	High-performance liquid chromatography
FDA	Food and Drug Administration
LOD	Loss on drying
L/S ratio	Liquid-to-solid mass flow ratio
MIT	Massachusetts Institute of Technology
NIR	Near-infrared (spectroscopy)
Ph.Eur.	Pharmacopoeia Europaea
RTD	Residence time distribution
s	Standard deviation
SUPAC	Scale-up and post-approval changes
TSG	Twin-screw granulator
USP	United States Pharmacopeia
\bar{x}	Arithmetic mean

List of publications

1. A. Schmidt; H. de Waard; K.-P. Moll; M. Krumme; P. Kleinebudde; Quantitative Assessment of Mass Flow Boundaries in Continuous Twin-screw Granulation, CHIMIA International Journal for Chemistry, 2016. 70(9): p. 604-609.
2. A. Schmidt; H. de Waard; K.-P. Moll; P. Kleinebudde; M. Krumme; Simplified end-to-end continuous manufacturing by feeding API suspensions in twin-screw wet granulation, European Journal of Pharmaceutics and Biopharmaceutics, submitted for publication.
3. A. Schmidt; H. de Waard; P. Kleinebudde; M. Krumme; Continuous single-step wet granulation with integrated in-barrel-drying, Pharmaceutical Research, submitted for publication.
4. M. Krumme; H. de Waard; K.-P. Moll; A. Schmidt; J. Taillemite; Method for preparing granules, European patent application.
5. M. Krumme; H. de Waard; F. Elbaz; K.-P. Moll; A. Schmidt; P. Kleinebudde; Method for preparing at least partially dried granules, European patent application.

Evaluation of authorship

Research article: Quantitative Assessment of Mass Flow Boundaries in Continuous Twin-screw Granulation.

author / co-author	idea [%]	study design [%]	experimental [%]	evaluation [%]	manuscript [%]
Adrian Schmidt	20	50	100	50	70
Hans de Waard	20	20	0	20	15
Klaus-Peter Moll	20	10	0	10	5
Markus Krumme	20	10	0	10	5
Peter Kleinebudde	20	10	0	10	5

Research article: Simplified end-to-end continuous manufacturing by feeding API suspensions in twin-screw wet granulation.

author / co-author	idea [%]	study design [%]	experimental [%]	evaluation [%]	manuscript [%]
Adrian Schmidt	20	50	100	50	70
Hans de Waard	20	20	0	20	15
Klaus-Peter Moll	20	10	0	10	5
Peter Kleinebudde	0	10	0	10	5
Markus Krumme	40	10	0	10	5

Research article: Continuous single-step wet granulation with integrated in-barrel-drying.

author / co-author	idea [%]	study design [%]	experimental [%]	evaluation [%]	manuscript [%]
Adrian Schmidt	20	50	100	50	70
Hans de Waard	20	25	0	25	20
Peter Kleinebudde	20	12.5	0	12.5	5
Markus Krumme	40	12.5	0	12.5	5

1 INTRODUCTION

1.1 Continuous manufacturing in pharmaceutical industries

1.1.1 Motivation

For decades, medicine has been produced in batch processes in pharmaceutical industries. In batch manufacturing, every single unit operation is processed separately (1). Typically, most material(s) are charged into the process equipment, before the process is started. Later, the process is stopped, the product is discharged, all at once, and then moved to the next unit operation (2). As consequence, a batch manufacturing line consists of multiple stops and starts in a series of unit operations (3). Such process interruptions cause not only inefficiency and delay in drug manufacturing, but also bear the risk for error and defects. Thereby costs and risks for drug shortages increase (4). On the long term, conventional batch manufacturing is not sustainable (5).

Therefore, health authorities, and in particular the U.S. Food and Drug Administration (FDA), emphasise actively the development of emerging technologies such as continuous manufacturing (6). Pharmaceutical manufacturing shall become more agile, flexible and robust, to ensure on-demand supply of high quality medicine (2). One of the emerging technologies to increase sustainability in pharmaceutical processing is continuous manufacturing (7). In contrast to batch manufacturing, raw material(s) and product(s) are charged continuously into the unit operation(s), for the entire duration of the process (2). Material(s) and/or products are created continuously, modified or transformed at a controlled rate over time (flow processing), before they are discharged continuously from the process. This principle is also called “one in, one out” (8).

In 2011, Janet Woodcock, CDER (Center for Drug Evaluation and Research) director at the FDA, predicted that in 25 years' time “current manufacturing practices are abandoned in favour of cleaner, flexible, more efficient continuous manufacturing” (9, 10). Ever since, regulators, pharmaceutical industry, academia and vendors have worked in close collaboration to make continuous manufacturing a reality. For example in 2014, the Novartis - Massachusetts Institute of Technology (MIT) Center, in cooperation with companies of the Continuous Manufacturing and Crystallisation (CMAC) Future Manufacturing Research Hub and the FDA, organised an International Symposium on Continuous Manufacturing of Pharmaceuticals, to review the state of research and to accelerate the implementation of continuous manufacturing. The symposium resulted in a comprehensive work package of guidance and gap analysis to accelerate the development of continuous processes in pharmaceutical industry (5, 11-18). In 2016, the work was followed by a second symposium, which addressed the regulatory environment in more detail (19).

One reason for the popularity of continuous manufacturing is its capacity to integrate multiple unit operations into a single manufacturing line. Since material is transferred immediately from one unit operation to the following unit operation, some process steps of a conventional batch manufacturing line may be omitted (e.g. work-up steps due to storage of intermediates). This thesis focusses on how to link chemical and pharmaceutical continuous manufacturing for a wet granulation operation. Thereby it moves the boundary of the pharmaceutical operation into the interface and provides one option to enable fully integrated end-to-end continuous manufacturing.

1.1.2 Advantages

So far, a global standard of operation principles with an established equipment basis, as well as high regulatory burdens for new technologies limited the promise and effort of pharmaceutical industry to change its batch manufacturing concept (20, 21). Times have changed and cost-pressure increases also for pharmaceuticals (22, 23). Likewise, in other industries such as food and chemical industry, continuous manufacturing could provide a high potential for increasing time- and cost-efficiency (24, 25). Thereby, pharmaceutical processing could get more competitive and sustainable for future. Continuous manufacturing provides various advantages over batch manufacturing in different aspects of the overall manufacturing process. For example, advantages can be found in the process flexibility and agility, the supply chain, in technical advances, in the improvement of product quality consistency and/or the ease for automation. In the following a few of those aspects are addressed.

One advantage of continuous manufacturing is an increased process flexibility and agility. Other than in batch manufacturing, the production volume of a continuous manufacturing process is not defined by equipment dimensions, but by process time (20). The afforded volume flexibility allows developing capabilities to supply niche markets that are currently uneconomical to serve because of the small product volumes linked to specific patient populations (orphan drugs, paediatric medicine, personalised medicine) (17). Furthermore, various batch sizes could be produced using one and the same equipment. Thereby, efforts for process scaling from lab-scale over piloting to commercial scale can be reduced. Thus, product development can be accelerated. Moreover, inventory could be reduced dramatically. In addition, the equipment itself can be designed in a smaller size. Both lead to a reduced footprint (reduced required facility capacity and hence lower costs) and to an increased process flexibility and agility. For example, mobile unit operations can be designed in a modular setup (26, 27). Thereby various manufacturing line configurations could be realised very flexible and in short time. Also in case of a troubleshooting with a single unit operation of the line, the equipment could be exchanged quickly (e.g. using a twin-module) without interrupting the entire manufacturing process for days or weeks.

Another advantage of continuous manufacturing can be found in the supply chain. In batch manufacturing, every unit operation is processed separately (Figure 1). After one batch manufacturing step is finished, the intermediate product has to be transferred to the next unit operation by using containers. Subsequently, batch equipment and containers have to be cleaned before a new batch can be processed. If the equipment of the following batch unit operation is not ready on time, material has to be stored intermediately (28). In some situations, material has to be stored for batch release purposes, before it can be further processed in the next manufacturing step. In other situations, materials have to be transported around the globe, before further processing them at a different manufacturing site. All this process interruptions and intermediate storage is inefficient and could potentially provoke product degradation and hence negatively impact the product quality (29). In contrast, in continuous manufacturing, unit operations offer the opportunity for physical co-location and a control concept as single manufacturing line. Material(s) and intermediate product(s) are directly transferred to the next unit operation which makes transport and intermediate storage redundant. Hence, efficiency increases and degradation risks of sensitive intermediate product can be reduced (2). Further, continuous manufacturing enables production on-demand. This holds true especially for end-to-end continuous manufacturing. A drug product could be manufactured starting from raw materials within days (instead of weeks or months for batch manufacturing) (30). Thereby, potential drug shortages could be addressed with significantly reduced response times.

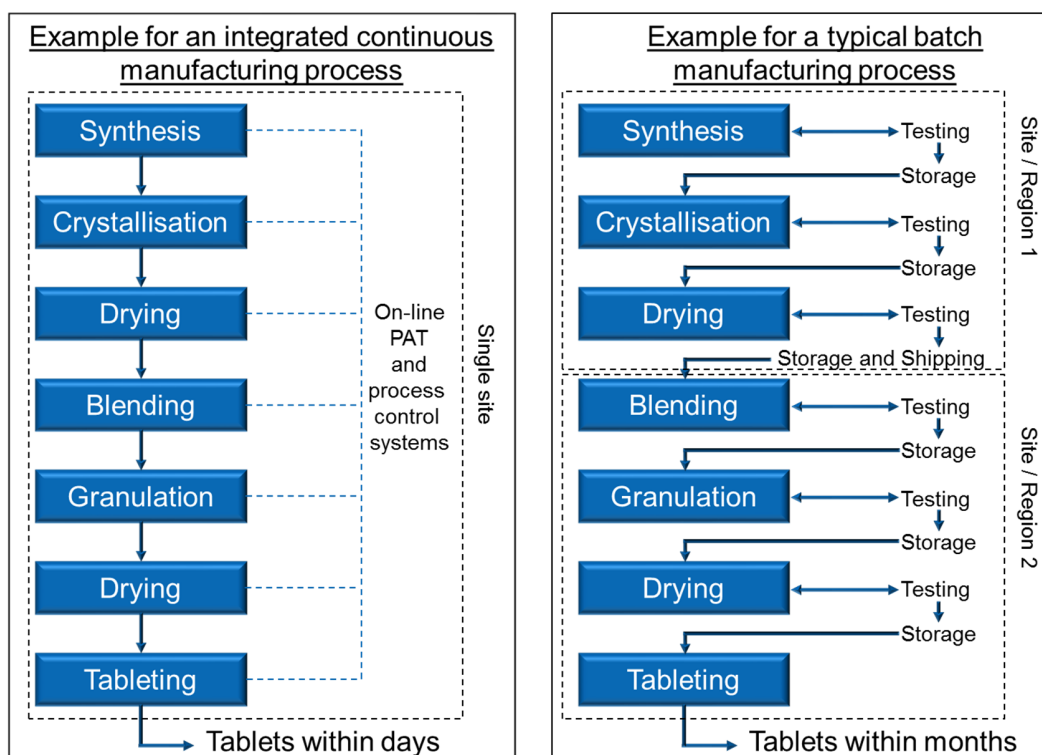


Figure 1: A comparison of the supply chains of a continuous and a batch manufacturing process.

Using continuous manufacturing, new technical advances are introduced to the manufacturing of pharmaceuticals. Examples are the continuous flow chemistry for the synthesis of active pharmaceutical ingredients (API's) and the continuous crystallisation of the synthesised API. So far, continuous flow chemistry has found limited implementation in pharmaceutical industry due to generally more complex synthesis of pharmaceuticals. However, it is already well implemented in petrochemical and bulk chemical industry (31). The benefits are numerous, for example: first, a fast synthesis enables the employment of new chemical pathways (for example via unstable intermediates) (32). Second, a large surface-to-volume ratio of the reactor provides exceptionally fast heat- and mass-transfer. Third, an improved yield by instantaneous mixing of small volumes (33). Fourth, an increased safety, achieved by better control of the smaller reactor volume (34). Fifth, a lower environmental footprint from a reduced solvent and catalyst consumption. And finally, well defined scale-up routes, such as by numbering-up (12, 31, 35). Another technical advance was introduced with the continuous crystallisation of the synthesised API. Continuous crystallisation aims for generating solids in flow over long periods of time and on pharmaceutical scales (36). Various methodologies have been employed and reported in literature including mixed-suspension-mixed-product-removal, plug-flow and continuous oscillatory flow reactors (37, 38). The big advantage of continuous crystallisation over batch is the enhanced impurity rejection, as well as the better reproducibility and control over the crystal size distribution in controlled steady-state (12). The crystal size distribution is an important critical quality attribute (CQA) of the crystallisation process since it affects directly the filtration time and efficiency, as well as later bulk properties of the finished API powder (39). The drawback of the controlled steady-state in continuous crystallisation processes are lower yields (no equilibrium) (40). However, this challenge could be overcome by using a controlled recycle of the mother liquor (12).

Another aspect is that continuous manufacturing provides opportunities for improved quality assurance through innovation in process development, process analysis and process control (41). In batch manufacturing, the release decision on the (intermediate) product quality is typically based only on a small fraction of the batch. In continuous manufacturing, however, the CQAs of the (intermediate) product can be monitored in continuous flow, upfront, within and/or after every single unit operation. This allows achieving a high data density to base the release decision on. Moreover, the CQAs of the (intermediate) product can be controlled while processing. Therefore, an automated quality control system evaluates the measurement data of the CQAs continuously and controls the critical process parameters (CPPs) of the single unit operations. CPPs are process parameters that impact significantly the CQAs of the (intermediate) product. Therefore, CPPs must be maintained in a well-defined range to ensure (intermediate) product quality (42). However, if the quality control system detects a disturbance in a CQA, it may respond/react automatically, for example, by using feed-forward and feed-backward loops (another or additional control mechanism could be the model-predictive control). As a response to a detected disturbance, the process controller manipulates the CPPs of the following unit operation to bring the product back into specifications. Further, as a reaction to a detected disturbance, the process controller

manipulates CPPs of the current/previous unit operation. In case that the material cannot be brought back into specifications, the system still could respond by diverting the material from the manufacturing line. This adaptive behaviour of the process in response to real-time knowledge of material attributes or process performance is a fundamental advantage of continuous manufacturing over batch processes and hence allow for a more consistent final product quality.

1.1.3 Challenges

Besides all the promising advantages of continuous manufacturing, it also introduces several challenges to be overcome and solved. Since people are familiar with batch processes, a new mind-set is needed and a substantial learning curve has to be taken (21, 23, 43). That includes not only industry, but also vendors, academia and regulatory authorities. A massive initial investment from all stakeholders is required to establish the necessary know-how and to implement first cases of industrial continuous processes. This can only be achieved in collaboration (44). Furthermore, there is a pressing need for developing appropriate continuous process equipment, as well as suitable measurement techniques to monitor and control product quality. For example, NIR is an often used technique to monitor and to control some CQAs of a material (8). This is because NIR is one of the most readily available process analytical techniques. It is a very flexible tool and hence finds many applications. But in fact, it is not always known if NIR also is the most appropriate tool for monitoring and controlling the CQA of interest (8).

Moreover, a pharmaceutical manufacturer has to ensure knowledge about what material (excipient and API) is contained in any drug product at any time. Thereby the manufacturer ensures material traceability (in a batch mode) in case of products that have to be recalled from the market due to later detected defects. For continuous manufacturing this is a challenging topic, since instead of reaction time, the process is controlled via the residence time. The understanding of the flow dynamics of the material in a continuous process is rather complex. It can be enhanced by performing experiments on the material residence time distribution (RTD) (2, 45). The RTD is the probability distribution for an infinitely small chunk of material to reside in an apparatus for a specific time. The RTD of a material in a specific process (chain) can be assumed from tracer or step change experiments and/or by modelling. However, the RTD of a material depends upon several factors and it is only an approximation of what is actually happening in the process. For example, some material could be exposed to layering in an individual unit operation. Hence, the residence time could be exceptionally prolonged for this material. Therefore, there is a general uncertainty about the traceability of materials throughout the continuous manufacturing process that needs to be addressed (46).

Other real or perceived general uncertainties can be found in the requirements for registration, validation and stability testing for continuous processes (47). Thereby risks are created, that could delay or fail the

approval of new products. Manufacturers may be risk-averse and choose the safe route for registration by developing the product via the well-known batch manufacturing. If approved, any change in the manufacturing process of already registered products would raise the need for re-approval with all its costs and uncertainties (48). This additional risk will further delay the implementation of continuous processes as a standard in pharmaceutical industries.

1.2 Integration of continuous manufacturing in pharmaceutical industry

The integration of unit operations into a continuous manufacturing line is a long-term goal for pharmaceutical industries. It will certainly be a stepwise approach to change-over to this new process paradigm. There are different levels of the integration of continuous manufacturing that can be distinguished, namely bin-to-bin processing of single disconnected unit operations, partial integration of multiple connected unit operations, chain integration for a chemical or pharmaceutical manufacturing line and full integration of all unit operations into a single end-to-end continuous manufacturing line (18). The bin-to-bin processing of single disconnected unit operations is the lowest level of the integration of continuous manufacturing. There are examples of already existing unit operations that are continuous processes by their nature, such as roller compaction, milling or tableting (2). Materials are charged continuously into, and products are discharged continuously from those equipment. The next level of the integration is the partial integration of multiple connected unit operations, for example by linking the previously mentioned roller compaction with a milling operation. A subsequent step would be to extend the number of integrated unit operations until the process line results in an entire chain for chemical or pharmaceutical manufacturing. A pharmaceutical process chain could consist for example out of a continuous blending, a roller compaction, a milling and a tableting operation. Finally, a link of the two process chains for chemical and pharmaceutical manufacturing would result in the ultimate level of integration of continuous manufacturing, namely in a fully integrated end-to-end continuous manufacturing line. In the following, various examples are given for the different levels of integration. However, it is started with examples for batch manufacturing steps, in order to already highlight how those process operations could benefit from a continuous mode.

1.2.1 Batch

1.2.1.1 Blending

Blending is an essential step in many pharmaceutical processes. The API is blended with other powder component(s), which thereby form all together a functional pharmaceutical formulation for the drug product. There is a variety of blenders available on the market. According to the scale-up and post-

approval changes (SUPAC) guidance of the FDA, the equipment can be classified into diffusion (tumble) mixers, convection mixers and pneumatic mixers (49). Thereby the choice for an appropriate blender depends on the material properties and the targeted blend uniformity (BU) (50). For example, the blending operation is influenced by the particle size and the shape, as well as by the concentration of the different blend components (51). Whereas for free flowing powders a tumble mixer could be used, convective systems would be more appropriate for cohesive powders (52).

Generally, BU is achieved by three blending mechanism that run simultaneously, namely convective, diffusive and shear mixing. Convective mixing thereby refers to blending due to bulk movement of the powder. Diffusive mixing refers to random movement of individual particles in the powder. Shear mixing refers to velocity gradients in the powder bed that are induced by internal blending elements (53). The BU is a crucial CQA of the blending and the overall manufacturing process, since it significantly impacts the content uniformity (CU) of the API in the final drug product. To evaluate the BU, sampling is a fundamental concern. Samples that are analysed for BU have to be representative for the state of the mixture. This so-called scale of scrutiny have to correspond to the dose unit that the patient may take (54). By using continuous manufacturing sampling-related issues could be mitigated. In continuous manufacturing, smaller volumes of the material are handled in continuous flow. The small volumes of material in continuous flow could be constantly analysed for BU by using online analytical measurements like near-infrared (NIR) spectroscopy, which increases the data density significantly on which the release decision is based on. Although similar measures could also be integrated in batch manufacturing equipment, in such equipment it may be more challenging to define a reliable measurement position. Another advantage of small material volumes in continuous flow is that the mixing could be enhanced.

1.2.1.2 Wet granulation

Generally, wet granulation is known as a process of particle enlargement. In wet granulation, powder particles are agglomerating into aggregates (granules) in which the original particles can still be distinguished (55). Wet granulation locks the BU and other material properties at the microscopic level of the agglomerated particle. It can be seen as a removal of degrees of freedom for the primary particles at a higher scale of scrutiny. Thereby, powder properties such as flow, densification and/or segregation tendency are modified as a prerequisite for following manufacturing steps, for example a tableting operation (56, 57). There are different types of granulators that can be distinguished, for example high-shear granulators and fluidised-bed granulators. However, all work in a similar way: a granulation liquid is added into the powder bed, in order to form nuclei and hence to initiate particle agglomeration. In high-shear granulators, agglomerates are formed by mixing the bed with an agitator while adding the liquid binder (58). Therefore, the agglomeration typically is very efficient, but solely a statistically controlled process, not a deterministic process. That is why often a sizing unit is integrated in order to reduce

agglomerates in size again. In fluidised-bed granulators, the powder bed is agitated by using a constant air stream. The powder bed is thereby fluidised while granulation liquid is sprayed through a nozzle into the bed. The agitation is less aggressive than mechanical stirring. Therefore, granules are typically obtained with a higher porosity after fluidised-bed granulation, compared to high-shear granulation.

A crucial CQA of the wet granulation process is the mean granule size and size distribution since both significantly impact the properties of the bulk material (e.g. flow). Therefore, it is important to determine an appropriate end-point of the granulation. A common technique to determine the granulation end-point in high-shear granulators for example, is the monitoring of the equipment's power consumption as a function of granulation time, while granulation liquid is added constantly (58). In a first stage of the granulation, the powder is wetted and only little granule growth is obtained. The power consumption remains constantly low. The second stage corresponds to the start of the agglomeration. An increase of the power consumption is observed. At the following third stage the power consumption reaches a plateau. This stage represents the achievement of a useful granule size. The fourth stage represents an over-wetting of the material. Increasing fluctuations are observed in the power consumption. In the final fifth stage, the material translates into a suspension. The equipment's power consumption drops down. Other measurement techniques to determine the end-point in granulation are for example imaging techniques, NIR or Raman spectroscopy. Still, as for the blending operation, it is challenging to define a reliable measurement position in batch processes. This could be overcome by using continuous manufacturing and its highly deterministic characteristic at high levels of scrutiny.

1.2.1.3 Drying

A wet granulation unit operation is followed by a drying operation. The drying operation removes the added granulation liquid, since the typical used amounts of water are detrimental for the following process steps (e.g. sticking to punch surfaces during tableting) and the final drug product quality (59, 60). Also for dryers, various types of equipment can be distinguished. Depending on the status of the material (i.e. liquid, pasty, solid), one or the other type of dryer should be used. An example of a dryer suitable to process liquid material is a spray dryer, for pasty material a drum dryer, and for solid material a fluidised-bed dryer. The drum dryer belongs to the group of conductive dryers, like belt or freeze dryers. Conductive dryers transfer heat for the evaporation of the liquid by contact. Additionally, in some dryers a gas stream or a vacuum is applied to enhance the drying rate. The drum dryer is a highly variable process equipment, suitable for material that forms a film like concentrated suspensions or pastes (61). The spray dryer is a process technique that sprays a liquid formulation into a drying chamber (47). Small droplets are dried by a hot drying gas within seconds. Due to the short exposure to high temperatures, spray drying has the advantage that this technique can also be used for heat-sensitive materials. The fluidised-bed dryer is one of the most commonly used drying techniques for solids in pharmaceutical

industry. In fluidised-bed drying, the wet material is fluidised and dried by a constant inlet air stream. Thereby a large contact area between the solids and the drying gas is created, which contributes to high rates of heat- and mass-transfer (62). Moreover, the fluidisation enables good mixing properties (63). All contributes to increased drying rates and hence shortened drying times.

In general, the drying process is based on simultaneous heat- and mass-transfer (63, 64). In the initial phase, the drying process is limited by the heat-transfer. In a first stage, the material is warmed up. The drying rate is low. In a second stage, the linear rate stage, water is steadily evaporated per time. The surface of the material remains saturated with moisture. In the first two stages, unbound moisture (liquid that is adsorbed by the solid and held only by weak cohesive forces) is evaporated. The product temperature remains relatively constant since heat is consumed by water evaporation. In the third stage, the system changes from heat-transfer-limited to mass-transfer-limited. In this phase, remaining moisture (bound moisture, absorbed by the solid or trapped in pores) has to diffuse to the particle surfaces first, before it can be evaporated. Thereby, less water is evaporated. As a result, more energy is provided to the heating of the material. The product temperature increases. This stage of the drying process is crucial and contributes significantly to the overall drying time.

A major CQA of the drying process is the residual moisture in the product. Therefore, it is important to determine the end-point of the drying process appropriately. For fluidised-bed drying, this can be done by using direct or indirect measurement methods. An indirect method that indicates a low residual moisture and thereby the end-point of the drying process is the monitoring of the exhaust air temperature. Since initially high amounts of energy are consumed by liquid evaporation, the exhaust air temperature is decreasing. Towards lower residual liquid amounts in the process, less energy is consumed by liquid evaporation. As a consequence, the exhaust air temperature is increasing. It equalises slowly with the inlet air temperature again. Thereby the end-point of the drying process can be determined. Direct measurement methods may use infrared moisture sensors or NIR spectroscopy to control the end-point of the drying process (65, 66). An advantage of a continuous drying process would be an enhanced process control, enabled by an enhanced material control. Thereby, risks of an over-drying of the material and material degradation could be reduced.

1.2.2 Bin-to-bin

1.2.2.1 Milling

Milling is a pharmaceutical unit operation, which is used to de-agglomerate powders or to reduce powders in particle size (47). On the one hand, the solubility, dissolution and bioavailability of API powders can be enhanced by using a milling operation (effect of the particle size reduction) (67). On the other hand, such a process could be used as a safety barrier to prevent fouling of following manufacturing steps. For

example, a mill can prevent a blocking of a tableting operation which could be caused by a few too coarse particles or powder agglomerates. Such powders can challenge an even filling of the tablet die and thereby cause variability in the tablet weight.

There are various types of mills on the market: colloid, disk, air jet, or a hammer mill, to name only some of them (68, 69). All equipment work with a comparable principle: material is charged continuously into the equipment. Then stress is applied to the material (e.g. by a mechanical rotor or by accelerating particles by air to collide against each other or to parts of the equipment) and a screening is conducted (e.g. by using sieves or air classifier). The hammer mill, for example, uses a rotor to break down the material and to push it through a sieve of particular size. After that, material is discharged continuously from the equipment. A major CQA of a milling unit operation certainly is the particle size and size distribution. Particle size and size distribution can be monitored online for example by optical or laser systems (70, 71).

1.2.2.2 Tableting

Most popular drug dosage forms are administered orally due to ease of ingestion, pain avoidance and hence higher patient compliance. Since oral dosage forms do not require sterility, they are also less expensive to manufacture (72). A well-known example of an oral drug dosage form is the tablet. In a tableting unit operation, materials are compacted in a tablet die by using two punches, an upper and a lower punch. Basically, there are two main types of tablet presses, namely the excenter and the rotary tablet press. The excenter tablet press is equipped with a single tablet die and one pair of punches. The tablet die is filled with powder by a movable filling shoe, which itself can be charged with material continuously. After that, the upper punch moves into the tablet die and the powder is compacted by applying a particular compaction pressure. For the excenter tablet press, the force is applied only via the upper punch. As a result, the properties may differ within a single tablet depending on the compaction side (e.g. higher tablet density at the upper tablet side). Finally, resulting tablets are discharged continuously from the equipment and another compaction cycle starts.

The rotary press is equipped with a turret (die table) on which a variable number of tablet dies and punches could be installed. While processing, the tablet die runs through a number of process units. At the filling unit, the die is filled with material either gravimetrically and/or by support of a forced feeder. The next step is the optional pre-compression unit, where punches pre-densify the powder in the die. Thereby air is released from the powder bed, which could prevent a later capping of the tablet (73). After that, the powder is compacted at the targeted force in the following compression unit. Other than for an excenter press, on a rotary press the force is applied via upper and lower punch. Thereby, the properties are more consistent within a single tablet. Finally, the tablet is discharged from the equipment.

There are several CQAs of the final tablet, for example the tablet weight, the hardness or the CU (74). Typically, all these CQAs are determined off-line, using wet chemical or other destructive analyses. For example, to determine the CU, several tablet samples are taken. Every tablet is then disintegrated in a specific liquid volume, in which the API dissolves. After that, the API concentration is determined in the liquid using HPLC. Subsequently, the content uniformity over all tablet samples can be calculated. However, there are also non-destructive online measurements available to indicate CU. For example, the CU is related to the tablet mass, which in turn affects the compaction pressure. The compaction pressure is a parameter that is easily and rapidly accessible. Therefore, the compaction pressure could be monitored to give an indication of the CU. However, this measurement is not very precise and could only be used for higher dose strengths as an indicator. Another measurement method that provides non-destructive online analysis of the CU for every single tablet is the NIR spectroscopy (75, 76).

1.2.3 Partial integration

The next higher level of integration of continuous manufacturing is the partial integration of multiple connected unit operations. One example for a partial integration is the link of the two unit operations wet granulation and drying. One system that was developed to combine continuous wet granulation and drying was the Easy Flow[®] system from L.B. Bohle (27). Therefore, a small volume single-pot high-shear granulator was designed. The granulator was equipped with a top-driven impeller, a chopper, a nozzle for continuous liquid spraying, a top port for continuous solid feed, a top side-port with an integrated sieve for the continuous discharge of granulated material and a scraper to reduce dead volume in the equipment (77). The working principle of this granulator is comparable to a continuous stirred-tank reactor. Material (solid and liquid) is charged continuously into the equipment and granulated. By centrifugal forces, induced by the impeller, granulated material is discharged continuously from the equipment. During development, a broad granule size distribution was observed in preliminary tests. Therefore, a sieve was integrated into the material discharge port. Thereby, too coarse granules were held back in the process and exposed again to the chopper (particle size reduction). After discharge, the wet granules were passing by a vacuum dryer, which was heated by infrared radiation. However, overall the Easy Flow[®] system still provided critical dead volume, which is why the development has been stopped finally.

Another way to combine a continuous wet granulation operation with a drying operation is by using a twin-screw granulator (TSG) and a fluidised-bed dryer. The TSG is comparable to a plug-flow reactor. Solid and liquid material is continuously fed into the barrel of the TSG and horizontally conveyed and granulated along two screws. Big advantages of the TSG are the low material hold-back and the reduced dead volume. The screws are self-cleaning and wiping away stagnant material. From the outlet of the TSG, wet granules are transferred (e.g. gravimetrically or by compressed air) to the fluidised-bed dryer. An example for such a process is the ConsiGma[®] 1 line (78-80). The ConsiGma[®] 1 is a lab-scale

equipment and designed as a small mobile module for plug and play. The fluidised-bed dryer is thereby optional and processed in batch mode. However, wet granules are gravimetrically continuously transferred to the dryer. Thereby, the quality of the wet granules is crucial since it impacts significantly the drying process. Depending on the particle size, a different stress has to be applied by air, in order to fluidise the powder bed. If granules get too coarse, it could be that the air supply is not sufficient to fluidise the powder bed and the drying will fail. In contrast, if granules remain too fine, it could be that particles are blown directly into the filter system of the fluidised-bed dryer. The drying efficiency would drop significantly. Therefore, the properties of wet granules from continuous twin-screw wet granulation need to be within a certain range.

1.2.4 Chain integration of chemical/pharmaceutical processes

1.2.4.1 Chain integration of pharmaceutical processes

The next level of integration of continuous manufacturing is the chain integration of an entire chemical or pharmaceutical manufacturing line. One example for an entire pharmaceutical manufacturing line is the continuous direct compression line from ConsiGma® (ConsiGma® CDC) (80). This line is commercially available from GEA and comprises the unit operations feeding, blending and compression. The ConsiGma® CDC provides the possibility to install up to six loss-in-weight powder feeders. The solid flow streams from every powder feeder are then combined in the blending unit operation, which consists of two agitated blending units, one at low- and one at high-shear. The feeding systems and blending units have to work hand-in-hand to ensure accurate blend composition and uniformity. For example, if the fluctuations in the solid mass feed rates of the powder feeders are increasing due to suboptimal bulk powder properties, the blending may require a longer processing. Therefore, an NIR sensor is used as online measurement tool to control BU. The powder blend is then transferred to and compacted on a rotary tablet press. Since the blend is transferred directly to the following tableting unit operation, the risk of segregation is reduced.

Another product in the portfolio from GEA is the ConsiGma® continuous tableting line (ConsiGma® CTL). This continuous manufacturing line comprises the unit operations feeding, blending, wet granulation, drying, tableting and coating (80). Since more unit operations are linked with each other, the complexity of the continuous process is increasing. Next to the previously described interplay between powder feeding and blending time and between wet granulation and fluidised-bed drying, another example is given by the interplay between granulation and tableting. For tableting, the flow and the densification of the powder bulk is crucial. Both properties are a function of the particle size, size distribution and/or morphology and can be enhanced by granulation (81). However, if the resulting material is under-granulated, it will behave

cohesively. For cohesive powder, it takes longer to fill the tablet die and therefore the tablet weight variability could be affected (82).

Another solution for continuous pharmaceutical manufacturing is the so-called Modular Continuous System (Modcos) (83). This modular system comprises the unit operations feeding, blending, wet granulation, drying, milling and tableting. For most of those unit operations the supplier Glatt can provide technical solutions in-house (e.g. blending, drying, milling, powder transport), for others the company has partnered up with other suppliers, such as Thermo Scientific Fisher (twin-screw wet granulation) or Fette (tableting).

In 2015, the FDA approved Orkambi® as the first continuously produced drug product. Orkambi® is a drug from Vertex against cystic fibrosis. The applied continuous process uses the ConsiGma® platform technology. It starts with feeding individual powder components and finishes with film-coated tablets (3). Thereby, the process displays an entire continuous pharmaceutical manufacturing line. In 2016, another drug product was approved by the FDA, when Janssen Supply Chain switched its production of the HIV-1 treatment Prezista® (film-coated tablet) from batch to continuous manufacturing (84). The continuous direct compression process thereby uses the platform design developed by the Engineering Research Center for Structured Organic Particulate Systems (C-SOPS).

1.2.4.2 Chain integration of chemical processes

A typical chemical manufacturing process consists of multiple synthesis steps, that include reaction-, extraction- and distillation steps. All steps would need to be conducted in continuous flow and require an adequate feeding, mixing, tempering, timing and level of control. Various successful examples have been demonstrated in literature, for example for aliskiren, efavirenz or pregabalin (85, 86). One study has demonstrated an entire manufacturing chain for drug substances in the size of a refrigerator (86). This system consists of various reconfigurable modules and is divided into an upstream and a downstream unit. The upstream unit thereby synthesises the API and includes reaction-depending multiple pumps, reactors, separators and/or pressure regulators. The downstream unit is dedicated to the purification and formulation of the liquid drug product and includes for example crystallisers and filters. Due to the modular setup, the system is very flexible and has been demonstrated applicable for the supply of various APIs on-demand, for example diphenhydramine or lidocaine.

Other chemical manufacturing lines, however, target finished API dry powder. For such processes, the API synthesis is followed by API crystallisation/purification, as well as by a drying of the API. The feasibility and advantages of continuous crystallisation have been highlighted already (87). After crystallisation, crystals are filtrated and washed in the following unit operations, in order to minimise the amount of impurities that is carried into downstream processes. The solid separation in continuous

filtration, including the washing of the solids, has been a seldom described technique in literature due to its complexity (12). A challenge could be the handling of high concentrated slurries. However, a novel filtration system has been reported recently, that finally could enable the handling of high concentrated slurries for particle ranges from 0.01 - 200 microns (35). The filtration system was shown to be capable for achieving suspension concentrations up to 60 % w/w for ibuprofen or 76 % w/w for lactose respectively. The filtration and isolation of the API is then followed by a drying operation. Although progress was made, a significant benefit of continuous over batch processing is not yet clear for filtration, isolation and drying (36).

1.2.5 End-to-end integration

The ultimate challenge of continuous manufacturing is a fully integrated continuous manufacturing line. Thereby continuous manufacturing of drug substance and continuous manufacture of drug product are linked. In 2007 Novartis launched together with the MIT the Novartis-MIT Center for Continuous Manufacturing (44). Novartis has committed significant funding over a period of 10 years to this collaboration, with the aim to transform the current manufacturing in the pharmaceutical industry into continuous mode (88). The project is focused on combining industrial expertise with the scientific environment of academia, in order to develop new technologies that will replace traditional batch manufacturing unit operations. In 2013, the collaboration presented a first fully integrated end-to-end continuous manufacturing process (30). This work proved the technical feasibility.

The process starts with a chemical intermediate and includes several manufacturing steps for the API synthesis and the API work-up (including drying). In the following combined hot melt extrusion and injection moulding unit operations, tablets were produced, containing 112 mg of aliskiren. The process was monitored and controlled via an automated control system. The manufacturing line was operated continuously end-to-end for time periods of up to eight hours. By changing from batch to continuous manufacturing, the total number of unit operations was reduced from 21 to 14. Additionally, the process residence time was shortened from 300 to 47 hours (47). However, after the successful demonstration of the feasibility, the next challenge would be the transfer of such technologies to an adequate scale for industry. Moreover, hot melt extrusion is limited in its applicability to thermostable APIs. Hence, other process technologies need to be exploited for end-to-end continuous manufacturing that could also be applied to thermosensitive materials.

1.3 Vision and aims of the thesis

1.3.1 Vision

Over the last years, continuous manufacturing is a relatively quickly evolving emerging technology in pharmaceutical processing. New technologies were introduced to enable the switch from batch to continuous processing. A variety of studies have focused on investigating formulation and process development of single continuous unit operations. Other studies have investigated the partial integration of multiple unit operations or the integration of an entire chemical or pharmaceutical continuous manufacturing chain (e.g. GEA ConsiGma® CTL). A natural extension is to link both process chains into a fully integrated end-to-end continuous manufacturing line. First attempts to study end-to-end continuous manufacturing have been reported, for example, for a hot melt extrusion unit operation. However, such a process setup is limited in its application for thermostable APIs. Therefore, new ways have to be explored to link chemical and pharmaceutical continuous manufacturing for more traditional unit operations, such as wet granulation. One unit operation uses a converted twin-screw extruder from hot melt extrusion to perform continuous wet granulation. In case of using the equipment for wet granulation, the operation is called twin-screw wet granulation. Since for hot melt extrusion the extruder was demonstrated to enable end-to-end continuous manufacturing, it is reasonable to envision a link between chemical and pharmaceutical continuous manufacturing for wet granulation by using the same equipment for twin-screw wet granulation. Therefore, continuous twin-screw wet granulation was investigated in detail for its potential to link chemical and pharmaceutical continuous manufacturing for wet granulation. In the following, continuous twin-screw wet granulation is introduced, before the aims are highlighted in more detail.

1.3.2 Continuous twin-screw wet granulation

1.3.2.1 Process setup of a twin-screw granulator

Next to its capability for continuous processing, the main driver for the popularity of the TSG is its high flexibility at a very compact design. In general, the TSG consists of the main parts barrel, two screws with screw elements, temperature control units and feeding systems for liquids and solids. The design of the TSG heavily depends on the type of equipment and the vendor. For example, the barrel of a TSG from Leistritz is designed as a block and the temperature control unit is surrounding the barrel. All temperature control blocks have to be mounted, disassembled and cleaned separately. Thereby the accessibility of the barrel and the screws is limited. In contrary, for a TSG from Thermo Fisher Scientific, the barrel consists of two parts: a lower barrel and an upper barrel. The temperature control unit is integrated into the equipment itself. It is installed inside the socket for the lower barrel. The advantage of such integrated

design is a very compact process setup and a lower contamination risk. Further, the barrels can be disassembled quickly as a block, together with the screws. The drawback of the integrated temperature control unit is a heterogeneous temperature distribution across the barrel and screws. Heating and cooling is supplied only to the lower barrel. By heat flux, heat is distributed to other compartments, such as the upper barrel or the screws. There are many other examples for differing details between TSGs. However, the following description of the features of a TSG is mainly focused on a lab-scale Pharma 11 from Thermo Fisher Scientific.

The lower and the upper barrel are segmented into eight barrel zones of equal size. The lower barrel is installed on a socket, in which the temperature control unit is integrated. The temperature control unit is assembled of several blocks, one for every barrel zone (not applicable for barrel zone 1). Every temperature control block consists of a cooling block (water-cooled), a heating block (250 W thermo element) and a temperature sensor. Thereby a precise individual temperature control is enabled for every single barrel zone. Limitations can be found in the outlined heat flux.

The upper barrel can be equipped with various ports (not applicable for barrel zone 8). One port that can be installed is a degassing vent port. Such port is commonly used in hot melt extrusion to release vapour and/or pressure build-up. Moreover, there are other ports that can be installed to feed solids or liquids into the TSG. The different flow streams together define the total material mass throughput, its solid/liquid composition, as well as the final formulation composition. Therefore, feeding has to be accurate and precise. Small fluctuations in the feed rate of solids and/or liquids could cause significant deviations in granule size and size distribution and can lead to poor product quality (89). In some cases, such fluctuations can even lead to a failing of the unit operation, due to over-wetting of the material and paste formation (90). Fluctuations in the liquid feed rate could be obtained depending on the used pumping system. Whereas with a peristaltic pump pulsations are obtained by definition, a micro gear or progressing cavity pump can feed liquids free of pulsations. Another impacting factor for fluctuations in the liquid feed is the liquid nozzle diameter of the TSG. Whereas large nozzle diameters tend to deliver liquids in dripping mode, a smaller nozzle diameter could deliver a similar feed as continuous liquid stream (depending on the liquid and the feed rate). To identify and to reduce fluctuations in the feed rates, a reliable control system is essential and has to be evaluated carefully. For solid feeding equipment (e.g. gravimetric powder feeder) for example, it has been reported that control could be insufficient, using only data provided by the equipment itself (89). Moving averages and other pre-treatment techniques of raw data may bias the information content that is fed back into the control loop and warrant careful interpretation of the actual performance.

The core part of the TSG is the co-rotating intermeshing twin-screws enclosed in the barrel. The Thermo Scientific Fisher TSG is characterised by the diameter and the length of its screws. The screw size defines the dimensions of the equipment and the material throughput that it can achieve. A high flexibility is provided in terms of the design of the screws. Basically, the screw setup is modular and comprises

various screw elements that can be assembled in the desired configuration. There are different types of screw elements, which are used to modify the process conditions in the TSG. Broadly, there are three types that can be distinguished, namely conveying elements, kneading elements (blocks) and mixing (combing) elements (91).

Conveying elements are mainly used for material transportation, since they are designed to impart low mechanical energy to the material. Conveying elements are mainly characterised by their pitch, which represents the axial distance between two adjacent flights. Compared to other traditional screw elements, the conveying element offers the largest space for material to fill (92). Such elements often are used in zones, where solids are fed into the TSG (91). A special variant of a conveying element is the (shouldered) wide throat element. Those screw elements provide even larger space to the material, but are not intermeshing. Wide throat elements allow the feeding of larger particles (agglomerates). Kneading elements are mainly used for mixing, densification and granulation of the material. They are typically used in blocks at different staggering angle (30, 60 or 90°) (91). Depending on the number of elements and the staggering angle, material is exposed to various shear forces since the space in the TSG is reduced significantly (fill-degree-dependent). Moreover, it has been described that kneading elements can introduce forward or reversing flow, when used at different staggering angle (93). Thereby, plug-flow of the material and axial mixing can be reduced and increased respectively, which in turn enhances the mixing in the TSG. Mixing elements are mainly used to distribute and to recombine material flow streams in order to provide a good mixing in a low shear environment (91). In some studies, mixing elements were reported also as sizing/milling elements (94, 95). Further, it has been described that those elements possess a lower capability of wiping away stagnant material, compared to conveying elements (92, 94).

1.3.2.2 Process parameter in twin-screw wet granulation

Process parameters in twin-screw wet granulation are parameters that define the material mass throughput and its composition (solid/liquid), the screw speed and the barrel zone temperature. The material mass throughput and its composition can be described in different ways. With a combination of two out of four parameters (solid mass flow rate, liquid mass flow rate, total material mass flow rate and liquid-to-solid ratio), this can be described. Depending on the choice of parameters, different aspects of the process are being emphasised. However, for the evaluation of results and of literature, it is important to highlight that whatever parameters are chosen, they will be confounded with each other. Other qualitative process parameters, such as the TSG fill-level and the RTD are impacted by these process parameters.

Firstly, liquid, solid, and total material mass flow rate obviously all impact the TSG fill-level. However, also the L/S ratio has an influence on the TSG fill-level, since it affects the material density (e.g. the density of

a liquid is usually higher than that of a bulk solid and the L/S ratio also impacts powder agglomeration). The TSG fill-level has been reported as a CPP for CQAs of the granulation process (e.g. particle size distribution or bulk/tapped density), as well as for CQAs of a following tableting process (e.g. tensile strength or disintegration time) (96). For the granulation unit operation, it has been demonstrated that with increasing TSG fill-level, the fraction of oversized granules was increasing. For a following tableting, a trend has been described for the tensile strength of tablets produced of granules from increasing TSG fill-level. With increasing TSG fill-level, the tensile strength of tablets was demonstrated to increase initially, before it decreased at higher TSG fill-level. Consequently, also the disintegration time was affected. With increasing TSG fill-level, the disintegration time of tablets was decreasing initially, before it increased at higher TSG fill-level. Secondly, the parameters that define the material throughput and its composition are all impacting the RTD (97-100). The RTD is another important parameter that for example affects the liquid distribution in the powder bed and thereby the particle agglomeration (size and size distribution) (101). Furthermore, the RTD and the TSG fill-level are linked. For example, increasing L/S ratios are described to increase the RTD (102). Although the total material mass flow rate is kept constant, the fill-level of the TSG increases. Finally, the liquid and total material mass flow rate, as well as the L/S ratio all together obviously influence the overall processed amount of water in the granulation. Whereas for the granulation process, the order of magnitude of the impact has to be defined per process and formulation, the processed amount of water certainly has a significant impact on the following drying operation. With increasing amounts of processed water, increasing drying times are required. Thereby, the material throughput of a continuous manufacturing line could be limited.

Another CPP is the screw speed. Generally, the screw speed defines how fast the material is conveyed within the TSG. Moreover, the screw speed has a direct impact on the shear rate and is linked to the RTD and the TSG fill-level. For example, increasing screw speeds increase the material transport in the TSG and thereby shorten the residence time (91). Simultaneously, the TSG fill-level is decreasing. However, the magnitude of the impact of the screw speed certainly depends on the investigated range.

Finally, the barrel temperature was reported as a CPP for granulation. It has been described that at higher barrel temperature, the process yields less fines and more coarse granules (79, 97, 103). In some studies, this effect was attributed to an increased solubility of solids in the granulation liquid, which in turn led to a stronger formation of liquid bridges (79, 97, 104). Other studies additionally highlighted a lower capacity for moisture absorption by certain powder components (e.g. MCC) at increasing temperature (103). Thereby less water would be absorbed by the formulation. Thus, increasing moisture would be obtained on particle surfaces, increasing the potential for forming liquid bridges.

1.3.3 Aims

This thesis aims for extending the toolbox of end-to-end continuous manufacturing by using twin-screw wet granulation. Therefore, this thesis provides one efficient and novel possibility for the interface to link chemical and pharmaceutical continuous manufacturing for wet granulation (Figure 2). It was hypothesised that this ambitious scope could be achieved, using an API suspension obtained from a continuous manufacturing process to feed a TSG directly. However, such innovative process technique also introduces uncommon challenges to the wet granulation operation, for example handling of high amounts of water in and after the twin-screw wet granulation operation.

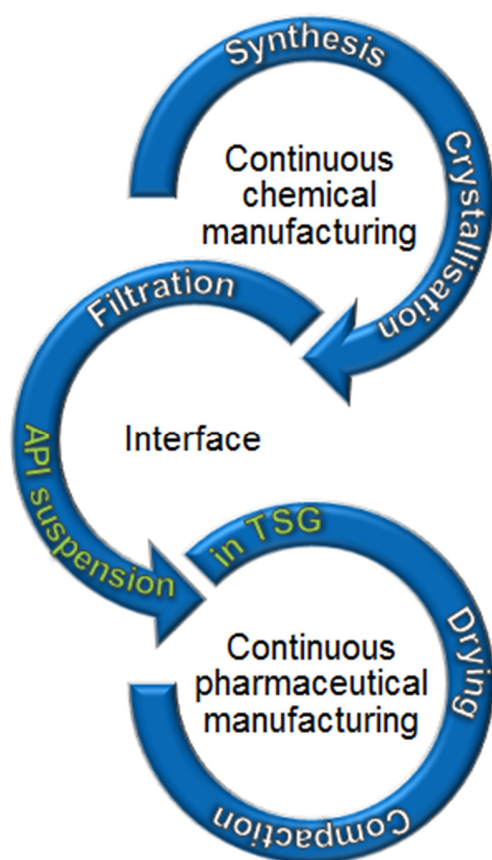


Figure 2: Link of continuous manufacturing of drug substance and continuous manufacture of drug product by API suspension feed in twin-screw wet granulation (green colour highlights the process investigated in the present thesis).

Therefore, the aims of this thesis are as follows:

- Develop appropriate formulation for the API suspension and for a powder formulation in wet granulation to enable API suspension feed in twin-screw wet granulation.
- Investigate the feasibility of API suspension feed in twin-screw wet granulation at the interface to link chemical and pharmaceutical continuous manufacturing.
- Compare twin-screw wet granulation with API suspension feed against the traditional dry API blend feed. Compare the granulation and granule properties, as well as the following compaction and resulting compact properties.
- Investigate in-barrel-drying as a solution for the increasing drying efforts after twin-screw wet granulation, caused by API suspension feed. Characterise and optimise the process by using design of experiments (DOE).
- Merge and investigate the API suspension feed and the in-barrel-drying in twin-screw wet granulation. Compare the process against traditional twin-screw wet granulation processes with dry API blend feed and fluidised-bed drying. Evaluate the resulting granules properties, the following compaction process, as well as the resulting compact properties.

1.4 Outline of the thesis

It was investigated whether continuous manufacturing of drug substance and continuous manufacture of drug product could be connected into a fully integrated continuous manufacturing line. Such a connection was hypothesised to be achieved by feeding an API suspension from the chemical process directly in a TSG. The suspension liquid could be directly used as granulation liquid. This could not only enable connecting chemical to pharmaceutical manufacturing, but could also result in omitting the typical drying step after API crystallisation and washing. Thereby manufacturing efficiency could be enhanced significantly. A major challenge of such process, however, is that the amount of water in the twin-screw wet granulation process is defined by the API suspension concentration on the one hand, and the

targeted API formulation load on the other hand. Such process setup could become challenging, especially when a high API load is targeted in the formulation. Increasing API loads in the formulation are achieved by increasing the liquid mass flow rate of the API suspension. Simultaneously, the amount of water in the process is increased, while the amount of excipients remains constant. Hence, the relative amount of water in the twin-screw wet granulation process increases. In contrast, in traditional twin-screw wet granulation, the API is dosed as dry blend, together with excipients. The granulation liquid is added independently, as much as needed, as little as possible.

In wet granulation, one CPP is the processed amount of water, or in case of twin-screw wet granulation the L/S ratio. Particular L/S ratios are needed to form nuclei and hence to induce particle agglomeration, whereas too high L/S ratios induce paste formation and hence a fouling of the unit operation. These effects (under-granulated material versus paste formation) depend not only on the processed amount of water, but also on the formulation. Hence, for the API suspension feed, formulation and the processed amount of water have to be balanced to ensure favourable granulation behaviour.

In a first chapter, considerations of the processed amount of water and an appropriate powder formulation are investigated to enable API suspension feed in twin-screw wet granulation. One way to decrease the relative amount of water in twin-screw wet granulation while keeping the formulation drug load constant is to increase the API suspension concentration. However, this approach is limited since upon changing the suspension concentration, the rheological behaviour is impacted and may affect the dosing of the suspension. Consequently, an appropriate formulation is developed, capable of being processed at high L/S ratios in twin-screw wet granulation with API suspension feed.

In chapter two, the feasibility of API suspension feed in twin-screw wet granulation is investigated by processing various API suspensions. The API suspension feed is compared against traditional API dry blend feed in twin-screw wet granulation, since according to literature the granulation behaviour can be impacted significantly by the granulation liquid and its viscosity (105). The granulation process and resulting granules properties (granule size distribution, flowability, morphology) are compared. For a particular L/S ratio, at which comparable granule properties are obtained, granules batches of both processes are compacted. The compaction process (using force-displacement-curves) and resulting compact properties (tensile strength, out-of-die porosity, friability, disintegration time, and dissolution rate) are compared.

By using API suspension feed, previously required API drying is omitted, since the suspending liquid has been used directly as granulation liquid. However, as a consequence of such a process setup, more extensive drying is required after the twin-screw wet granulation operation. According to literature, screw conveyors can be used as efficient and truly continuous drying systems. In other industries, like food, agricultural or mining, screw conveyors are already operated as pre- and/or post-dryer (106-108). The big advantage of a screw conveyor dryer is the controlled material throughput, its compact design and cost

efficiency. The TSG, as a type of screw conveyor, provides the function of individual segmented temperature control of barrel zones. It is hypothesised that by heating certain parts of the equipment, wet granulation and (pre-) drying could be combined inside the barrels, from now on referred to as in-barrel-drying.

Although in a different context and with a completely different scope, a study has indicated the possibility of receiving dried granules after twin-screw wet granulation at higher temperatures (109). Actually, it was aimed to enhance the tabletability of a poorly compactible drug, using twin-screw wet granulation at barrel zone temperatures up to 90 °C. Since only a very low amount of water (5 %) was processed, dried granules were obtained for specific settings.

In the final third chapter, the drying capability by in-barrel-drying in a TSG is investigated specifically. A robust process setup for in-barrel-drying is investigated by evaluating various possibilities for venting. After that, critical factors and their appropriate ranges are studied systematically by using DOE. A design space for achieving (pre-) dried granules is identified. Finally, the API suspension feed and the in-barrel-drying are merged in twin-screw wet granulation. This process is investigated in detail and compared against the traditional twin-screw wet granulation processes with API dry blend feed and fluidised-bed drying. Granules (granule size distribution, flowability) and compact properties (tensile strength, out-of-die porosity, disintegration time) are therefore studied and compared for all process setups.

2 MATERIALS AND METHODS

2.1 Materials

Ibuprofen (ibuprofen 25, BASF, Ludwigshafen, Germany) and lumefantrine (lumefantrine DS, Zhejiang Medicine Co., Zhejiang, China) were used as model drug substances. Other materials used for granulation were spray-dried lactose monohydrate (lactose) (Foremost® 316 Fast Flo®, Kerry Bio-Science, Beloit, USA), microcrystalline cellulose (MCC) (Vivapur® 102, JRS Pharma, Rosenberg, Germany), sodium carboxymethylcellulose (croscarmellose sodium Ph.Eur.) (Na-CMC) (Primellose®, DFE Pharma, Goch, Germany), polyvinylpyrrolidone K30 (povidone K30 Ph.Eur.) (PVP K30) (Plasdone® K-29/32, Ashland, Covington, USA), magnesium stearate (MgSt) (magnesium stearate Ph.Eur., Faci, Carasco, Italy), sodium pyrophosphate ($\text{Na}_4\text{P}_2\text{O}_7$) (sodium pyrophosphate 98 %, Alfa Aesar, Thermo Fisher Scientific, Heysham, UK) and polysorbate 80 (Tween® 80, Croda International, Snaith, UK). Demineralised water has been used as granulation liquid.

2.2 Methods

2.2.1 Manufacturing methods

2.2.1.1 Preparation of granulation powder blends

Whenever an API was contained in the powder blend, it was sieved manually through a 1 mm mesh before use. All components for the powder blend were dispensed in a mixing drum of appropriate size (fill volume approximately 75 %) and mixed, using a turbula blender T10A (Willy A. Bachofen, Muttenz, Switzerland) for 5 min at 25 rpm (Table 1-3). Although magnesium stearate is typically added in a separate short blending step in order to have it only as an external phase, it was blended together with the other components to avoid an additional blending step (110). Powder blends were prepared in batch sizes ranging between 1.5 and 4.5 kg. Following blending, powder blends were sieved manually through a 1 mm mesh.

Materials and Methods

Table 1: Tested formulations during formulation screening to enable API suspension feed.

Component	Formulations based on [% w/w]				
	Lactose	Lactose-MCC	MCC	MCC-Na-CMC	Na-CMC
Ibuprofen	60				
Lactose	36	18	-	-	-
MCC	-	18	36	28	-
Na-CMC	-	-	-	8	36
PVP K30	2.5				
MgSt	1.5				

Table 2: Formulation compositions used during the investigation on ibuprofen suspension feed.
(CMC= critical micelle concentration)

Component	Ibuprofen blend feed [% w/w]					Ibuprofen suspension feed [% w/w]	
	A. MCC-Na- CMC based	B. Na ₄ P ₂ O ₇ in the blend	C. Na ₄ P ₂ O ₇ in the liquid	D. Polysorbate 80 (↓ CMC)	E. Polysorbate 80 (↑ CMC)	F. Na ₄ P ₂ O ₇ in the liquid (PVP in the blend)	G. Na ₄ P ₂ O ₇ in the liquid (PVP in the liquid)
Ibuprofen	60.0	60.0	60.0	61.5	60.3	60.0 *	60.0 *
MCC	28.0	25.5	25.5	26.2	25.6	25.5	25.5
Na-CMC	8.0	8.0	8.0	8.2	8.0	8.0	8.0
PVP K30	2.5	2.5	2.5	2.6	2.5	2.5	2.5 *
MgSt	1.5	1.5	1.5	1.5	1.5	1.5	1.5
Na ₄ P ₂ O ₇	-	2.5	2.5 *	-	-	2.5 *	2.5 *
Polysorbate 80	-	-	-	2.6x10 ⁻³ *	2.0 *	-	-

* Components were processed via the granulation liquid.

Materials and Methods

Table 3: Formulation compositions used during the investigation on in-barrel-drying.

Component	Characterisation of in-barrel-drying [% w/w]	Comparison in-barrel-drying and fluidised-bed drying [% w/w]
Lumefantrine	20.0	20.0 *
Lactose	35.0	
MCC	33.5	33.0
Na-CMC	6.0	
PVP K30	4.0	
MgSt	1.5	
Polysorbate 80	-	0.5 *

* Components were processed via the granulation liquid.

2.2.1.2 Screening of API suspensions and preparation of the granulation liquid

Screening for processable ibuprofen suspensions

Ibuprofen was sieved manually through a 1 mm mesh. To aid the wetting of ibuprofen in the granulation liquid and to obtain a suspension, either sodium pyrophosphate or polysorbate 80 was added. The suspending agent was dissolved, before ibuprofen was added slowly. Approximately 50 g of ibuprofen was suspended every 5 minutes. Any visual change in the rheological behaviour of the suspension was noted. The solutions and suspensions were stirred constantly using a magnetic stirrer or an overhead stirrer equipped with a four-blade agitator. Furthermore, suspensions with ibuprofen concentrations between 30 to 60 % w/w were tested for their pumpability and processability using a progressing cavity pump NM003BY11S12B (Netzsch, Selb, Germany). Therefore, the suspension was processed at several pump speeds between 500 to 2500 rpm and the liquid mass flow rate was monitored using a dynamic balance (K-Sampler K-SFS-24, Coperion, Stuttgart, Germany).

Preparation of processable ibuprofen suspensions

Ibuprofen was sieved manually through a 1 mm mesh. After that, ibuprofen was suspended slowly (approximately 50 g every 5 min), either in a sodium pyrophosphate or a polysorbate 80 solution, until the desired concentration was achieved. The ibuprofen concentration in the suspensions was chosen such that the amount of water that is dosed to the granulation was minimised while simultaneously maintaining adequate rheological behaviour for processing. For the twin-screw wet granulation with ibuprofen suspension feed, the ibuprofen concentration in the suspensions ranged between 30 to 53 % w/w, in order to achieve L/S ratios between 1.4 and 0.5 respectively. The solutions and suspensions were stirred constantly to ensure a uniform liquid using either a magnetic stirrer or an overhead stirrer equipped with a

four-blade agitator. Produced batch sizes ranged between 0.6 and 1.0 kg, depending on the ibuprofen concentration in the suspension.

Preparation of processable lumefantrine suspensions

Lumefantrine was sieved manually through a 1 mm mesh. Polysorbate 80 was dissolved in the granulation liquid to aid lumefantrine wetting and to obtain a suspension. After that, lumefantrine was added in small portions (approximately 25 g every 5 minutes) until the targeted suspension concentration was achieved. For investigating the in-barrel-drying process setup, the drug load in the suspension was 35 % w/w. For all other experiments with a lumefantrine suspension, the drug load in the suspension was 25 % w/w. The suspension was manufactured in batch sizes of 400 g. To ensure a homogeneous solution or suspension, the liquid was stirred constantly using a magnetic stirrer.

2.2.1.3 Twin-screw wet granulation

Twin-screw wet granulation was performed using a co-rotating Pharma 11 mm TSG (Thermo Scientific Pharma 11 Twin-screw Extruder, Thermo Fisher Scientific, Karlsruhe, Germany). The TSG was equipped with screws (screw diameter (D): 11 mm; screw length: $40 \frac{3}{4} D$) in the configuration 1 D conveying element (CE), 4 D long helix CE, 18 D CE, 1 $\frac{1}{2} D$ kneading elements at 60° staggering angle, 1 D CE, 1 $\frac{1}{4} D$ kneading elements at 30° staggering angle, 10 D CE and 4 D distributive flow elements (Figure 3). To minimise the amount of large lumps, the kneading zones were separated by a conveying element (92). The solids blend was fed in barrel zone 1 using a Brabender gravimetric feeder (DDW-MD0-MT-1, Brabender, Duisburg, Germany). The granulation liquid was fed at different positions in the twin-screw wet granulation. For L/S ratios below 0.15, the liquid was fed using a syringe pump PHD 4400 (Harvard Apparatus, Holliston, USA). For L/S ratios above 0.15, either a progressing cavity pump NM003BY11S12B (Netzsch, Selb, Germany) or an HPLC pump Smartline pump 100 (Knauer, Berlin, Germany) was used.

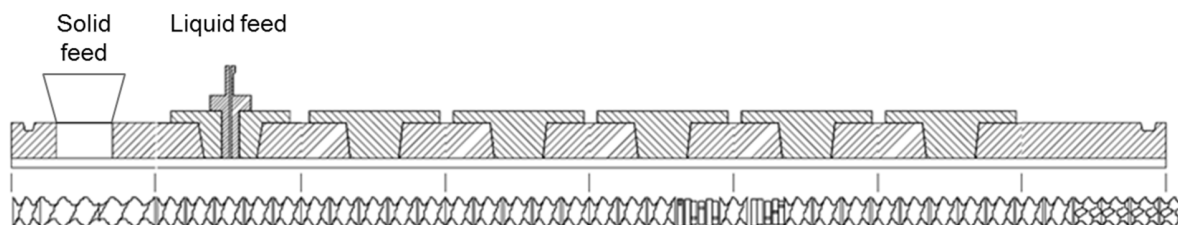


Figure 3: The screw configuration. In this example, the solid feed port is installed in barrel zone 1 and the liquid feed port in barrel zone 2. The setting of those ports may vary between experiments.

Formulation screening and investigation on ibuprofen suspension feed

The investigation was performed, using ibuprofen as a model drug substance. An overview of the experimental setup is given in Figure 4 and 5. Twin-screw wet granulation was performed in triplicate over 20 to 25 minutes. The screw speed was kept constant at 250 rpm. The solid mass flow rate was set to 500 g/h, independent whether the ibuprofen was dosed with the blend or as suspension (i.e. solids processed via the dry blend plus solids processed via the granulation liquid were equal to 500 g/h). The processed amount of water has been adapted, in order to obtain granules manufactured at different L/S ratios between 0.1 and 3.2. For the formulation screening, the liquid was fed to barrel zone 5, whereas for the investigation of ibuprofen suspension feed it was fed to barrel zone 2. The barrel zone temperature was kept constant at 20 °C. Cooling water was supplied at 7 °C temperature by a chiller (Unichiller 320Tw, Huber, Offenburg, Germany). Before experiments were started, the granulator was tempered until the barrel zone temperature stabilised. After 10 minutes processing time the wet granule mass flow was monitored over a further 10 minutes while granules were collected on a dynamic balance (K-Sampler K-SFS-24, Coperion, Stuttgart, Germany). The variation in the wet granule mass flow was determined by calculating the relative standard deviation of the five seconds mass intervals over a period of 10 minutes. Finally, the applied L/S ratio was verified by measuring the product LOD using a moisture analyser (HS153, Mettler Toledo, Greifensee, Switzerland). For the formulation screening, the residual water content was verified before the wet granule mass flow was monitored, whereas for the investigation on ibuprofen suspension feed it was measured thereafter. The sample (5 - 6 g) was dried at 105 °C temperature, until the loss in weight was less than 1 mg over 50 seconds. The collected wet granules were further processed in a fluidised-bed drying unit operation in a batch size of approximately 120 g. For one experimental setup, wet granules from the same batch (L/S ratio 0.7) were dried additionally in an oven (Thermo Scientific Heratherm, Thermo Fisher Scientific, Karlsruhe, Germany) for 20 hours at 60 °C temperature. A comparable batch size was taken of approximately 120 g.

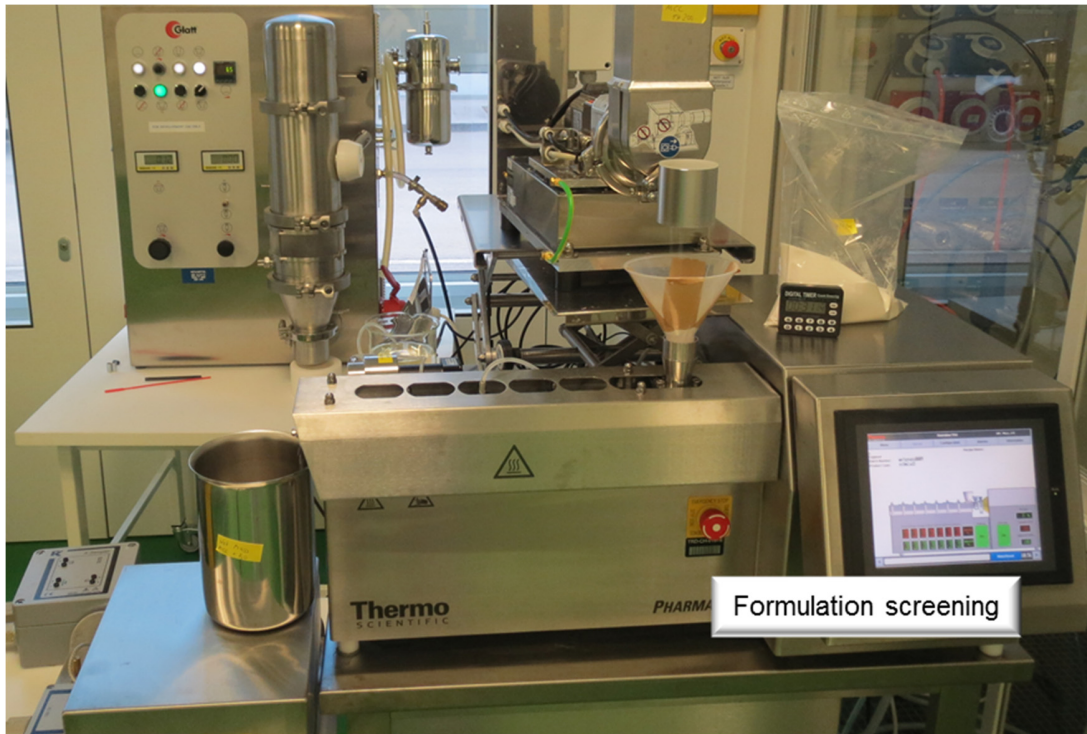


Figure 4: Process setup for the formulation screening to enable API suspension feed. The wet granules from the TSG Pharma 11 were collected on a dynamic balance and then dried in a Mini-Glatt fluidised-bed dryer.



Figure 5: Process setup for the comparison of twin-screw wet granulation with API suspension feed and API dry blend feed. The solid (API blend or excipients blend) was fed using a twin-screw loss-in-weight powder feeder. The liquid (API suspension, suspending agent solution, or pure water) was fed using a progressing cavity pump.

Investigating in-barrel-drying

Process setup

For the in-barrel-drying, a robust setup for venting was investigated. Only for experiments of the process setup for in-barrel-drying, the Pharma 11 mm TSG was equipped with 2 screws in the simplified configuration: 1 D CE, ¼ D kneading element, 2 D long helix CE, ¼ D kneading element, 2 D long helix CE, ¼ D kneading element and 35 D CE. The screw speed was 250 rpm. Only a liquid was fed. A 35 % w/w lumefantrine suspension was injected in barrel zone 1 at liquid mass flow rates between 200 and 800 g/h (L/S ratio 1.8). In the following 3 barrel zones (2 to 4), the barrel zone temperature was set to 200 °C. In those barrel zones, it was targeted to evaporate water and to discharge the moisture sufficiently. The temperature of the other barrel zones (5 to 8) was kept at 20 °C. Whenever the temperature profile was changed, it was waited until the heating performance stabilised. For venting, either degassing vent ports were used or the port was kept open (no port attached to it). Another setup that was tested for lumefantrine, was investigating if sufficient venting could be achieved by using closed barrel zone ports and by moving the evaporation zone towards the natural opening at the end of the TSG (barrel zones 6 to 8). Therefore, the temperature profile was changed. Instead of heating barrel zones 2 to 4, the barrel zones 6 to 8 were heated. Other parameters were kept the same as described above.

Another set of experiments was performed with MCC. The solid was fed constantly at a feed rate of 250 g/h in barrel zone 1. Water was fed to barrel zone 2 at various feed rates, in order to achieve L/S ratios in a range between 0.6 and 3.6. As for lumefantrine, in the following 3 barrel zones (3 to 5) water evaporation was targeted. The barrel zone temperature in the evaporation zone was 150 °C. For the other barrel zones the temperature was 20 °C. For venting, either a degassing vent port, a liquid feed port without nozzle or no port at all was used in the particular barrel zones. In another experimental setting, the use of degassing vent ports was fixed and the screw elements in the zone of water evaporation and moisture discharge were exchanged. Instead of CE, long helix conveying elements were used. Another type of screw element, the wide throat elements, were tested on a Pharma 16 mm TSG (Thermo Scientific Pharma 16 Twin-screw Extruder, Thermo Fisher Scientific, Karlsruhe, Germany) since such elements were not available for the Pharma 11. The screws (D: 16 mm; screw length: 53 ¼ D) were equipped with 47 D CE, 2 D long helix CE, ¼ D kneading element and 4 D wide throat elements in the barrel zone 6. One degassing vent port was installed in barrel zone 6. The screw speed was set to 250 rpm. MCC was fed constantly at 700 g/h to barrel zone 1. Water was added in barrel zone 2 (L/S ratios between 0.7 - 1.6). Barrel zones 3 to 5 were set to 20 °C barrel temperature, whereas barrel zones 6 to 8 were operated at temperatures up to 100 °C.

Characterisation of in-barrel-drying

The investigation of in-barrel-drying was performed on the Pharma 11 mm TSG using lumefantrine as a model drug substance. In-barrel-drying was performed over a process run time of 20 minutes. The granulation liquid was added to barrel zone 2. The TSG was divided into two different temperature zones. One temperature zone included barrel zones 2 to 5 and was defined as “pre-heating” zone. The other temperature zone included barrel zones 6 to 8 and was defined as “evaporation” zone. Barrel zone 1 could not be controlled in temperature. Temperature settings were investigated in the range of 20 - 110 °C (pre-heating zone) and 160 - 220 °C (evaporation zone). At start-up and whenever temperature settings were changed, the TSG was equilibrated until the heating performance stabilised and for at least 45 minutes before experiments were started. For cooling of the barrels, a chiller (Thermo Scientific NesLab Thermoflex 1400, Thermo Fisher Scientific, Karlsruhe, Germany) was used, supplying the TSG with water at 15 °C. Other process parameters were investigated in the range 240 to 610 g/h (total material mass flow rate), 0.5 to 1.0 (L/S ratio) and 40 to 350 rpm (screw speed). Throughout the process, all process parameters were monitored using the data logging software provided by Thermo Fisher. After 20 minutes process run time, the product temperature was assessed using a contact thermometer (Thermocouple Traceable®, VWR, Radnor, USA). The product temperature was measured on granules at different spots, directly after the material exited the TSG. Only the highest product temperature was taken into account for further evaluation, since it is the most critical in terms of potential degradation. At the time point 17 to 20 minutes, granules were collected for LOD analysis. After LOD analysis, the dried granules were taken for determining the particle size distribution.

Comparison in-barrel-drying and fluidised-bed drying

For in-barrel-drying, the parameters were set as follows: the total material mass flow rate was 360 g/h, the L/S ratio was 0.6, the screw speed was 50 rpm, the pre-heating zone temperature was 100 °C and the evaporation zone temperature was 215 °C. If needed, the screw speed was adapted within narrow ranges (+ 7 / - 5 rpm). The screw speed was adapted to control the product LOD in narrow ranges, while keeping the product temperature below the melting point of lumefantrine (128 °C). The process was operated for 140 minutes to collect a sufficient amount of granules for the following compaction unit operation. Granules were collected from 20 minutes onwards. Granules were collected to verify the product LOD at time points 20, 50, 80, 110 and 140 minutes. At least every 10 minutes, the product temperature was measured.

For fluidised-bed drying, the total material mass flow rate and the L/S ratio were kept constant. The screw speed was 47 rpm and all barrel zones were kept at constant temperature of 20 °C. The process was operated for 140 minutes. Granules were collected between 20 to 140 minutes process run time. At time points 20 and 140 minutes, granules were collected to verify the applied L/S ratio via measurements of the product LOD. Granules from 20 to 50 minutes, 50 to 80 minutes, 80 to 110 minutes and 110 to 140

minutes were defined as sub-batch and dried using a fluidised-bed dryer (Mini-Glatt 5, Glatt, Binzen, Germany).

2.2.1.4 Fluidised-bed drying

Wet granules were dried using a fluidised-bed dryer (Mini-Glatt 5, Glatt, Binzen, Germany) at an inlet air temperature of 65 °C. The inlet air temperature was selected below the melting point of ibuprofen and fixed for all other experiments, in order to exclude any material degradation towards low residual moisture and hence high product temperature. The fluidised-bed dryer was initially pre-heated at an air flow of 0.1 bar for at least 1 hour. The exhaust air temperature stabilised around 40 °C. Material was loaded into the equipment and the air flow was increased until proper fluidisation of the powder bed was observed (range was adjusted such that the pressure drop was between 0.1 - 1.0 bar). For coarse granules (typically produced at high L/S ratios), the air flow was decreased during drying, since the required air flow level for powder fluidisation was decreasing with the evaporation of moisture. The filters were unclogged every 5 seconds using compressed air. When the exhaust air temperature reached values around 40 °C, the drying process was interrupted and the product LOD was checked. If the product LOD of the granules was comparable to the LOD of the original powder blend, the drying was stopped. If not, drying was continued. The drying time varied between 8 and 49 minutes. Before the material was discharged from the dryer, the filters were unclogged every second over 1 minute, in order to collect most of the fines. Since the focus was on twin-screw wet granulation, the fluidised-bed drying process was not optimised and kept constant at the listed parameters.

2.2.1.5 Compaction

Before compaction, dried granules were sieved manually (1 mm mesh). The compacts were manufactured on a fully instrumented compaction simulator (Stylcam® 200R, Medelpharm, Beynost, France) to mimic a Fette P1200. A gravimetric feed shoe was used. Displacement and pressure gauges for upper and lower punch enabled the evaluation of force-displacement-curves. 500 mg round flat face compacts with a diameter of 11.28 mm were manufactured. A dwell time of 13 ms was applied constantly. For ibuprofen granules, compacts were manufactured at compaction pressures of 60, 100 or 140 MPa, 3 (for formulation screening) or 10 (for investigating ibuprofen suspension feed) compacts each. The compacts were directly analysed for dimensions and breaking force. Another 32 compacts were manufactured at 100 MPa for evaluating other compact properties (friability, disintegration time and dissolution rate). For lumefantrine granules, compacts were manufactured at compaction pressures of 50, 100, 150, 200, 250 or 300 MPa, 10 compacts each. The compacts were directly analysed for dimensions

and breaking force. Another 25 compacts were manufactured at 100 MPa for evaluating other compact properties (friability and disintegration time).

2.2.2 Analytical methods

2.2.2.1 Particle size distribution of powders and granules

The particle size distribution was measured using dynamic image analysis. Therefore, a Camsizer XT (Camsizer XT, Retsch Technology, Haan, Germany) was used. The Camsizer was equipped with an X-Jet module. The air dispersion pressure was set to 30 kPa to de-agglomerate powder particles without destroying granules. The dispersed particles pass in front of two LED light sources and the shadows are captured by 2 digital cameras. The basic camera detects coarse particles, whereas the zoom camera is optimised to detect small particles. In a small measuring window the optical paths of both cameras intersect and the particle size distribution is analysed. Various parameters (e.g. Feret/Martin diameter, various widths and lengths, sphericity) can be calculated to evaluate the particle size. The smallest of all maximum chord lengths of the particle projections ($x_{c \min}$) was used to calculate the particle size. For further evaluation, the particle size descriptor x_{50} was used, which corresponds to 50 % of the particles smaller than the given size with respect to their volume.

2.2.2.2 Helium density of granules (true density)

The true density was determined from granule samples that were stored in a desiccator at room temperature and a relative humidity of 43 ± 1 % (saturated potassium carbonate solution) for approximately 48 hours, using a helium pycnometer (AccuPyc 1340 V2.0, Micromeritics, Norcross, USA). The measurements were conducted in triplicate (5 purging runs, 34.5 Pa/min equilibration rate, 2 g sample size).

2.2.2.3 Bulk and tapped density

The bulk and tapped density were measured, using a 250 ml measuring cylinder (graduated to 2 ml) and a tapped density tester (STAV 2003, J.Engelsmann, Ludwigshafen, Germany). For ibuprofen granules, the bulk and tapped density were evaluated based on an initial untapped sample volume of 100 ml. For lumefantrine granules, the bulk and tapped density were evaluated according to the Pharmacopoeia Europaea (Ph.Eur.) 2.9.34. (111), based on a sample size of 100 g. If the powder density was too low, a smaller sample size was used, such that the untapped volume was in between 150 and 250 ml. For the

tapped density, the powder sample was tapped 500 and 1250 times and the volume was read (V_{500} and V_{1250}). If the difference between V_{500} and V_{1250} exceeded 2 ml, another 1250 taps were carried out. The difference between V_{1250} and V_{2500} was then observed less than or equal to 2 ml. The tapped density was calculated using either the V_{1250} or the V_{2500} . The Hausner ratio was calculated by dividing the tapped density by the bulk density.

2.2.2.4 Scanning electron microscopy

Samples from granule batches were gold sputtered using a high vacuum coater (Leica EN ACE600, Leica Microsystems, Wetzlar, Germany), until a layer thickness of approximately 8 nm was achieved. Images were taken under vacuum conditions (operating voltage 6 to 8 kV; magnification 25 to 100 times; working distance 6 to 28 mm) using a scanning electron microscope (SUPRA 40, Carl Zeiss, Oberkochen, Germany).

2.2.2.5 Compact porosity

The compact porosity (in all experiments the out-of-die porosity was used) was calculated from the thickness, diameter and mass of the compact, as well as the true density of the former granules. Compact thickness and diameter were measured, using a calliper (Traceable®, VWR, Radnor, USA). For ibuprofen compacts, the compact thickness and diameter were measured on 3 compacts immediately after compaction. For lumefantrine compacts, the compact thickness of 10 compacts immediately after compaction was used together with the punch diameter.

2.2.2.6 Tensile strength

The breaking force was measured immediately after the compaction and after dimensions were determined, using a hardness tester (Pharmatron MultiTest 50, Pharmatron, Thun, Switzerland). The tensile strength was then calculated, using the breaking force, the compact thickness and the diameter of the compact (Equation 1) (112). For ibuprofen compacts the tensile strength was measured for 3 compacts, whereas for lumefantrine compacts 10 measures were taken.

$$\text{Tensile strength} = \frac{2 \times F}{\pi \times d \times t}$$

Equation 1: Calculating the tensile strength [MPa] from the breaking force [N] (F), the compact thickness [mm] (t) and the diameter [mm] (d) of the compact.

2.2.2.7 Friability

The friability was measured from compacts manufactured at 100 MPa, using an abrasion and friability tester (AE-1, Charles Ischi, Zuchwil, Switzerland). The measurement was performed as described in the Ph.Eur. 2.9.7 (111).

2.2.2.8 Disintegration time

The disintegration time was measured from compacts manufactured at 100 MPa, using a disintegration tester (Pharmatron DisiTest 50, Pharmatron, Thun, Switzerland). The test was performed as described in the Ph. Eur. 2.9.1 for test apparatus A (111). The immersion fluid was demineralised water, which was tempered to 37 ± 0.5 °C. For ibuprofen compacts, the disintegration time was determined from 3 compacts and for lumefantrine compacts it was measured from 6 compacts.

2.2.2.9 Dissolution rate of ibuprofen compacts

The dissolution rate was measured from compacts manufactured at 100 MPa, using a dissolution tester (AT7 Smart double bath, Sotax, Aesch, Switzerland). The measurement was performed for 3 compacts and according to the USP dissolution test method for ibuprofen tablets (113). A paddle apparatus has been used. After 60 min, the paddle speed was increased from 50 to 200 rpm and after 75 min, a final measurement cycle was performed. During a measurement cycle the media was pumped from the dissolution vessel to an in-line UV-spectrometer (Lambda 25, PerkinElmer instruments, Schwerzenbach, Switzerland) and back again to the vessel. UV-measurements were performed at a wavelength of 222 nm using a 1 mm measuring cell.

2.2.2.10 Wettability of ibuprofen powder blends

The powder wettability was measured using the sorption method and a force tensiometer (K100 Mk2, Krüss, Hamburg, Germany). 1.0 g of powder was weighed into a small glass cylinder, which was covered with a filter on one side. The powder was tapped manually (approximately 200 times) always to a comparable volume of 2.2 ml, to achieve a comparable powder density across the samples (approximately 0.45 g/ml). The cylinder was then attached to the microbalance of the equipment and brought automatically in contact with the test liquid (speed to raise the platform with the liquid: 6 mm/min; surface detection: 0.01 g). The increase in mass by liquid sorption was measured over time. Basically, this method uses the Washburn equation to calculate the contact angle. However, for this setting the

sorption kinetics of two ibuprofen powder blends in two liquids were compared. The wettability was tested for an ibuprofen powder blend comprising sodium pyrophosphate in the test liquid water and compared against an ibuprofen powder blend without sodium pyrophosphate in a 3.4 % w/w sodium pyrophosphate solution. A faster increase of the mass over time typically indicates better wettability.

2.2.2.11 Dissolved amount of Ibuprofen

The dissolved amount of ibuprofen was determined for two solutions of sodium pyrophosphate (1.60 % w/w and 3.36 % w/w) and for two solutions of polysorbate 80 (0.32 % w/w and 0.34×10^{-3} % w/w). 25 g of liquid was stirred using a magnetic stirrer bar during the addition of 10 g ibuprofen. The suspension was filtered after 1, 5 and 10 minutes. The ibuprofen content was measured from the filtrates using a UV-spectrometer (Lambda 25, PerkinElmer instruments, Schwerzenbach, Switzerland). UV-measurements were performed at a wavelength of 222 nm using a 1 mm measuring cell.

2.2.2.12 Design of experiments

For the in-barrel-drying process, firstly, a screening DOE was performed. 5 factors were selected, namely the total material mass flow rate, the L/S ratio, the screw speed and the temperatures in the pre-heating and in the evaporation barrel zones. Factors were coded as -1 (lower level), 0 (centre point level) and +1 (upper level). A 29-run fractional factorial three-level central composite face-centred design (2^{5-1}) has been selected in order to get access to main, interaction and quadratic effects (Figure 6a). Following factor ranges were investigated: 240 to 500 g/h (total material mass flow rate), 0.6 to 1.0 (L/S ratio), 50 to 350 rpm (screw speed), 20 to 100 °C (pre-heating zone temperature) and 160 to 200 °C (evaporation zone temperature).

Secondly, an optimisation DOE was performed. The basic modelling of quadratic effects based on 3 factor levels from the central composite face-centred design was found to be insufficient. Therefore, a 31-run fractional factorial central composite circumscribed design (2^{5-1}) has been selected (Figure 6b). For such a design, the star points are located outside the definition of the factor range. Thereby the model estimates quadratic effects based on 5 levels. The design included an additional single experiment in the corner of highest temperatures in the barrel zones and lowest screw speed, total material mass flow rate and L/S ratio. Following factor ranges were investigated: 360 to 560 g/h (total material mass flow rate), 0.6 to 0.8 (L/S ratio), 50 to 100 rpm (screw speed), 60 to 100 °C (pre-heating zone temperature) and 205 to 215 °C (evaporation zone temperature).

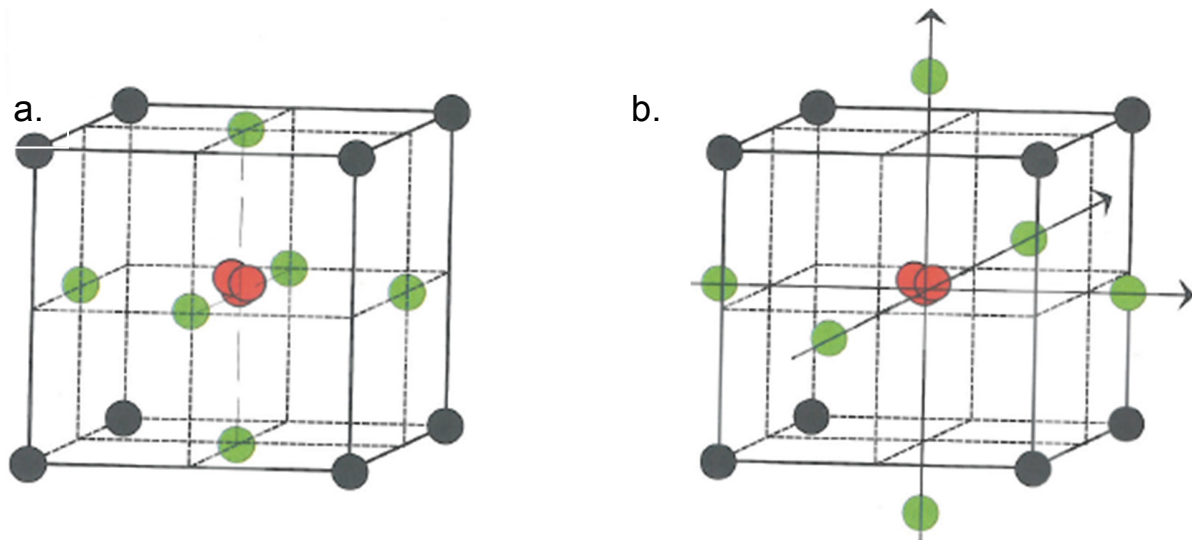


Figure 6: (a) Central composite face-centred design in three factors. (b) Central composite circumscribed design in three factors.

The product LOD, the evaporated mass of water (= introduced amount of water by solid and liquid feed minus residual amount of water in the product), the drying efficiency (= evaporated amount of water divided by introduced amount of water by liquid feed), the product temperature and the granule size x_{50} were evaluated as process responses. Initially, every potential term was included in the model for the evaluation of the single responses (Equation 2).

$$\text{Response (y)} = \beta_0 + \beta_1 x_1 + \beta_2 x_2 + \beta_3 x_3 + \beta_4 x_4 + \beta_5 x_5 + \beta_{12} x_1 x_2 + \beta_{13} x_1 x_3 + \beta_{14} x_1 x_4 + \beta_{15} x_1 x_5 + \beta_{23} x_2 x_3 + \beta_{24} x_2 x_4 + \beta_{25} x_2 x_5 + \beta_{34} x_3 x_4 + \beta_{45} x_4 x_5 + \beta_{11} x_1^2 + \beta_{22} x_2^2 + \beta_{33} x_3^2 + \beta_{44} x_4^2 + \beta_{55} x_5^2 + \varepsilon$$

Equation 2: Model equation where y is the response, β_0 is the constant term, x_i are the factors (in this example 5 factors), β_i are the model parameters and ε is the residual response variation.

A model was fitted using multiple linear regression. The response distribution was checked and it was determined if data transformation was needed. Using backward regression of non-significant terms, the model was refined. All models were checked for model quality based on 4 quality parameters: goodness of fit (R^2), goodness of prediction (Q^2), model validity and reproducibility. The R^2 represents how well the model explains the obtained response variation. The Q^2 estimates the predictive power of the model. The model validity and the reproducibility give a measure for the lack of fit of the model and the pure error. The best model quality is represented by the value 1. However, the acceptance criteria for the model were set to R^2 and Q^2 higher than 0.5 and the difference between the two smaller than 0.2 - 0.3. The model validity must be higher than 0.25 to indicate a sufficiently low model error. The p-value was set to 0.05. The acceptance criterion for the reproducibility was set higher than 0.5. The values of the

Materials and Methods

coefficients in the coefficient plots were scaled and centred, whereas values of the coefficients in pareto plots were normalised over all process responses.

Experiments were designed and evaluated using the DOE software MODDE (version 11.0.1, Sartorius, Aubagne, France).

3 RESULTS AND DISCUSSION

3.1 Considerations to enable API suspension feed in twin-screw wet granulation

3.1.1 Background and objectives

The L/S ratio is a crucial process parameter in twin-screw wet granulation, since it significantly impacts the granulation behaviour of the formulation. The granulation behaviour can roughly be divided into different stages, depending on the L/S ratio:

- At low L/S ratios, particles remain as a dry and free-flowing powder,
- At slightly higher L/S ratios, nuclei are formed,
- At medium L/S ratios, particles will grow steadily,
- At high L/S ratios, the material is over-wetted and a paste is formed (90, 114).

It is furthermore highly dependent on the formulation/composition at what specific L/S ratio, which granulation behaviour can be observed (115). Since the L/S ratio is fixed for the API suspension feed in twin-screw wet granulation, the composition of the formulation was used to control the granulation behaviour.

Therefore, the objectives were to define:

- which ibuprofen concentrations could be processed in a suspension.
- the L/S ratio in twin-screw wet granulation with API suspension feed that has to be processed, based on the suspension composition and a targeted drug load in the final formulation.
- which excipients formulation would show suitable granulation behaviour with the expected L/S ratio in twin-screw wet granulation.

3.1.2 Screening of API suspensions

In order to assess which ibuprofen concentrations could be processed in a suspension, first a suitable pump was selected and various suspensions were assessed for their processability. Broadly, two types of pumps, namely the progressing cavity and the centrifugal pump, are considered suitable for pumping of suspensions (116). The centrifugal pump consists of two parts, the housing and the rotating impeller (Figure 7a). The pump uses the rotating impeller to increase centrifugal forces to the liquid to induce flow (117). Thereby the centrifugal pump is a rotodynamic pump. The progressing cavity pump (also called single-screw pump or Moineau pump) is a positive displacement pump. It consists of a helix-shaped screw (rotor) located in a double-threaded rubber stator housing (Figure 7b) (116). As the screw rotates within the stator, the liquid is displaced along the length of the pump.

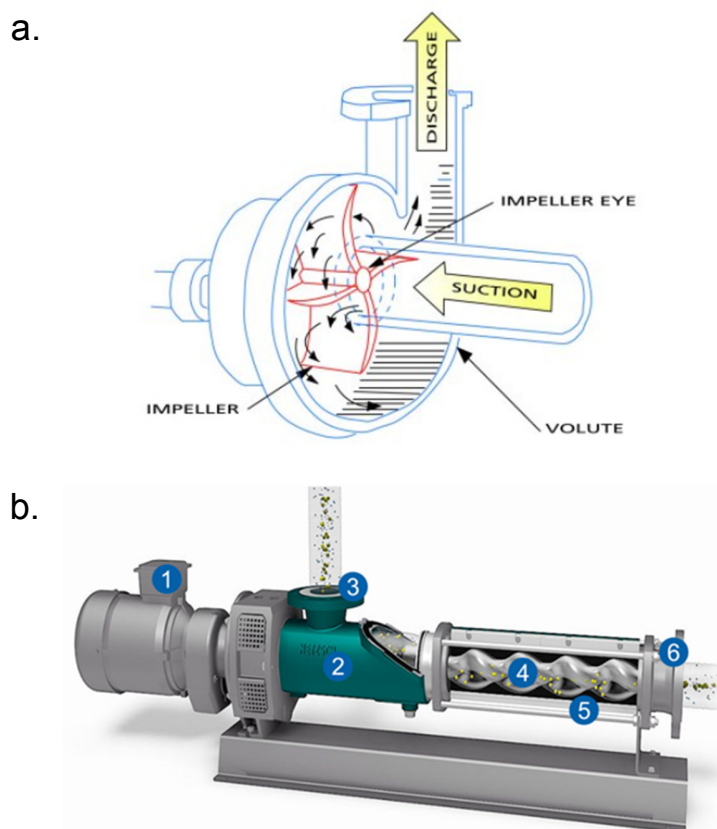


Figure 7: (a) Components of a centrifugal pump (118); (b) Components of the Nemo® progressing cavity pump with particular modifications for API suspension feed: 1. Frequency inverter, 2. Sucking chamber with stirring elements on the drive, 3. Inlet (sucking side), 4. Rotor, 5. Stator, 6. Outlet (pressure side) (119).

Both pump systems provide a continuous, low pulsation flow of the suspension, which is desirable to ensure good liquid (and API) distribution in the wet granulation. However, there are considerable

Results and Discussion

differences. At a constant pump speed of a centrifugal pump, the pump efficiency and the pressure the pump can supply to the liquid decrease with an increase in the solid load of the suspension (116, 120). Moreover, from a practical point of view, centrifugal pumps are typically operated in flow ranges of kilograms per minute, whereas for this study 100 - 1500 g/h were targeted. At a constant pump speed of a progressing cavity pump, the pump efficiency and the pressure are relatively constant and initially even increase with increasing suspension concentrations. By using a frequency inverter, the selected pump could also be operated within the targeted liquid flow ranges. Therefore, a progressing cavity pump has been selected for this study to process suspensions (Figure 8).



Figure 8: Setup of the progressing cavity pump.

Since suspensions are rather complex systems, extensive data of the pump process is required to exclude potential deviations in the pump performance due to suspension flow at different solid concentration (116). For example, the aqueous mixture could change its flow behaviour from Newtonian to non-Newtonian behaviour, if the solid concentration exceeds a threshold (i.e. the viscosity is not constant anymore upon changing time and/or shear rate) (121). Upon increasing suspension concentrations, the viscosity typically increases (122, 123). Thereby, a higher pressure is required to convey the suspension in a pipeline (e.g. due to friction losses) (124). Thus it could happen, that upon a certain solid load (and viscosity) the pump might not be capable anymore to convey the liquid (116, 120). However, too low viscous liquids could be of disadvantage too. According to Stokes' law, the settling velocity of suspended solid particles is impacted among other parameters (particle/fluid mass density or particle size), also by the viscosity (Equation 3) (125). Therefore, a rapid settling of solid particles could be the result of a too low viscosity suspension. As a consequence, a solid layer could build up on the bottom of a pipeline, if the suspension is not mixed steadily and/or the velocity in the pipeline is too low.

Results and Discussion

Thus, a blockage of the pipe could be obtained. Hence, it is meaningful to find a good balance between the concentration and the handling of the suspension in flow.

$$v = \frac{2 (\rho_p - \rho_f) \times g \times r^2}{9 \times \mu}$$

Equation 3: Calculating the settling velocity according to Stokes' law; v = settling velocity of spheres in a fluid [m/s]; ρ_p = mass density of the solid particles [kg/m³]; ρ_f = mass density of the fluid [kg/m³]; g = gravitational acceleration [m/s²]; r = particle radius [m]; μ = dynamic viscosity [Pa × s].

In order to minimise the amount of water that needs to be processed, it was tested which maximum ibuprofen suspension concentration could be processed (e.g. with regards to viscosity) (upper process window boundary). In order to enhance also the flexibility and the applicability of API suspension feed in twin-screw wet granulation, ibuprofen suspension concentrations down to 30 % w/w were further investigated for their processability (e.g. with regards to settling). Lower ibuprofen concentrations were not tested, since the water amount that would need to be processed in the granulation would get unreasonable high (lower process window boundary). Thereby, a process window for ibuprofen suspensions was set up (details on the used methodology are listed in section 2.2.1.2 (screening of API suspensions and preparation of the granulation liquid)).

In a first step, the ibuprofen had to be suspended in the liquid. It is well-known that ibuprofen has a low solubility in water (approximately 0.06 mg/ml) and is poorly wettable in addition (126). Even by applying intensive stirring, it was not possible to suspend the ibuprofen in water. Therefore, a suspending agent, either sodium pyrophosphate or polysorbate 80, was dissolved in the suspending liquid (35). The sodium pyrophosphate supports the dispersing of powder particles by electrostatic interactions, whereas polysorbate 80 provides steric stabilisation of the suspension. After adding the suspending agent, ibuprofen was successfully suspended in the liquid.

In a second step, the ibuprofen concentration in the suspension was increased slowly. Upon a certain concentration, the change in fluidity of the suspension could be observed visually. Whereas an ibuprofen suspension of 55 % w/w could still be stirred by using a magnetic stirrer and formed a vortex while stirring, higher ibuprofen suspension concentrations required a mechanical stirrer and showed material build-up around the stirrer (Figure 9). This observation can be explained by increasing particle-particle interactions between dispersed ibuprofen particles with increasing solid load and agrees well with what is described in literature (127). Furthermore, it was observed that this visual finding matched well with the experienced processability of those suspensions in the pumping process. While ibuprofen suspensions up to 55 % w/w were conveyed reliably, the pumping of higher concentrated suspensions failed since material was not sucked into the pump anymore. Hence, an estimate for the highest processable ibuprofen load in suspension was found at 55 % w/w. To make up for unexpected process variations

Results and Discussion

(safety buffer) and to increase thereby the reliability of the ibuprofen suspension feed in twin-screw wet granulation, for this study a maximum ibuprofen load of 53 % w/w was used in the suspension.

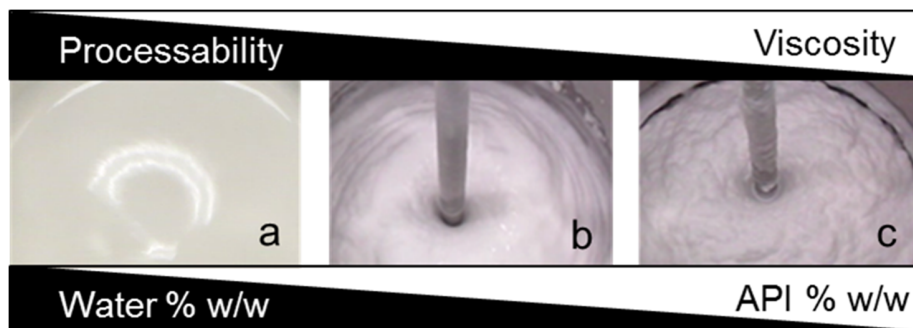


Figure 9: Visual inspection of ibuprofen suspensions of (a) 55.0 % w/w; (b) 57.5 % w/w; (c) 60.0 % w/w. Within a narrow range of ibuprofen suspension concentrations, the rheological behaviour of the suspension changed significantly and thereby its processability. Ibuprofen suspension concentrations above 55.0 % w/w could not be pumped.

Finally, lower concentrated ibuprofen suspensions were verified for their processability. It was shown that the liquid mass flow rate was comparable at similar pump speed for all investigated liquids (Figure 10). This agrees well with the described relatively low dependency of the progressing cavity pump on changing viscosities (118). Moreover, it was shown that the pump process was stable over a reasonable period of time for the later investigation of ibuprofen suspension feed in twin-screw wet granulation (Figure 11). Thus, effects of the suspension concentration on the pump performance can be excluded for ibuprofen concentrations between 30 to 53 % w/w.

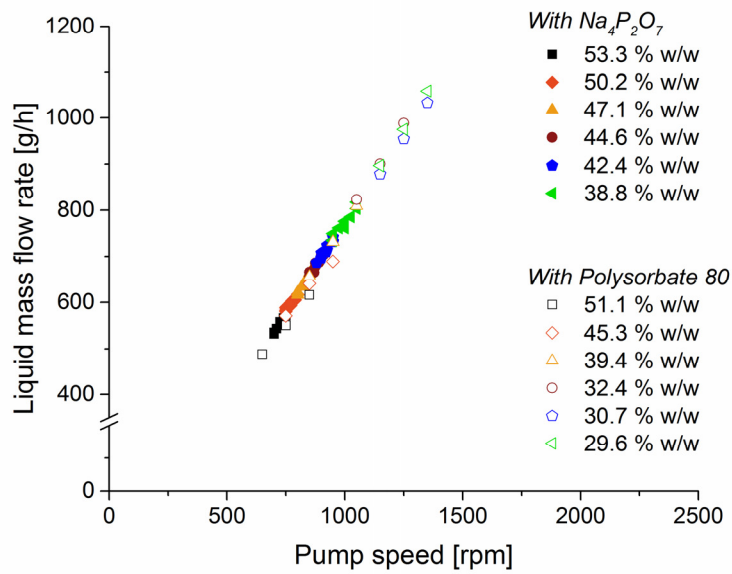


Figure 10: Pump calibrations of various ibuprofen suspensions at different concentration. (individual calibration points plotted)

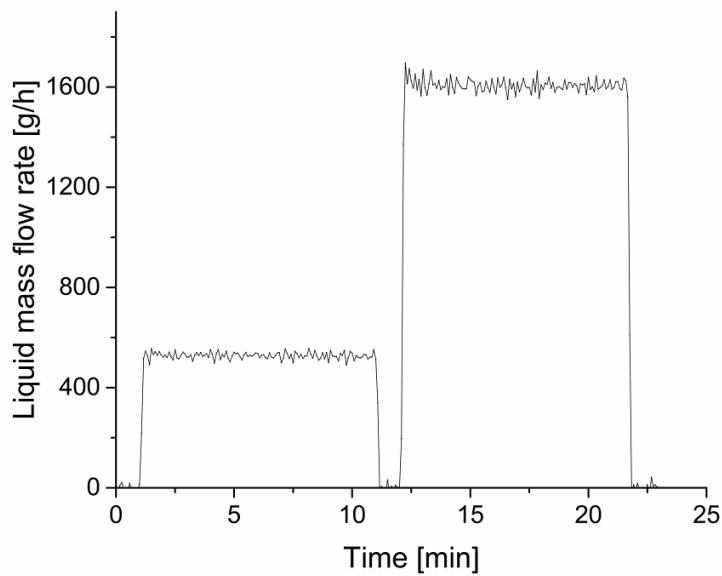


Figure 11: The liquid mass flow rate as function of time at two pump levels for a 50 % w/w ibuprofen suspension. (measurement frequency 0.2 Hz; individual experiment for illustration)

Results and Discussion

In order to define the L/S ratio in twin-screw wet granulation with API suspension feed, the amount of water was calculated that would need to be processed for the individual suspensions to achieve the targeted drug load. Since challenges for the API suspension feed in twin-screw wet granulation especially arise when it is concerned with high drug loads in the final formulation (leading to unreasonable high L/S ratios which burden the granulation and the subsequent drying step), those were focused on and investigated in this study. A drug load of 60 % w/w ibuprofen was targeted. The L/S ratio was determined (Equation 4). For the highest tested ibuprofen suspension concentration of 53.3 % w/w (including 2.2 % w/w Na₄P₂O₇), an expected L/S ratio of 0.50 was calculated for twin-screw wet granulation with API suspension feed (Equation 5). For the lowest tested ibuprofen suspension concentration of 29.6 % w/w (including 0.2 % w/w polysorbate 80), an expected L/S ratio of 1.40 was calculated (Equation 6). Hence, an L/S ratio process window for twin-screw wet granulation with ibuprofen suspension feed can be expected between 0.50 and 1.40.

$$\text{Expected L/S ratio} = L_S \times \frac{DS_P}{DS_S}$$

Equation 4: Calculating the expected L/S ratio in twin-screw wet granulation with API suspension feed for an individual API suspension and targeted drug load in the final formulation.; DS_P= mass fraction of the drug load in the final formulation; L_S= mass fraction of the liquid in the suspension; DS_S= mass fraction of the drug substance in the suspension.

$$\text{Lowest expected L/S ratio} = 0.44 \times \frac{0.60}{0.53} = 0.50$$

Equation 5: Calculation of the lowest expected L/S ratio in twin-screw wet granulation with ibuprofen suspension feed.

$$\text{Highest expected L/S ratio} = 0.70 \times \frac{0.60}{0.30} = 1.40$$

Equation 6: Calculation of the highest expected L/S ratio in twin-screw wet granulation with ibuprofen suspension feed.

3.1.3 Analytical method development for L/S ratio-dependent formulation screening

Parts of this section have been published in the research article “Quantitative Assessment of Mass Flow Boundaries in Continuous Twin-screw Granulation.”.

In order to define a suitable formulation to process the ibuprofen suspensions, two quantitative methods were developed to define the L/S ratio process window for twin-screw wet granulation. In traditional high-shear granulation, typically, such quantitative L/S ratio boundaries are determined directly or through indirect torque measurements. The impeller torque thereby correlates reasonably well with changes in the granule size distribution. However, in twin-screw wet granulation, such torque measurements often are not precise enough since the equipment is also designed for melt processes, which result in much higher torque. As result of this equipment design the measurement of low torques is not easily available and imprecise data would be obtained. That is why the operator typically still determines the L/S ratio boundaries and granule quality based on visual observation of the material behaviour in twin-screw wet granulation. The visual inspection is based on the observations no or insufficient granulation, steady granule growth and paste formation with increasing L/S ratio.

In order to study the required/tolerated L/S ratio in twin-screw wet granulation, several powder formulations were investigated (Table 1). Each formulation contained 60 % w/w of the model drug substance ibuprofen (targeted ibuprofen formulation load for the later study on ibuprofen suspension feed). Moreover, the formulation contained 2.5 % w/w polyvinylpyrrolidone K30 as a binder and 1.5 % w/w magnesium stearate as a lubricant. The other 36 % w/w was either lactose, MCC, Na-CMC, a mixture of lactose and MCC (1:1) or a mixture of MCC and Na-CMC (28:8) (Table 1). For the MCC-Na-CMC based mixture, Na-CMC was selected at lower concentration to reflect a realistic formulation for pharmaceutical formulation development. By changing the ‘filler’ (lactose, MCC, Na-CMC), the water uptake capacity of the formulation was changed intentionally, which was assumed to lead to different L/S ratio granulation windows. Lactose is well-known as brittle filler and is highly soluble in water. The water uptake capacity was therefore assumed to be rather small. MCC is a plastic filler, practically insoluble in water. It is known that particular amounts of water can be incorporated in the polymer structure of MCC. Na-CMC is typically used as a disintegrant. Due to its polycarboxymethylether-groups it can bind high amounts of water, which lead to a swelling and finally cause its disintegrating function. However, due to its high water uptake capacity, it was used as filler/disintegrant in this study. All formulations were granulated in twin-screw wet granulation with subsequent fluidised-bed drying. Various L/S ratios were applied to determine the granulation behaviour and the L/S ratio process window for twin-screw wet granulation. Details on the used methodology are listed in the sections 2.2.1.3 (in twin-screw wet granulation and in formulation screening and investigation on ibuprofen suspension feed), 2.2.1.4 (fluidised-bed drying) and in 2.2.2.1 (particle size distribution of powders and granules).

Results and Discussion

Visually, it was observed that these different formulations indeed require different L/S ratio boundaries for granulation (Figure 12). For example, in case of a lactose based formulation, the visual findings of no granulation, granule growth and paste formation were found within a relatively narrow range at low L/S ratios (i.e. small changes in the L/S ratio showed an immediate impact on the granulation). In case of an MCC based formulation, a higher L/S ratio was required to initiate granule growth. The granulation window was wider and thereby less sensitive to small changes in the L/S ratio. The Na-CMC based formulation showed the widest granulation window in this study at very high L/S ratios. This agrees well with the previously outlined presumption about the water uptake capacity of the single fillers. Although these results were expected and intuitive, they illustrate the need for a quantitative method to detect the granulation process boundaries.

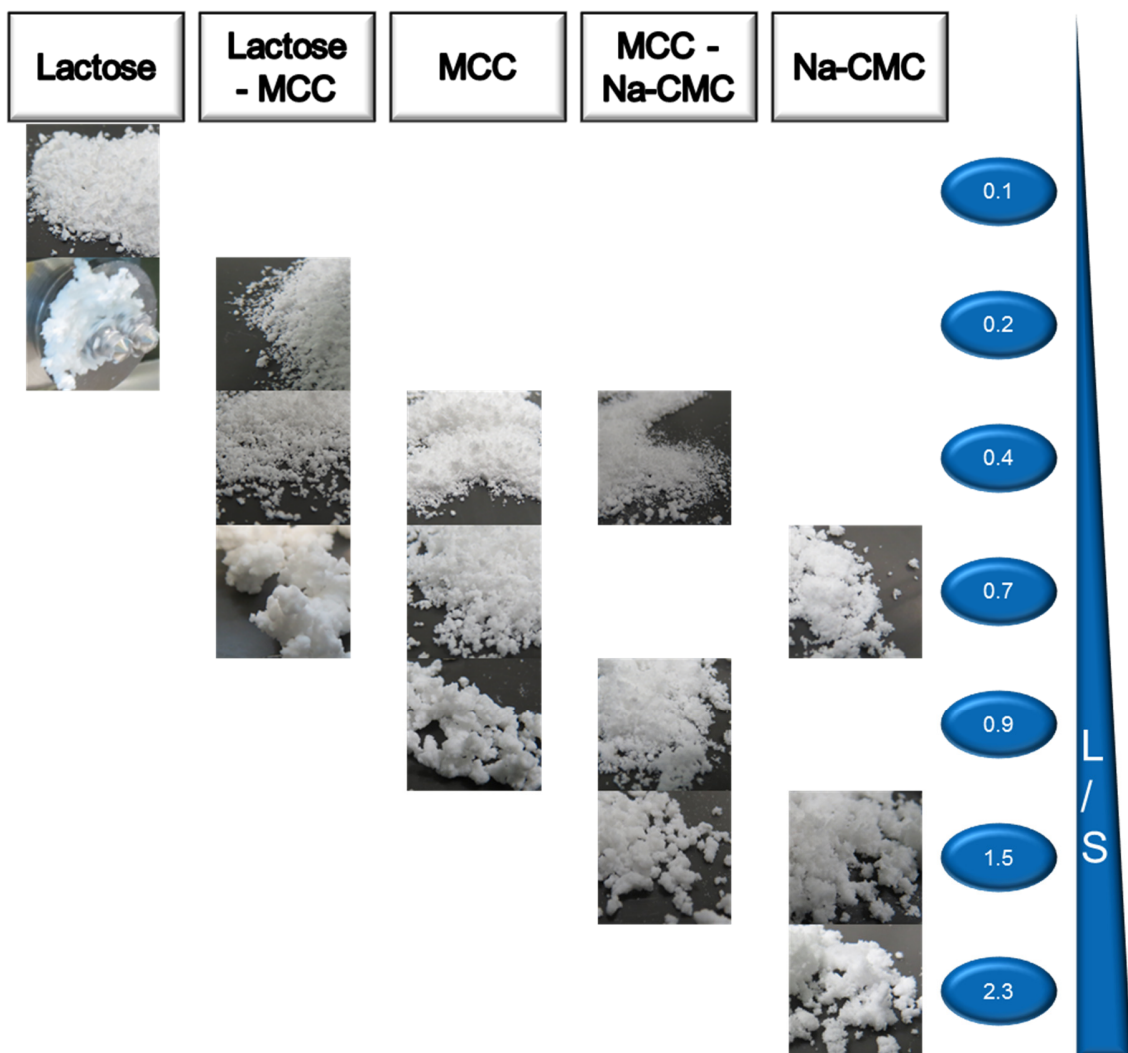


Figure 12: Visual observations of the twin-screw wet granulation behaviour of a lactose based, lactose-MCC based, MCC based, MCC-Na-CMC based and Na-CMC based ibuprofen formulation with increasing L/S ratios. Formulations showed no granulation, granule growth and formation of paste at and within different L/S ratio ranges.

Results and Discussion

Some authors have started to address this need for quantitative L/S ratio boundaries in wet granulation. In one study it is claimed that L/S ratio boundaries could be monitored by using NIR (115). It is assumed that added water distributes either inside of, or on the surface of the powder particles. Water on the surface of powders would then be detected immediately by a change in the NIR output signal. This change is stated as lower L/S ratio boundary. Another change in the NIR output signal is stated when powder particle surfaces are saturated and exceeding amounts of water are added (= upper L/S ratio boundary). Within the range between lower and upper L/S ratio, desirable granulation behaviour is claimed. However, the NIR output signal is rather complex and influenced by various attributes, such as particle size and shape, or density. This makes it complicated to attribute single effects from the spectra.

Therefore, two different quantitative methods were investigated for their applicability to detect the upper and lower L/S ratio boundary of the granulation window. A first method was based on the hypothesis that the mass flow of the material would significantly change at the TSG exit once the material is over-wetted and a paste is formed. A second method evaluates the onset of particle agglomeration by using the dried granule size. If sufficient water gets present on particle surfaces, a significant change in granule growth would be expected. Those two hypotheses were tested and are illustrated in the following for the MCC based formulation.

The upper L/S ratio boundary (the boundary towards over-wetted product) of the granulation window was assessed, by determining the mass flow variation of the wet granule mass as function of the L/S ratio at the TSG exit. The idea behind this method is based on the increasing fluctuation of the mass flow of over-wetted granules media due to increased lumping (Figure 13).

The wet granule mass flow variation represents the relative standard deviation of the 5 seconds mass intervals, monitored over a period of 10 minutes. A consistent wet granule mass flow was observed up to an L/S ratio where the onset of over-wetting was found (Figure 13). Above this L/S ratio, material started to stick and to accumulate on metal surfaces of the TSG, especially at the exit of the TSG. For example the MCC based formulation; the averaged relative standard deviation increased from 3 % at an L/S ratio of 0.4, to 7 % at an L/S ratio of 0.9 and to 71 % at an L/S ratio of 1.1.

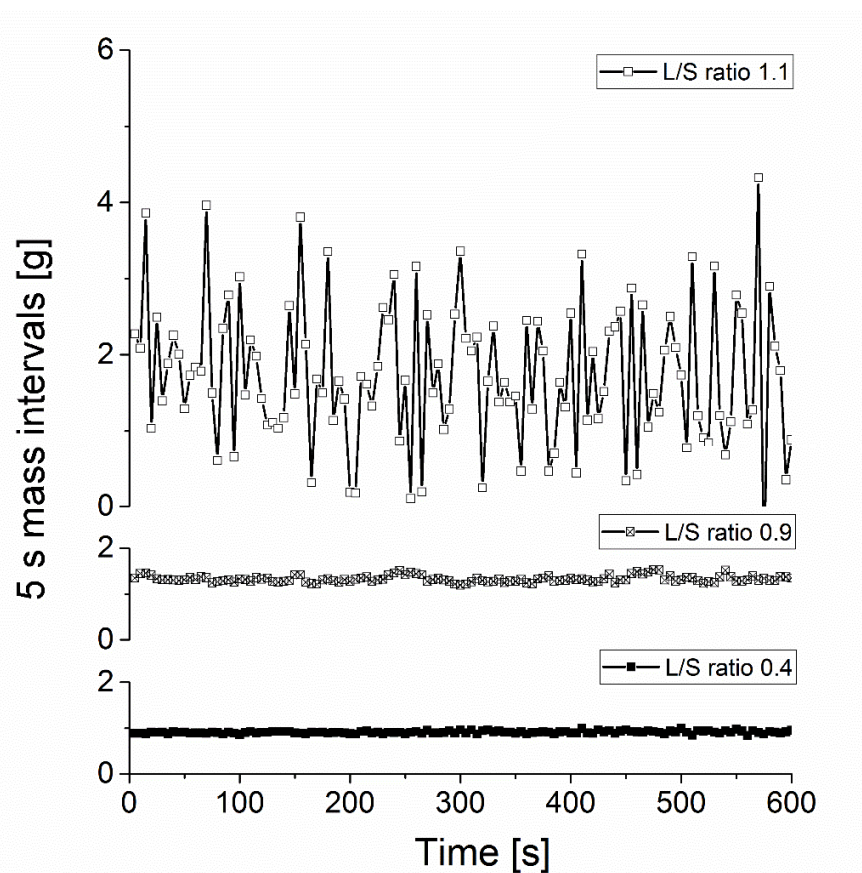


Figure 13: Wet granule mass flow rate [g/5 s] monitored over 10 minutes at different L/S ratios. (illustrated for an individual measurement of an MCC based ibuprofen formulation)

The lower L/S ratio boundary of the granulation window was assessed, by determining the dried granule size distribution (volume based) as function of the L/S ratio. In more detail, the x_{50} descriptor was evaluated. With increasing L/S ratio, a reduction in the fraction of fines and an increase in the fraction of coarse were found (Figure 14). Consequently, the granule size x_{50} was increasing with an increase in L/S ratio. For example for the MCC based formulation; the averaged granule size x_{50} increased from 153 μm at an L/S ratio of 0.4, to 281 μm at an L/S ratio of 0.7 and to 1916 μm at an L/S ratio of 0.9.

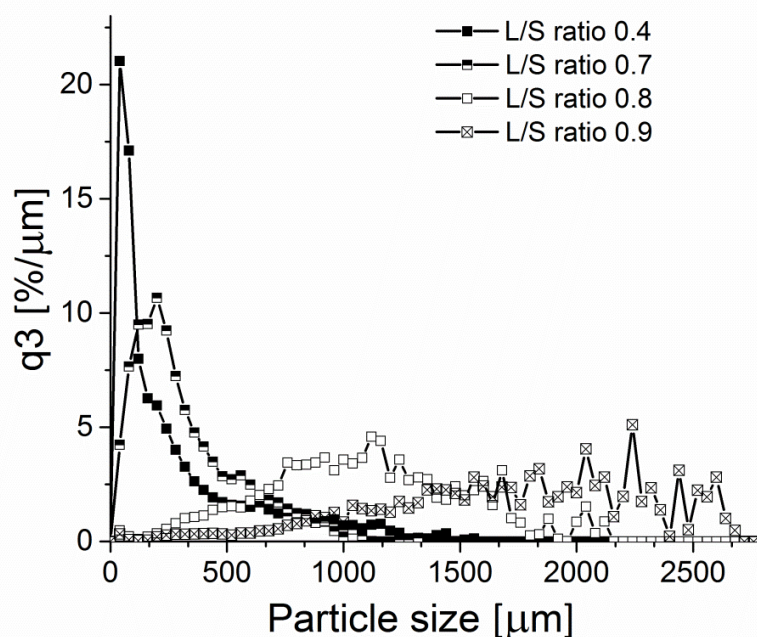


Figure 14: Particle size distribution of dried granules produced at different L/S ratios in twin-screw wet granulation. (illustrated for an individual measurement of an MCC based ibuprofen formulation)

In a next step, both methods have been used in combination to detect the L/S ratio-dependent granulation window (Figure 15). The upper L/S ratio boundary was detected by a change in gradient of the wet granule mass flow variation as function of the L/S ratio. The lower L/S ratio boundary was detected by a change in gradient of the dried granule size x_{50} as function of the L/S ratio. Hence, the upper boundary can be determined while the process is running (online), whereas the lower boundary is determined after completion of the run (offline). It puts the process between the minimum effective liquid concentration for granulation and the maximum tolerable liquid concentration based on the transition of the material to a liquid-dominated behaviour. The sharper these transitions are, the better the determination. In the cases of this study, the transitions were reasonable sharp. For example for the MCC based formulation; the upper L/S ratio boundary was found at an L/S ratio of 1.1, whereas the lower L/S ratio boundary was indicated at an L/S ratio of 0.7. Hence, the granulation window for the MCC based formulation was found in between the L/S ratios 0.7 and 1.1.

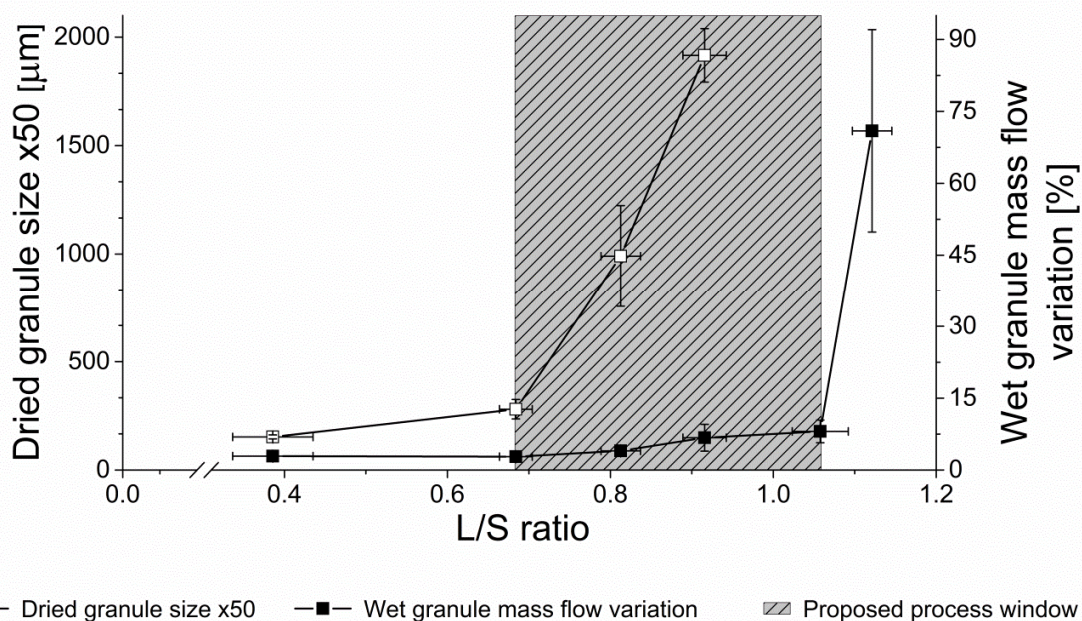


Figure 15: The L/S ratio-dependent granulation window of an MCC based formulation. The upper L/S ratio boundary is detected by a change in gradient for the wet granule mass flow variation. The lower L/S ratio boundary is detected by a change in gradient for the dried granule size x_{50} . ($\bar{x} \pm s$; $n=3$)

3.1.4 Formulation screening and selection

Parts of this section have been published in the research article “Quantitative Assessment of Mass Flow Boundaries in Continuous Twin-screw Granulation.”.

After establishing this quantitative method to detect the L/S ratio-dependent granulation window, the L/S ratio boundaries were evaluated for all formulations (Table 1). As indicated by visual observations, the fillers significantly impacted the location and the size of the L/S ratio-dependent granulation window. For the lactose based formulation, the window was found narrow and at very low L/S ratios (between 0.10 and 0.13), whereas the window was seen broader and at higher L/S ratios for the MCC based formulation (between 0.7 and 1.1), followed by the Na-CMC based formulation (L/S ratios between 1.2 and 3.0) (Figure 16). The granulation windows of the filler combinations lactose-MCC and MCC-Na-CMC were found in between the windows of the formulations based on either one of these fillers.

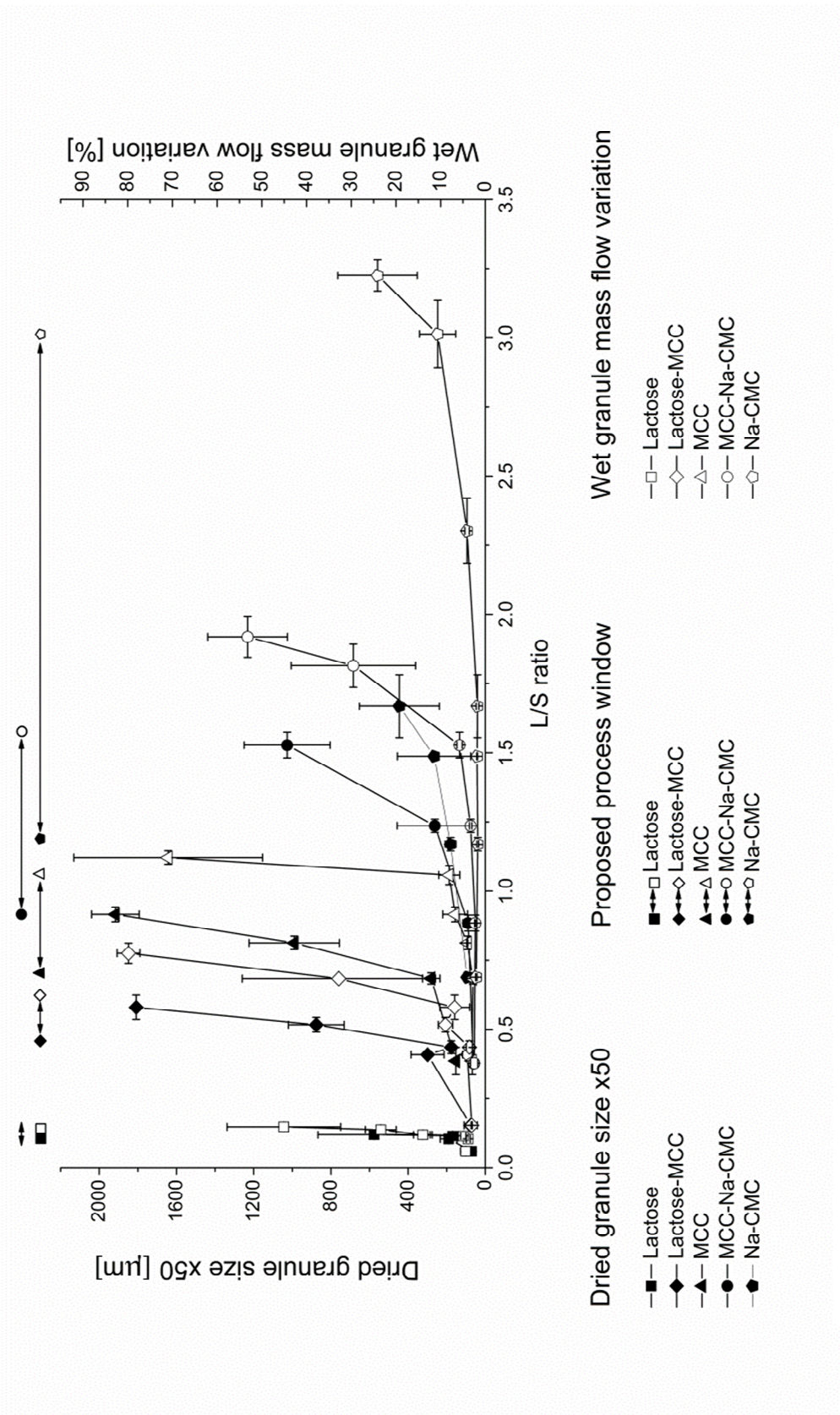


Figure 16: The L/S ratio-dependent granulation window of a lactose, lactose-MCC, MCC, MCC-Na-CMC and Na-CMC based formulation. The upper L/S ratio boundary is detected by a change in gradient for the wet granule mass flow variation. The lower L/S ratio boundary is detected by a change in gradient for the dried granule size x_{50} . ($\bar{x} \pm s$; $n=3$)

Results and Discussion

Further, an impact for the applied L/S ratio in twin-screw wet granulation was shown on the granules properties such as the tapped density or the flowability (indicated by the Hausner ratio) (details on the used methodology are listed in section 2.2.2.3 (bulk and tapped density)). For most formulations, it was found that with increasing L/S ratio the tapped density and the Hausner ratio decreased (Table 4 and Figure 17). For the MCC based formulation, for example, the tapped density decreased from 0.51 g/cm³ to 0.41 g/cm³ and the Hausner ratio decreased from 1.14 to 1.06 for an L/S ratio of 0.4 and 0.9, respectively. Both observations were probably triggered by an increasing granule size that was obtained at increasing L/S ratios. Whereas a decreasing Hausner ratio indicates an enhanced flowability of the powder bulk and is favourable for example for a following compaction unit operation, a decreasing tapped density indicates increasing air entrapment in the powder bulk and could challenge a subsequent compaction process.

Table 4: Bulk and tapped density [g/cm³] of granules from various ibuprofen formulations and L/S ratios.

L/S ratio	Bulk density $\bar{x} \pm s$ [g/cm ³]	Tapped density $\bar{x} \pm s$ [g/cm ³]
Lactose		
0.06	0.46 ± 0.01	0.52 ± 0.01
0.10	0.50 ± 0.01	0.56 ± 0.01
0.11	0.46 ± 0.03	0.52 ± 0.04
0.12	0.43 ± 0.02	0.47 ± 0.03
Lactose-MCC		
0.15	0.44 ± 0.03	0.50 ± 0.04
0.41	0.43 ± 0.01	0.47 ± 0.00
0.44	0.42 ± 0.02	0.46 ± 0.01
0.52	0.41 ± 0.01	0.45 ± 0.02
0.58	0.39 ± 0.02	0.41 ± 0.03
MCC		
0.39	0.44 ± 0.02	0.51 ± 0.03
0.68	0.42 ± 0.01	0.47 ± 0.00
0.81	0.42 ± 0.01	0.46 ± 0.03
0.92	0.39 ± 0.01	0.41 ± 0.01
MCC-Na-CMC		
0.38	0.36 ± 0.05	0.41 ± 0.04
0.88	0.40 ± 0.00	0.46 ± 0.01
1.24	0.35 ± 0.02	0.39 ± 0.02
1.53	0.31 ± 0.03	0.33 ± 0.03
Na-CMC		
0.69	0.33 ± 0.02	0.37 ± 0.01
1.17	0.32 ± 0.02	0.35 ± 0.02
1.49	0.31 ± 0.03	0.34 ± 0.03
1.67	0.34 ± 0.01	0.38 ± 0.01

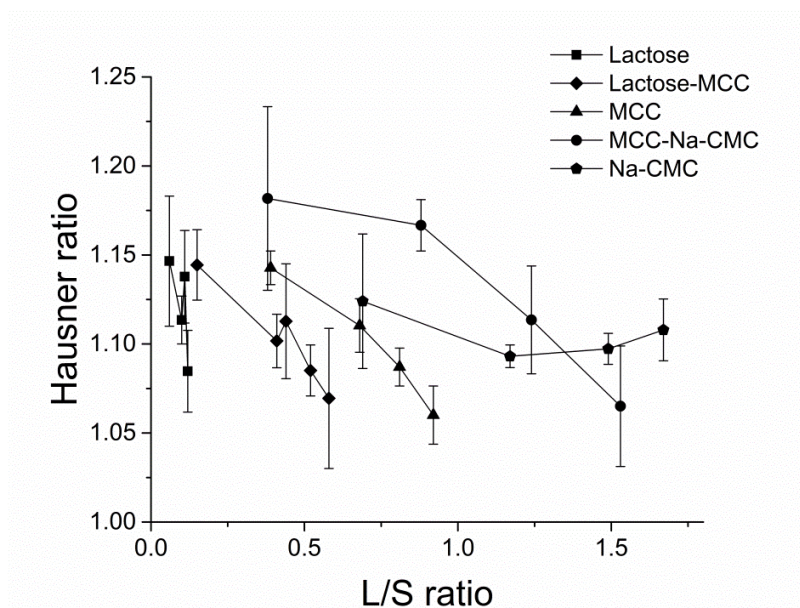


Figure 17: The granule flowability was evaluated as function of the L/S ratio in wet granulation using the Hausner ratio. ($\bar{x} \pm s$; $n=3$)

During compaction, a trend was shown that the mass variability of the compacts of granules from the lactose and MCC based formulations initially improved with increasing L/S ratio (Figure 18) (details on the used methodology are listed in section 2.2.1.5 (compaction)). However, above certain L/S ratios the mass variability of the compacts was found to increase again. For the MCC based formulation, for example, the compact mass variability dropped initially from 1.3 % at an L/S ratio of 0.4 to 0.7 % at an L/S ratio of 0.7, before it increased again to 1.1 % at an L/S ratio of 0.9. The initial improvement of the compact mass variability can be attributed to the previous described enhanced granule flowability with increasing L/S ratio. The filling of the tablet die is thereby more reproducible. However, simultaneously the tendency to entrap air in the powder bulk was increasing for granules produced at higher L/S ratios (reflected in a decreasing tapped density). Thereby the mass variability of the compacts was increasing again at higher L/S ratios. For some formulations, the initial decrease of the compact mass variability with increasing L/S ratios was not displayed, which is assumed to be caused by the selected range of L/S ratios. However, it was shown that a balance has to be found between flow and densification properties of the granule powder pack. Such compromise was obtained towards the lower side of the granulation window. Furthermore, towards the upper side of the granulation window the granulation resulted in relatively coarse granules (Figure 16). An additional process step was required before tableting (e.g. milling). Hence, granulation should be performed preferably at the lower side of the granulation window.

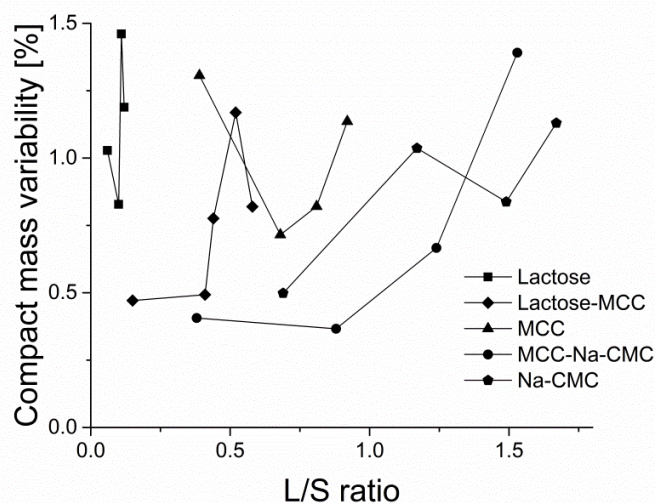


Figure 18: The compact mass variability calculated over 32 compaction cycles for compacts of granules of different formulations produced at different L/S ratios. (compaction pressure 100 MPa)

Finally, the MCC-Na-CMC based formulation was selected for the further investigation on ibuprofen suspension feed in twin-screw wet granulation with expected L/S ratios between 0.5 and 1.4. This decision was based on several reasons. First, the MCC-Na-CMC based formulation showed a relatively wide granulation window, which enabled also to work with more diluted suspensions (e.g. with ibuprofen suspension concentrations down to 30 % w/w, which correlates with an L/S ratio of up to 1.4). Although already outside the proposed granulation window, at a lower L/S ratio of 0.5, the MCC-Na-CMC based formulation showed still a relatively low compact mass variability. For the MCC based formulation in comparison, coarse granules up to paste formation were obtained for the targeted L/S ratio range. Second, it was shown, that as expected, a disintegrant was required in the formulation, in order to achieve reasonable disintegration times and dissolution of ibuprofen compacts, that would enable judging changes in tablet quality. Those two quality parameters of a tablet are essential to judge product quality and hence are valuable to be evaluated in a comparison between API suspension feed and traditional API blend feed. Overall, the MCC-Na-CMC based ibuprofen formulation showed a reasonable mechanical resistance (tensile strength between 1.0 MPa at 60 MPa compaction pressure and 1.9 MPa at 140 MPa compaction pressure), as well as a reasonable dissolution rate for ibuprofen (100 % dissolved in less than 5 minutes) (Figure 19 and Figure 20) (details on the used methodology are listed in the sections 2.2.2.6 (tensile strength), 2.2.2.8 (disintegration time) and 2.2.2.9 (dissolution rate of ibuprofen compacts)).

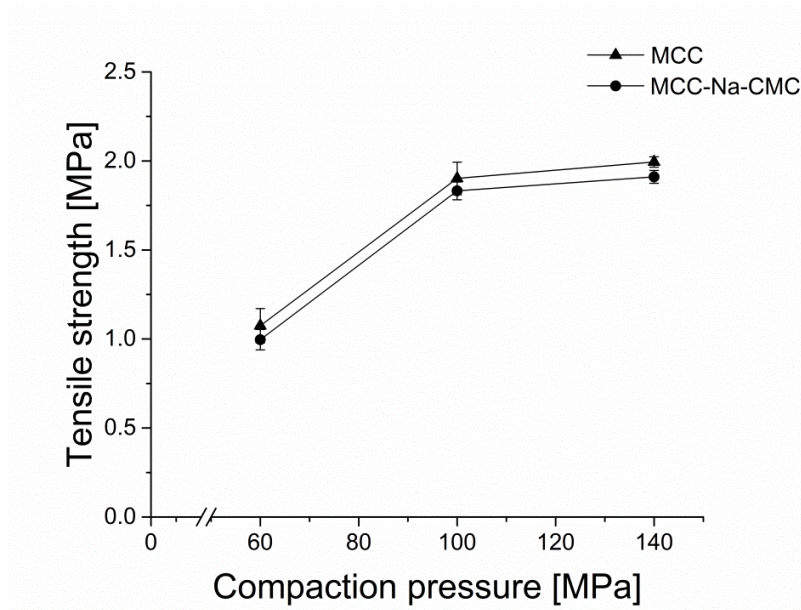


Figure 19: The tensile strength as function of the compaction pressure for an MCC (granules produced at an L/S ratio of 0.9) and an MCC-Na-CMC (granules produced at an L/S ratio of 1.5) based formulation. ($\bar{x} \pm s$; n=3)

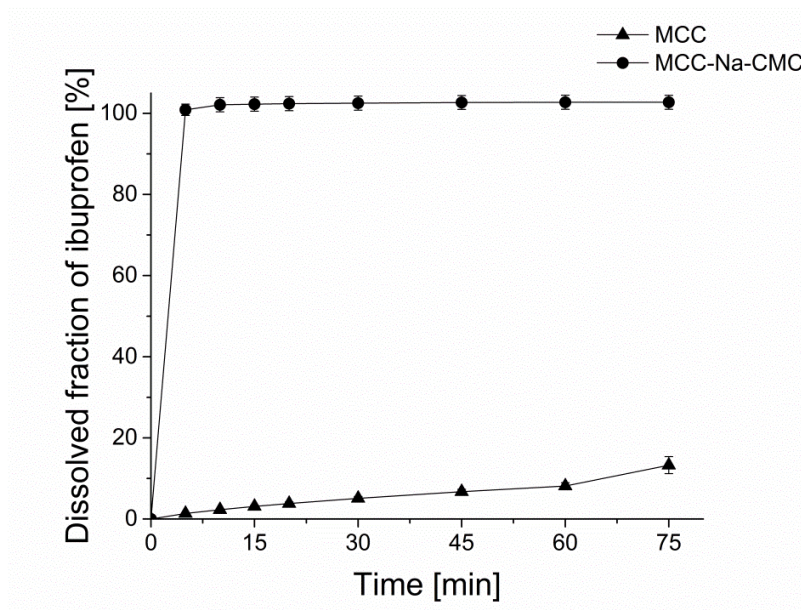


Figure 20: The dissolved fraction of ibuprofen as function of the time for an MCC (granules produced at an L/S ratio of 0.9) and an MCC-Na-CMC (granules produced at an L/S ratio of 1.5) based formulation. (compaction pressure 100 MPa, $\bar{x} \pm s$; n=3)

3.1.5 Summary

Prerequisites for enabling ibuprofen suspension feed in twin-screw wet granulation were evaluated. First, a precise and reliable pumping process was shown for ibuprofen suspension concentrations between 30 and 55 % w/w (as safety buffer, the upper ibuprofen concentration limit in the suspension was set to 53 % w/w). Higher ibuprofen concentrations were demonstrated to affect the flow behaviour of the suspension significantly and thereby its processability. Lower ibuprofen concentrations were not tested in order to restrict the amount of water that is dosed simultaneously with the ibuprofen. With the suspension composition and the targeted ibuprofen load of 60 % w/w in the final formulation, the expected range of L/S ratios in twin-screw wet granulation was calculated to 0.5 - 1.4.

Second, a suitable formulation was selected for the expected L/S ratio range in twin-screw wet granulation. A quantitative method was developed to assess L/S ratio boundaries for a formulation-specific granulation window. It was shown, that the upper L/S ratio boundary of the granulation window was indicated by a change in gradient of the wet granule mass flow variation as function of the L/S ratio. The lower L/S ratio boundary of the granulation window was indicated by a change in gradient of the dried granule size x_{50} as function of the L/S ratio. Thereby, a granulation window was detected quantitatively for a formulation. Moreover, granule flow properties were demonstrated to improve with increasing L/S ratio. However, it was shown that the tendency of the powder bulk to entrap air increases simultaneously (decreasing tapped density). The compact mass variability was shown to decrease initially with increasing L/S ratio, probably due to improving granule flow. At higher L/S ratios, the compact mass variability increases again with increasing L/S ratio (increasing amounts of air entrapped in the powder bulk). Thereby, it was demonstrated that the granulation should be preferably conducted at the lower side of the proposed granulation window. Finally, an MCC-Na-CMC based formulation was selected. It provides a relatively broad granulation window and provides reasonable disintegration times and dissolution of ibuprofen compacts that enable the comparison of ibuprofen suspension feed and traditional ibuprofen blend feed in twin-screw wet granulation.

3.2 Comparison of API suspension feed and traditional API blend feed

3.2.1 Background and objectives

In this chapter, the selected MCC-Na-CMC based formulation was used to study twin-screw wet granulation with API suspension feed (proof of concept) (Table 2 formulation A). A minor change was made by replacing a fraction of the MCC by the sodium pyrophosphate, which was needed to prepare and to stabilise the ibuprofen suspension. Thereby, the targeted final formulation composition was 60.0 % w/w of ibuprofen, 25.5 % w/w of MCC, 8.0 % w/w of Na-CMC, 2.5 % w/w of sodium pyrophosphate and of polyvinylpyrrolidone K30 (PVP), and 1.5 % w/w of magnesium stearate (Table 2 formulation F). Further, the API suspension feed was compared against the traditional API blend feed in twin-screw wet granulation (Table 2 formulation B).

Therefore, the objectives were to investigate:

- the particle agglomeration behaviour of ibuprofen suspension feed in twin-screw wet granulation (granule growth and paste formation) and to compare it against traditional ibuprofen dry blend feed.
- granule (granule size distribution, flowability, morphology) and compact properties (tensile strength, out-of-die porosity, friability, disintegration time, and ibuprofen dissolution rate) of the two process setups, ibuprofen suspension feed and dry blend feed.

3.2.2 Comparison of granulation behaviour in twin-screw wet granulation

Parts of this section are submitted for publication in the research article “Simplified end-to-end continuous manufacturing by feeding API suspensions in twin-screw wet granulation.”.

In order to investigate the agglomeration behaviour in the twin-screw wet granulation process with ibuprofen suspension feed and to compare it against traditional ibuprofen dry blend feed, the particle agglomeration was first evaluated visually (Table 2 formulation B and F). Both formulations were granulated in twin-screw wet granulation with subsequent fluidised-bed drying. Various L/S ratios were applied to determine the granulation behaviour and the L/S ratio process window for twin-screw wet granulation (details on the used methodology are listed in the sections 2.2.1.2 (screening of API suspensions and preparation of the granulation liquid), 2.2.1.3 (in twin-screw wet granulation and in formulation screening and investigation on ibuprofen suspension feed), 2.2.1.4 (fluidised-bed drying) and 2.2.2.1 (particle size distribution of powders and granules)). For the ibuprofen dry blend feed, particle agglomeration for wet granules was found visually for L/S ratios between 0.7 and 0.9 (Figure 21). Above an L/S ratio of 1.0, paste was being formed. However, intensive particle agglomeration was shown

already at lower L/S ratios for the ibuprofen suspension feed. Particle agglomeration of wet granules was observed for L/S ratios between 0.7 and 0.8. For L/S ratios above 0.8, paste was being formed. Although the formulations have been identical qualitatively and quantitatively for both process setups, considerable differences were obtained in the granulation behaviour.

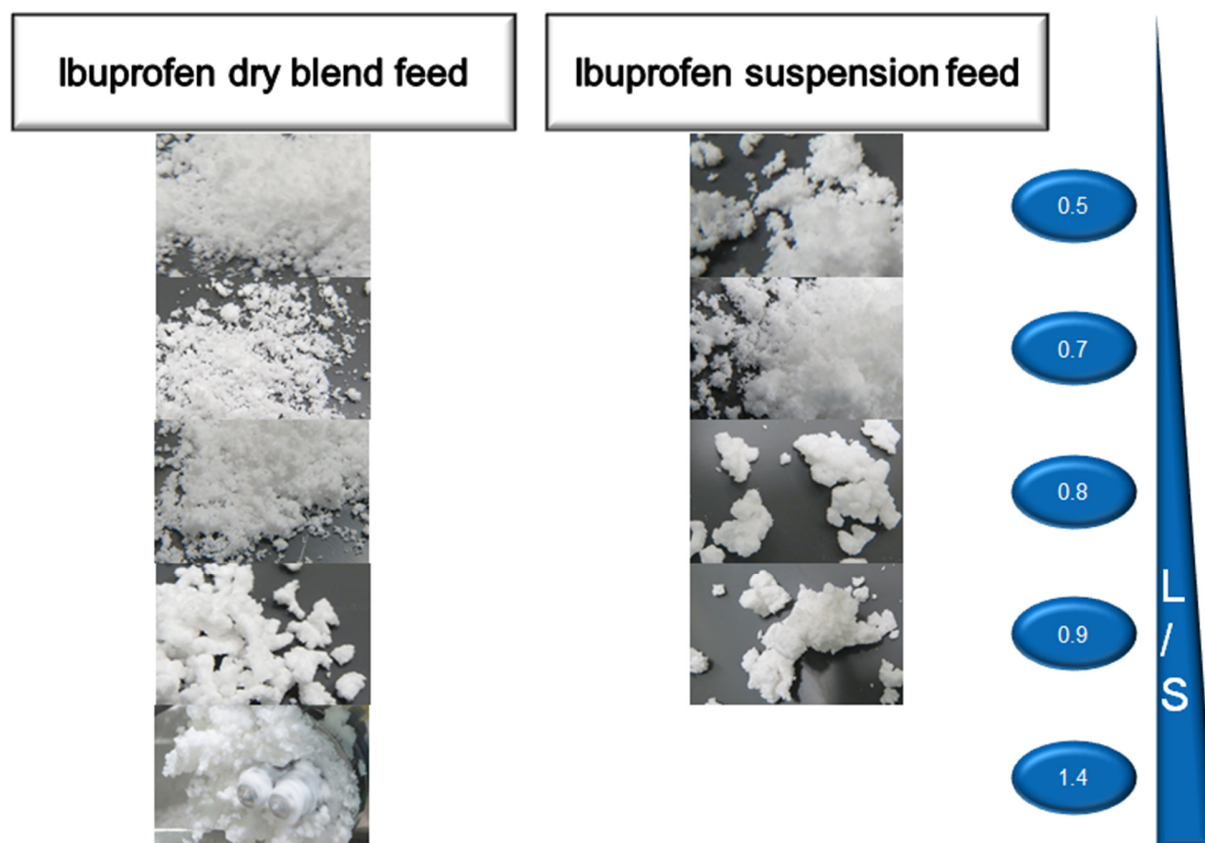


Figure 21: Visual observations of the twin-screw wet granulation behaviour for ibuprofen dry blend and ibuprofen suspension feed.

To confirm the differences found visually in their granulation behaviour, the quantitative method that was evaluated in the previous chapter (3.1.3) has been used. The onset of particle agglomeration was evaluated by studying the dried granule size x_{50} as function of the L/S ratio (Figure 22). Paste formation, and thereby over-wetting of the material, was evaluated by studying the wet granule mass flow variation at the TSG exit as function of the L/S ratio. After evaluation, the onset of particle granulation (change in the gradient of the dried granule size x_{50} as function of the L/S ratio) could not be detected quantitatively. Although with increasing L/S ratio an increasing particle agglomeration was observed visually for wet granules, after drying a relatively small dried granule size x_{50} was found for all L/S ratios. This observation was consistent for ibuprofen suspension and ibuprofen blend feed. Thereby, no granulation window could be assessed.

Results and Discussion

However, in the measure of the upper L/S ratio boundary, significant differences were obtained between ibuprofen suspension and ibuprofen blend feed. As assessed in the previous visual observations, paste was being formed at lower L/S ratios for the ibuprofen suspension feed, compared to the ibuprofen blend feed. For the ibuprofen blend feed, paste was being formed above an L/S ratio of 1.0, whereas for the ibuprofen suspension feed paste was formed above an L/S ratio of 0.8. Hence, the granulation behaviour of the two processes ibuprofen suspension and ibuprofen blend feed was different.

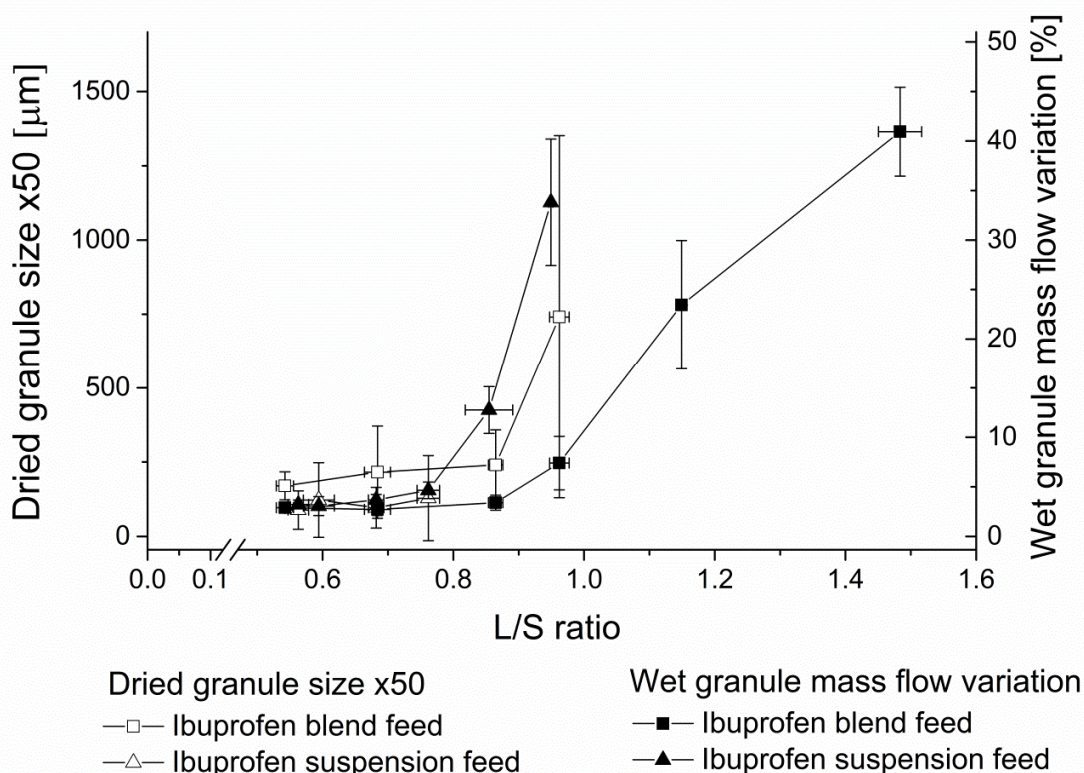


Figure 22: The dried granule size x_{50} and the wet granule mass flow variation as function of the L/S ratio. Particle agglomeration differed significantly in initial tests for ibuprofen suspension and ibuprofen blend feed. ($\bar{x} \pm s$; $n=3$)

In a next step, it was investigated why the visually observed difference in the wet particle growth was diminished after fluidised-bed drying. Therefore, two hypotheses were formed. First, it was hypothesised that only weak granules were formed due to a partial non-activation of the binder polyvinylpyrrolidone K30. It was assumed that due to the short residence time in the TSG and/or due to the viscous granulation liquid (e.g. a suspension); the PVP K30 did not dissolve completely and therefore was activated only partially. Such an effect was described in literature for the binder hydroxypropylmethyl cellulose (HPMC) (90). It has been shown that the binding effect of HPMC and therefore the particle

Results and Discussion

agglomeration was increased, when the binder was processed dissolved in the liquid phase. Second, it was hypothesised that granules initially were formed but then sized down again due to attrition and breakage in fluidised-bed drying. Especially for coarse wet granules that were obtained at higher L/S ratios, a high air flow was needed to achieve proper fluidisation of the powder bed in fluidised-bed drying. Thereby stress could have provoked also attrition and breakage. In literature sizing effects were described for different drying processes (128).

Both hypotheses were tested, using the ibuprofen suspension feed and an L/S ratio of 0.7, for which intensive particle agglomeration of wet granules was observed. The first hypothesis was investigated by processing the binder PVP K30 pre-dissolved in the granulation liquid instead of having it undissolved in the powder blend (Figure 23) (Table 2 formulations F and G). For both processes (pre-dissolved and undissolved binder), the dried granule size distribution was comparable. Hence, it was indicated that the process time was sufficient for the PVP K30 to dissolve and to act as a binder in the granulation. Therefore, the first hypothesis was not holding true.

The second hypothesis was investigated by minimising potential attrition and breakage during drying. Instead of fluidised-bed drying, the gentler oven drying was used. After drying, a significant difference was demonstrated in the dried granule size distribution between the two drying processes (Figure 23). Whereas after fluidised-bed drying a monomodal particle size distribution with a high fraction of fines was found, a bimodal particle size distribution and a high fraction of coarse granules was found after oven drying. Hence, it was indicated that potentially weak granules were sized by attrition and breakage during fluidised-bed drying and thereby visual observed differences in the wet granule size between ibuprofen suspension and ibuprofen blend feed were diminished (Figure 21).

This example shows a limitation of the proposed method to detect the L/S ratio boundaries quantitatively in twin-screw wet granulation. By using the dried granule size x_{50} , an impact of the subsequent drying process is incorporated in the measure of the lower L/S ratio boundary. In order to exclude such effect, particle size measurements should be conducted on wet granules, before drying. Furthermore, by the attrition and breakage during fluidised-bed drying it was indicated, that the manufacturing process may require improvement to gain more robust granules. This could be achieved for example by using a different binder or by increasing the binder concentration in the formulation. However, both actions can affect simultaneously the tolerated L/S ratio in twin-screw wet granulation and thereby the processability of ibuprofen suspension feed. For example, by increasing the binder concentration in the formulation, typically less granulation liquid is required to achieve comparable particle agglomeration. Therefore, the significant difference in paste formation was focused to study the difference in granulation behaviour between ibuprofen suspension feed and blend feed in twin-screw wet granulation.

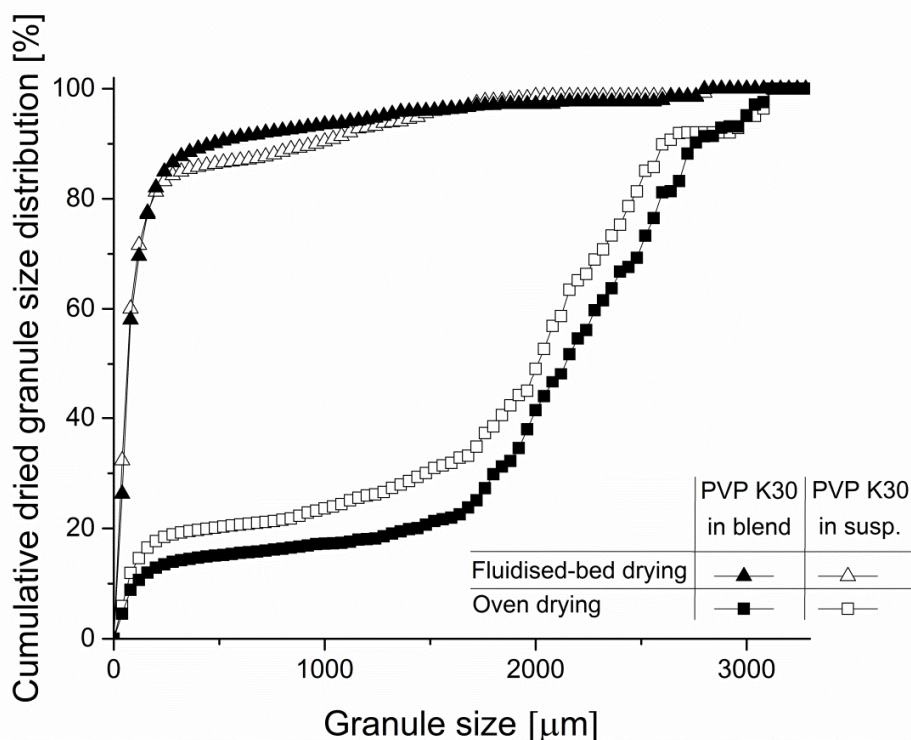


Figure 23: Comparison of the cumulative dried granule size distribution for granules from ibuprofen suspension feed with PVP K30 processed dissolved in the suspension versus PVP K30 processed undissolved in the blend (L/S ratio 0.7). Wet granules were dried either by fluidised-bed drying or by oven drying. (n=1)

Although the formulation was qualitatively and quantitatively identical for both processes, a difference was detected in the L/S ratio at which paste has been formed (Table 2 formulations B and F). The ibuprofen suspension and ibuprofen blend feed differed only in the way the sodium pyrophosphate and the ibuprofen were added to the twin-screw wet granulation process. For the ibuprofen suspension feed, the suspending agent sodium pyrophosphate was added dissolved in the granulation liquid and the ibuprofen was suspended. However, for the ibuprofen blend feed the two components were fed as solids via the powder blend. Hence, it was hypothesised that either the way the sodium pyrophosphate or the way the ibuprofen was added in the twin-screw wet granulation had caused the observed difference in paste formation.

As a first hypothesis, it was tested if the difference in paste formation could be attributed to the mode of ibuprofen addition. Therefore, the way of processing sodium pyrophosphate was changed. For both, ibuprofen suspension feed and blend feed, the sodium pyrophosphate was processed dissolved via the granulation liquid (Table 2 formulations C and F). It was shown, that the previously observed difference in paste formation thereby was eliminated (Figure 24). For both processes, paste formation was found

Results and Discussion

above an L/S ratio of 0.8. This finding is inconsistent with literature. It has been described, that increasingly viscous granulation liquids (e.g. an ibuprofen suspension), would lead to a poorer liquid distribution in the powder bed and thereby it would affect powder agglomeration (114). However, the mode of addition of the ibuprofen was shown not to influence the granulation behaviour in twin-screw wet granulation.

Simultaneously, the other hypothesis was shown to be valid. Indeed, it was found that the sodium pyrophosphate and its mode of addition significantly impacted the paste formation in twin-screw wet granulation. When comparing the original MCC-Na-CMC based formulation from the formulation screening with the modified MCC-Na-CMC based formulation for the ibuprofen suspension feed, for which 2.5 % w/w of the MCC were substituted by sodium pyrophosphate, paste formation was found at significantly lower L/S ratios (Figure 24) (Table 2 formulations A and B). For the MCC-Na-CMC based formulation without sodium pyrophosphate, paste formation was observed at an L/S ratio above 1.5. However, for the MCC-Na-CMC based formulation with sodium pyrophosphate, paste formation was observed already at an L/S ratio above 1.0. If the sodium pyrophosphate was then processed dissolved via the granulation liquid, paste formation was observed at even lower L/S ratios (above L/S ratios of 0.8) (Table 2 formulations C). A different activated sodium pyrophosphate concentration could have influenced the difference in paste formation between the ibuprofen suspension and the ibuprofen blend feed. For the ibuprofen suspension feed, all sodium pyrophosphate was activated since it was processed dissolved in the liquid. In contrast, for the ibuprofen blend feed the concentration of activated sodium pyrophosphate might have been lower since it was processed as solid and needed to dissolve first. As mentioned for the previous example of the binder HPMC, maybe the residence time in the TSG was too short and sodium pyrophosphate was dissolved only partially. Therefore, the activated concentration of sodium pyrophosphate could have been higher for the ibuprofen suspension feed, which in turn led to a paste formation at lower L/S ratios compared to the ibuprofen blend feed.

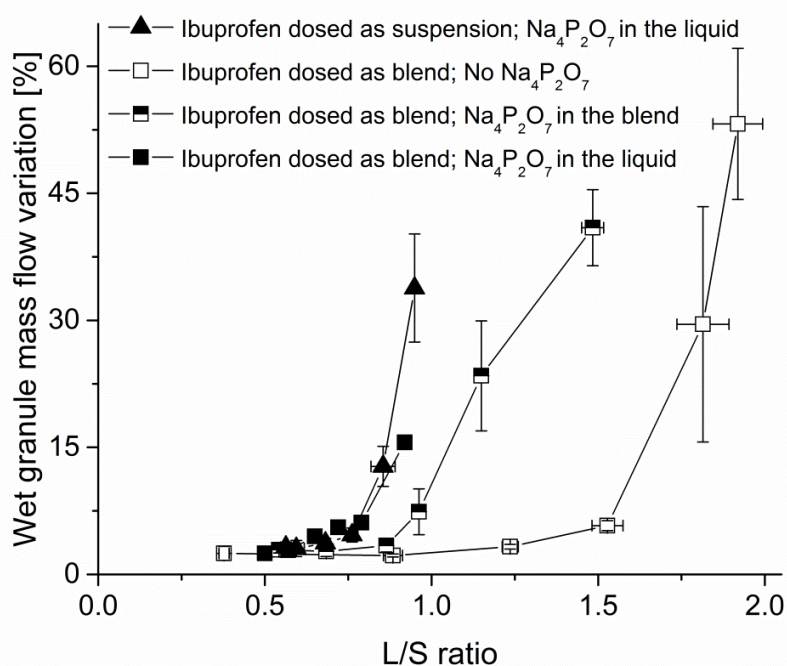


Figure 24: The onset of paste formation in twin-screw wet granulation was indicated by a significant change in gradient of the wet granule mass flow variation as function of the L/S ratio. Paste formation was observed above comparable L/S ratios for ibuprofen suspension feed and blend feed, when $\text{Na}_4\text{P}_2\text{O}_7$ was processed in the liquid. Paste formation was shifted towards higher L/S ratios when $\text{Na}_4\text{P}_2\text{O}_7$ was fed via the powder blend. In the absence of $\text{Na}_4\text{P}_2\text{O}_7$, paste formation was shifted towards even higher L/S ratios. (ibuprofen blend feed, $\text{Na}_4\text{P}_2\text{O}_7$ in the liquid: $n=1$; others: $\bar{x} \pm s$; $n=3$)

One possibility to explain the effect of the sodium pyrophosphate is by an enhanced particle agglomeration due to an increased wettability of the powder blend in the granulation liquid. In wet granulation, additives like wetting or suspending agents are typically used to improve the granulation behaviour of formulations with hydrophobic components (129). Thereby the wetting is improved and particle agglomeration is induced at lower amounts of granulation liquid. Another possibility to explain the effect of the sodium pyrophosphate is the hypothesis that it affects the dissolved amount of ibuprofen. Sodium pyrophosphate is a strong base, whereas ibuprofen is a strong acid. The dissolved amount of ibuprofen could have changed based on a change in pH. According to literature the solubility of solids is of significant impact for the particle agglomeration (130-132). The higher the dissolved fraction of solids, the less granulation liquid is required for particle agglomeration.

Both outlined hypotheses were tested. To test the first hypothesis, it was studied if an enhanced wettability of the powder blend in the granulation liquid had induced particle agglomeration at lower L/S

Results and Discussion

ratios in twin-screw wet granulation. The wettability was tested for the ibuprofen blend formulation, including sodium pyrophosphate, in pure water, and compared against the wettability of the ibuprofen blend formulation without sodium pyrophosphate in a 3.4 % w/w aqueous sodium pyrophosphate solution (simulated test conditions for complete dissolution of the suspending agent) (details on the used methodology are listed in section 2.2.2.10 (wettability of ibuprofen powder blends)). The results showed a faster mass increase for the powder formulation including sodium pyrophosphate with water as the liquid (Figure 25). This finding was contrary to the assumption of the first hypothesis, that the mass increase would be faster for the powder formulation without suspending agent in the aqueous 3.4 % w/w sodium pyrophosphate solution. However, the results may support the second hypothesis of changing ibuprofen solubility. The slower liquid uptake (increase in mass) of the powder formulation without sodium pyrophosphate could be explained by a faster ibuprofen dissolution in the aqueous 3.4 % w/w sodium pyrophosphate solution. The viscosity of the liquid and the structure of the pore system may have changed due to ibuprofen dissolution, which in turn could have resulted in a slower liquid uptake.

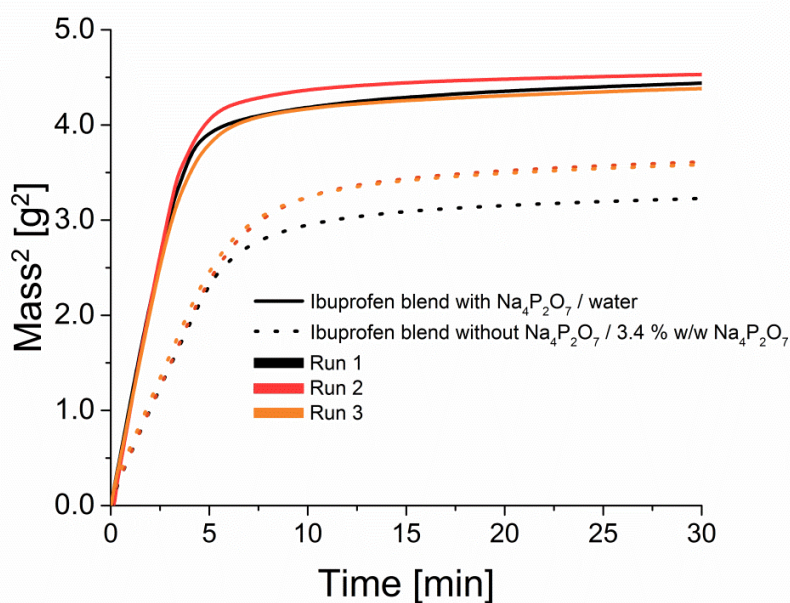


Figure 25: The increase in mass by water uptake, plotted over time for an ibuprofen blend with sodium pyrophosphate in water and for an ibuprofen blend without sodium pyrophosphate in an aqueous 3.4 % w/w sodium pyrophosphate solution. (individual experiments)

To test the second hypothesis, it was verified if the dissolved amount of ibuprofen was affected by increasing concentrations of activated sodium pyrophosphate and if thereby the granulation behaviour was changed. Therefore, the dissolved amount of ibuprofen was tested in two aqueous sodium pyrophosphate solutions (details on the used methodology are listed in section 2.2.2.11 (dissolved

Results and Discussion

amount of ibuprofen)). A 3.4 % w/w sodium pyrophosphate solution thereby simulates applied test conditions in twin-screw wet granulation (L/S ratio 0.7) for complete dissolution of the suspending agent. However, a 1.6 % w/w sodium pyrophosphate solution was selected to mimic a situation for a partial dissolution of the suspending agent in twin-screw wet granulation. The dissolved amount of ibuprofen was determined for suspensions after 1, 5 and 10 minutes respectively. It was found that the dissolved fraction of ibuprofen significantly depended on the (activated) concentration of sodium pyrophosphate in the water (Figure 26). The dissolved amount of ibuprofen increased from 14 mg/ml to 25 mg/ml for the 1.6 % w/w and the 3.4 % w/w sodium pyrophosphate solution, respectively. Moreover, it was shown that the dissolved amount of ibuprofen is relatively constant over time after 1 minute, indicating a quick dissolution of ibuprofen. The impact of pH on the dissolved amount of the ibuprofen in the liquid was found to be negligible. The pH was 9.8 for the 1.6 % w/w sodium pyrophosphate solution, whereas for the 3.4 % w/w sodium pyrophosphate solution the pH was 9.9. Instead, it was assumed, that the capability of sodium pyrophosphate to form soluble complexes could be enhanced and that thereby the dissolved fraction of ibuprofen was increased (133).

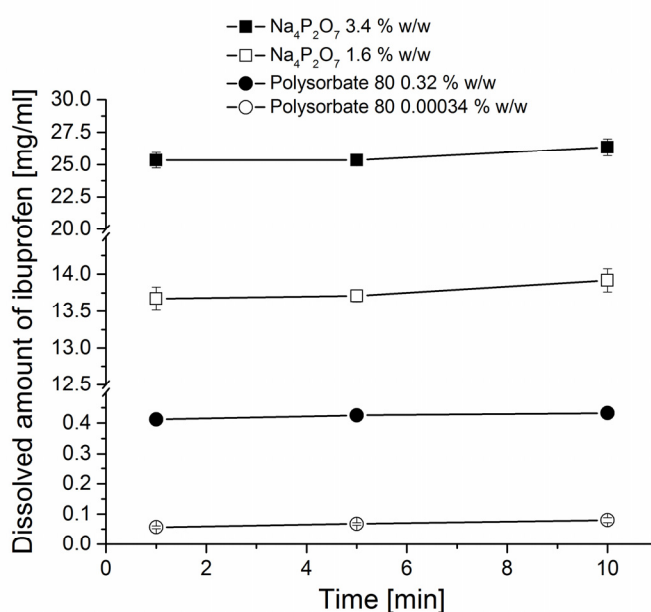


Figure 26: The dissolved amount of ibuprofen in aqueous sodium pyrophosphate and polysorbate 80 solutions. ($\bar{x} \pm s$; n=3)

Based on this, it was hypothesised that the underlying mechanism for the difference in paste formation for ibuprofen suspension and ibuprofen blend feed during twin-screw wet granulation, probably lies in different concentrations of activated sodium pyrophosphate. For the ibuprofen suspension feed, the sodium pyrophosphate was processed pre-dissolved in the granulation liquid (= fully activated). Thereby, relatively high amounts of ibuprofen were dissolved, which in turn impacted the L/S ratio in the process

Results and Discussion

and the particle agglomeration. The L/S ratio in the process was actually higher due to the partial dissolution of solid components. For example, for the ibuprofen suspension feed in twin-screw wet granulation and a targeted L/S ratio of 0.7, an aqueous 3.4 % w/w sodium pyrophosphate solution was used as a dispersing medium. A solid mass throughput of 500 g/h was set. Consequently, the water mass throughput was 350 g/h. Determined in off-line experiments, 25 mg/ml of ibuprofen dissolves in the selected dispersing liquid, meaning 9 g/h of the processed 300 g/h of ibuprofen (60 % w/w drug load) were dissolved. Additionally, all sodium pyrophosphate was dissolved (13 g/h); meaning that together with the dissolved amount of ibuprofen, 21 g/h of the 500 g/h solids were dissolved at least. Thereby, the actual L/S ratio is increased by at least 0.03. Such a small value should not make a big difference for the investigated MCC-Na-CMC based formulation. However, the in-process solubility is also not reflected in this estimation (e.g. enhanced dissolution by the intensive mixing of the screws). In fact, paste formation was observed at lower L/S ratios when sodium pyrophosphate was processed via the granulation liquid. In contrast, when the sodium pyrophosphate was processed as solid in the blend for the ibuprofen blend feed, the suspending agent needed to dissolve first, before it affected the dissolved amount of ibuprofen. Lower amounts of sodium pyrophosphate and/or ibuprofen were dissolved, which in turn led to a paste formation at higher L/S ratios in twin-screw wet granulation.

To confirm this hypothesis, the dissolved amount of ibuprofen in water was changed intentionally. Thereto polysorbate 80 was used as an additive. For one liquid, polysorbate 80 was used below its critical micelle concentration (CMC) of 0.13×10^{-2} % w/w, whereas for another liquid polysorbate 80 was used above its CMC (Table 2 formulations D and E). As expected, the dissolved amount of ibuprofen increased from approximately 0.06 mg/ml for the 0.34×10^{-3} % w/w polysorbate 80 solution (below CMC) to 0.41 mg/ml for the 0.32 % w/w polysorbate 80 solution (above CMC). Moreover, it was found that the dissolved fraction of ibuprofen in polysorbate 80 solutions was lower, compared to sodium pyrophosphate solutions.

Since the dissolved amount of ibuprofen was increasing for the solutions polysorbate 80 0.34×10^{-3} % w/w and 0.32 % w/w, and sodium pyrophosphate 1.6 % w/w and 3.4 % w/w, paste formation in twin-screw wet granulation with those granulation liquids was expected in the opposite order (details on the used methodology are listed in the sections 2.2.1.2 (screening of API suspensions and preparation of the granulation liquid), 2.2.1.3 (in twin-screw wet granulation and in formulation screening and investigation on ibuprofen suspension feed)). Paste formation in twin-screw wet granulation with those granulation liquids indeed was found in the opposite order (Figure 27). For the 3.4 % w/w sodium pyrophosphate solution, paste formation was found at an L/S ratio above 0.8, followed by a paste formation at an L/S ratio above 1.0 for the 1.6 % w/w sodium pyrophosphate solution. For the 0.32 % w/w polysorbate 80 solution, paste formation was observed at an L/S ratio above 1.3 and for the 0.34×10^{-3} % w/w polysorbate 80 solution paste was formed at an L/S ratio above 1.5. Hence, the initial hypothesis that the dissolved amount of ibuprofen varied depending on the concentration of activated sodium pyrophosphate and thereby impacted the agglomeration behaviour can be considered as valid.

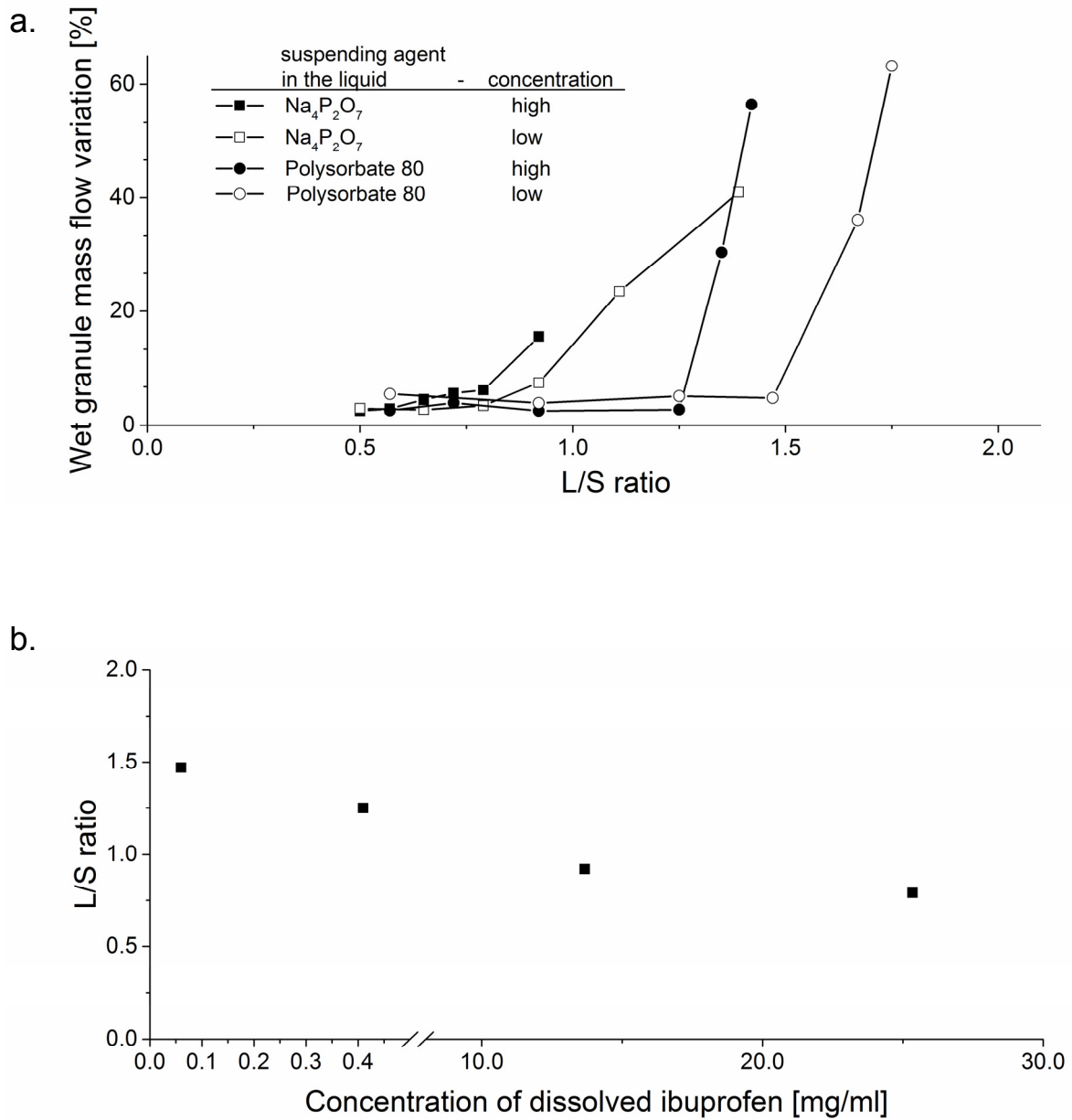


Figure 27: (a) Paste formation in twin-screw wet granulation with ibuprofen blend feed. Sodium pyrophosphate and polysorbate 80 solutions were used as granulation liquid at high and low concentration. Paste formation was indicated by a change in gradient of the wet granule mass flow variation as function of the L/S ratio. (n=1); (b) Correlation of the onset of paste formation as function of the dissolved amount of ibuprofen. (n=1)

In the setup of this study, the suspending agent was required in order to suspend and stabilise the API (ibuprofen) initially in the granulation liquid water. However, in an end-to-end continuous manufacturing line setup, suspending agents may not be used. In such a setup, the API is already obtained in suspension after the chemical operations API crystallisation and work-up. Thus, any variability in the granulation behaviour in a subsequent twin-screw wet granulation process due to an increasing dissolved amount of solid components in the granulation liquid can be excluded. As a consequence, higher amounts of liquid are tolerated, but are also required to start particle agglomeration. If the variation in the dissolved amount of solid components can be excluded, ibuprofen suspension feed and ibuprofen blend feed were demonstrated comparable in their particle agglomeration behaviour in twin-screw wet granulation (Figure 24).

3.2.3 Comparison of granule and compact properties

Parts of this section are submitted for publication in the research article “Simplified end-to-end continuous manufacturing by feeding API suspensions in twin-screw wet granulation.”.

After fluidised-bed drying, the properties of granules from ibuprofen suspension and the ibuprofen blend feed were analysed and compared (details on the used methodology are listed in the sections 2.2.2.3 (bulk and tapped density) and 2.2.2.4 (scanning electron microscopy)). For both processes, the needle-shaped ibuprofen was found well granulated after twin-screw wet granulation and fluidised-bed drying (Figure 28). Granules were found rectangular to round-shaped in their appearance. No significant difference was found in the granule morphology between the ibuprofen suspension and the ibuprofen blend feed. Furthermore, the flow properties of granules were evaluated using the Hausner ratio. Overall, the Hausner ratio was comparable for both process setups at comparable L/S ratios and indicated good flow properties (Table 5). For an L/S ratio of 0.5, for example, the Hausner ratio was 1.16 for granules from the ibuprofen suspension feed, whereas for granules from the ibuprofen blend feed the ratio was found at 1.17. For another L/S ratio of 0.7, the values for the Hausner ratio were found vice versa. Consequently, granules from both processes were comparable in their morphology and flow properties. However, this finding has to be considered with care. It could partially be a result of diminished differences in the dried granule size distribution between ibuprofen suspension feed and blend feed after fluidised-bed drying (described in the previous section 3.2.2).

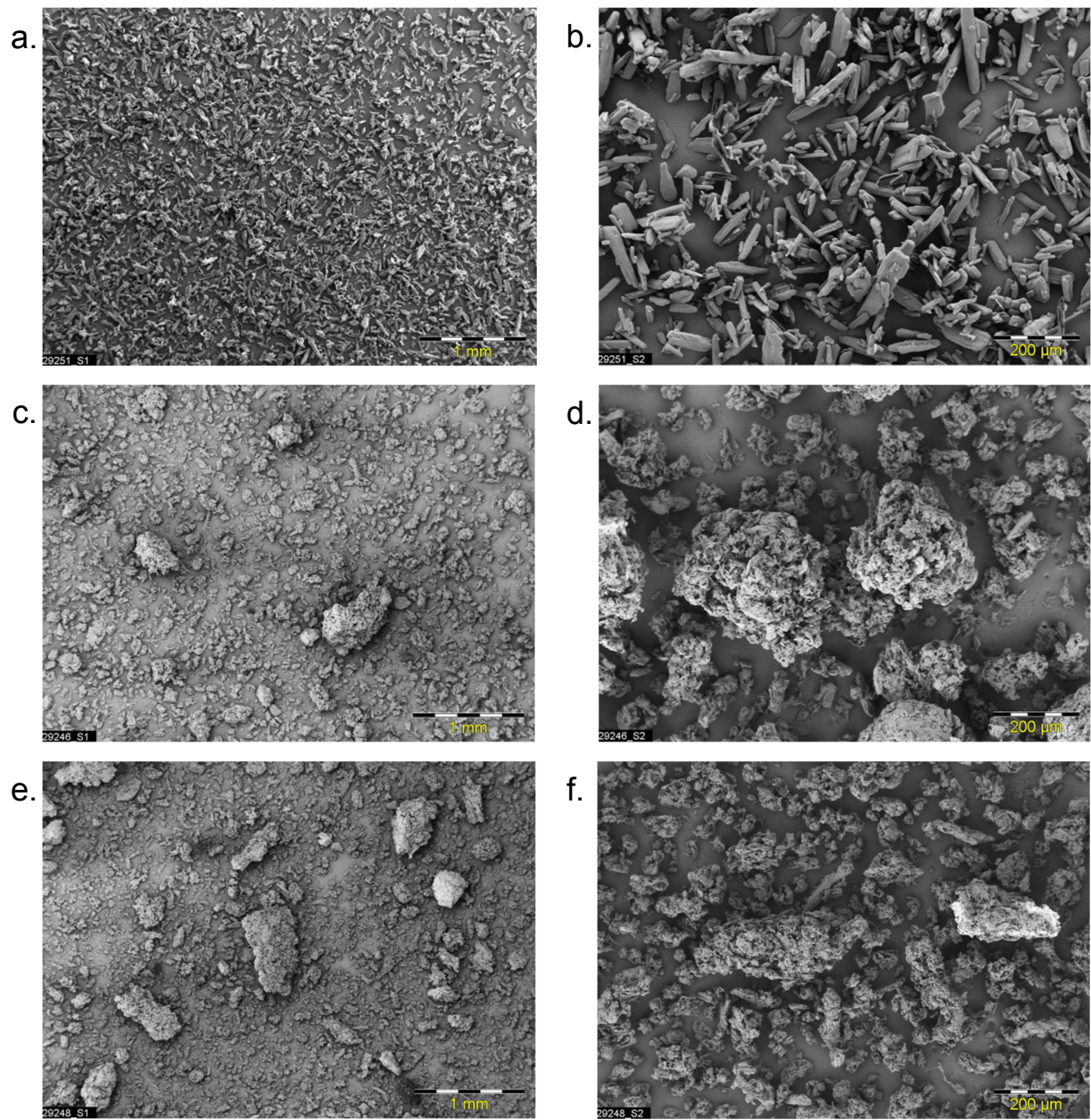


Figure 28: SEM pictures (a) and (b) from particles of ibuprofen 25; (c) and (d) of dried granules (L/S ratio 0.50) from the ibuprofen suspension feed; (e) and (f) of dried granules (L/S ratio 0.50) from the ibuprofen blend feed.

Results and Discussion

Table 5: Bulk and tapped density [g/cm³] of granules from ibuprofen suspension feed and blend feed, as well as the Hausner ratio. Granules were manufactured at various L/S ratios.

L/S ratio	Bulk density $\bar{x} \pm s$ [g/cm ³]	Tapped density $\bar{x} \pm s$ [g/cm ³]	Hausner ratio
Ibuprofen suspension feed			
0.50	0.41 ± 0.02	0.48 ± 0.03	1.16 ± 0.02
0.57	0.39 ± 0.03	0.46 ± 0.03	1.18 ± 0.01
0.65	0.39 ± 0.01	0.45 ± 0.01	1.17 ± 0.02
0.72	0.39 ± 0.01	0.45 ± 0.01	1.16 ± 0.01
Ibuprofen blend feed			
0.50	0.37 ± 0.01	0.44 ± 0.01	1.17 ± 0.01
0.65	0.39 ± 0.01	0.46 ± 0.01	1.17 ± 0.02
0.79	0.39 ± 0.01	0.45 ± 0.01	1.15 ± 0.02
0.92	0.36 ± 0.02	0.38 ± 0.03	1.07 ± 0.03

Finally, the compaction behaviour and compact properties were investigated for comparable granule batches from both processes (second run of granules manufactured at an L/S ratio of 0.50). Details on the used methodology are listed in the sections 2.2.1.5 (compaction), 2.2.2.2 (helium density of granules), 2.2.2.5 (compact porosity), 2.2.2.6 (tensile strength), 2.2.2.7 (friability), 2.2.2.8 (disintegration time) and 2.2.2.9 (dissolution rate of ibuprofen compacts). The compaction behaviour was evaluated and compared using force-displacement-curves (Figure 29). The force-displacement-curves for granules from both processes were found almost overlaying, which indicated comparable particle packing in the tablet die and compressibility. This finding is in line with the previous described comparable flow properties (evaluated by the Hausner ratio) and powder packing (tapped density) of the dried granules (Table 5). The variability in compact mass was found to be rather small for both processes (relative standard deviation below 0.5 %; n= 32).

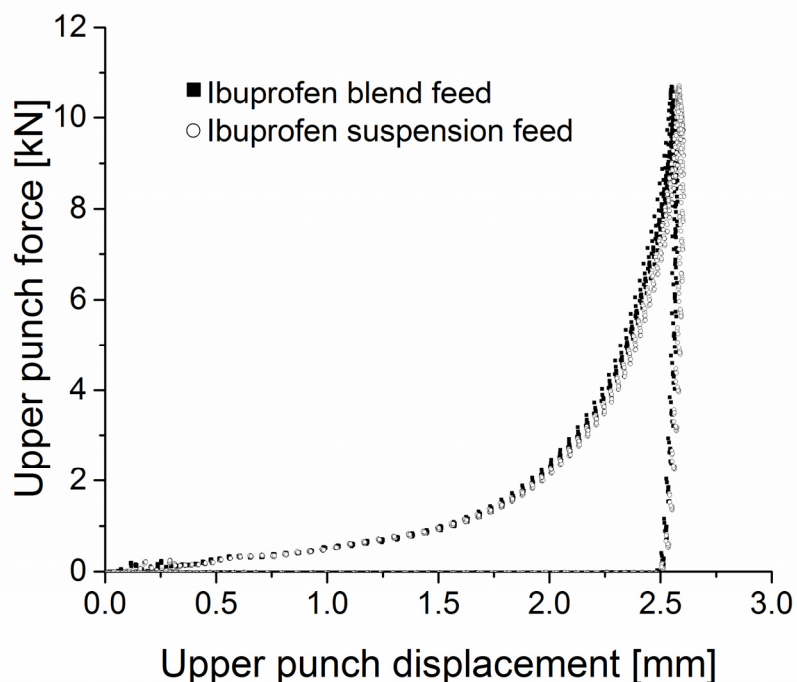


Figure 29: Force-displacement-curves for 10 compaction cycles of granules from ibuprofen suspension feed and of granules from ibuprofen blend feed. (L/S ratio 0.50; individual compaction cycles are plotted; targeted compaction force was 10 kN)

The tensile strength of compacts of granules from the ibuprofen suspension feed was found to be slightly, but consistently higher than that of compacts of granules from ibuprofen blend feed (Figure 30). The tensile strength increased from 1.1 MPa at 60 MPa compaction pressure, to 1.8 MPa at 100 MPa compaction pressure and to 1.9 MPa at 140 MPa compaction pressure for the ibuprofen suspension feed. However, for the ibuprofen blend feed, the tensile strength increased from 0.9 MPa at 60 MPa compaction pressure to 1.4 MPa at 100 MPa compaction pressure and to 1.7 MPa at 140 MPa compaction pressure. This finding is consistent with what has been reported in literature. According to literature, higher fractions of recrystallised ibuprofen in the formulation enhances the compressibility and increases the strength of the compact (134). For the ibuprofen suspension feed, sodium pyrophosphate was processed dissolved in the granulation liquid and triggered a higher dissolved amount of ibuprofen in the granulation process. After the following fluidised-bed drying process, thus, the dissolved ibuprofen recrystallised. This resulted in a higher fraction of recrystallised ibuprofen for the ibuprofen suspension feed, compared to the ibuprofen blend feed. Thereby the compressibility was enhanced and a higher tensile strength of manufactured compacts was found for the ibuprofen suspension feed. However, a low friability was shown for compacts from both processes (compaction pressure 100 MPa). The friability was found below 0.2 %.

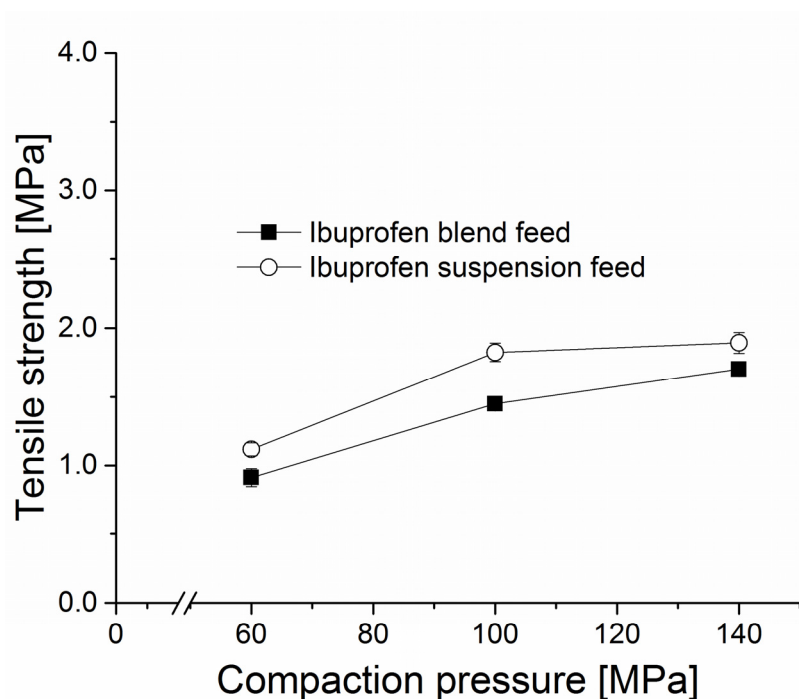


Figure 30: The tensile strength as function of the compaction pressure for compacts of granules from ibuprofen suspension feed and of granules from ibuprofen blend feed (L/S ratio 0.50). ($\bar{x} \pm s$; n=10)

The findings for the out-of-die porosity were in line with the previous data of the compact tensile strength. The out-of-die porosity decreased from 15.9 % at 60 MPa compaction pressure to 9.8 % at 140 MPa compaction pressure for the ibuprofen suspension feed (Figure 31). For the ibuprofen blend feed, the out-of-die porosity decreased from 17.3 % at 60 MPa compaction pressure to 11.2 % at 140 MPa compaction pressure. Therefore, the out-of-die porosity was found to be slightly, but consistently lower for compacts of granules from the ibuprofen suspension feed compared to compacts of granules from the ibuprofen blend feed. Thereby, particle-particle-interactions were intensified, which in turn explains the higher tensile strength of compacts of granules from the ibuprofen suspension feed.

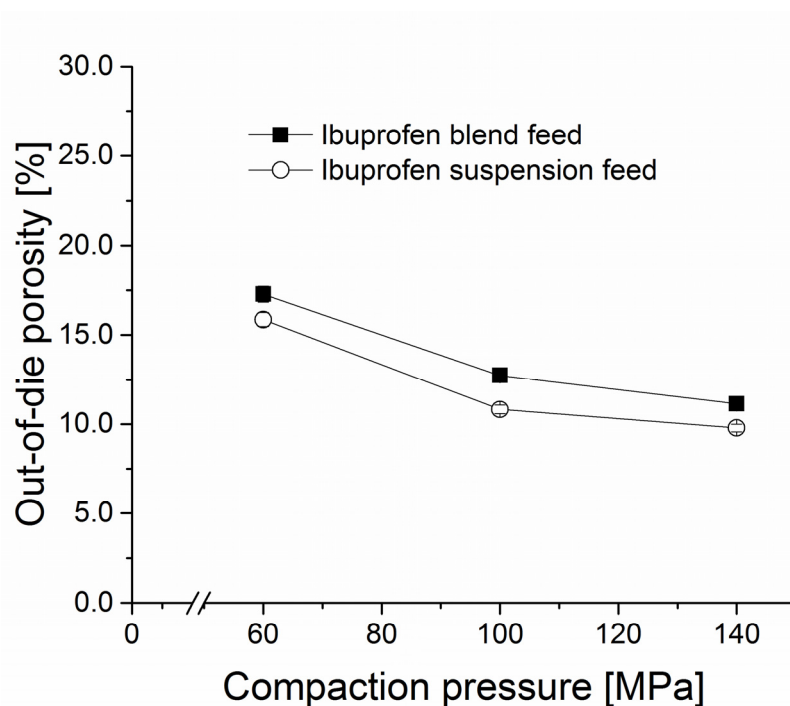


Figure 31: The out-of-die porosity as function of the compaction pressure for compacts of granules from ibuprofen suspension feed and of granules from ibuprofen blend feed (L/S ratio 0.50). ($\bar{x} \pm s$; n=10)

The dissolution of compacts from the ibuprofen suspension feed was found to be slightly slower compared to compacts from the ibuprofen blend feed (Figure 32). This observation can be attributed to the lower out-of-die porosity that was found for compacts from the ibuprofen suspension feed. Since the dissolution medium cannot penetrate into the compacts as quick as for compacts with a higher porosity (ibuprofen blend feed), the disintegration time was prolonged slightly (disintegration time of compacts of granules from the ibuprofen suspension feed was 7 minutes, whereas for compacts of granules from the ibuprofen blend feed it was 4 minutes (\bar{x} , n= 10); compacts manufactured at a compaction pressure of 100 MPa), which in turn resulted in a prolonged dissolution. Moreover, it was found that the MCC-Na-CMC based ibuprofen formulation that comprises sodium pyrophosphate showed a prolonged dissolution, compared to the previous tested MCC-Na-CMC based ibuprofen formulation without sodium pyrophosphate (Figure 21 and 33) (Table 2 formulation A and B). Compacts of the MCC-Na-CMC based ibuprofen formulation without sodium pyrophosphate (Figure 21) showed dissolution within 5 minutes, whereas compacts of the MCC-Na-CMC based ibuprofen formulation with sodium pyrophosphate (Figure 32) dissolved completely within 10 minutes. This can be attributed to the different process conditions during twin-screw wet granulation. The MCC-Na-CMC based formulation without sodium pyrophosphate was granulated at an L/S ratio of 1.5, whereas for the MCC-Na-CMC based formulation with sodium

pyrophosphate an L/S ratio of 0.5 was used. Different granule properties resulted, which in turn affected the disintegration and dissolution of subsequent manufactured compacts.

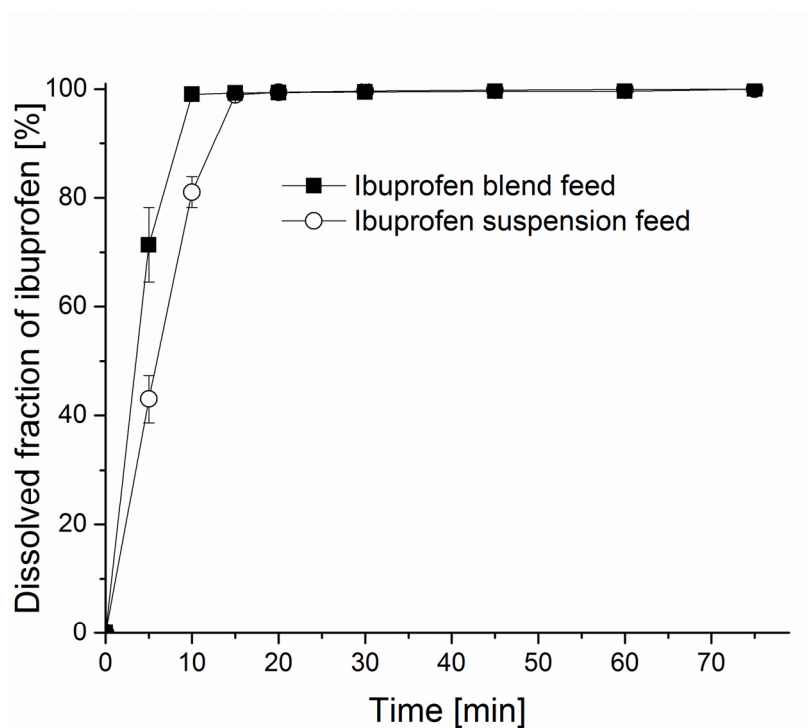


Figure 32: Dissolved fraction of ibuprofen as function of time for compacts of granules from ibuprofen suspension feed and of granules from ibuprofen blend feed (L/S ratio 0.50). (compaction pressure 100 MPa, $\bar{x} \pm s$; n=3)

3.2.4 Summary

In this chapter, the proof of concept of ibuprofen suspension feed in twin-screw wet granulation was demonstrated. Various ibuprofen suspensions were successfully processed. Thereby it was shown that the granulation behaviour between ibuprofen suspension feed and traditional ibuprofen dry blend feed in twin-screw wet granulation is comparable. Moreover, comparable granules properties were obtained from both process setups (Hausner ratio, granule morphology). However, potential differences could have been diminished by attrition and breakage of granules in the selected fluidised-bed drying. Another comparison with a more gentle drying process would therefore be of great interest. For comparable granule batches from both processes, the compressibility was comparable. However, minor differences were shown in the compact properties. Compacts of granules from the ibuprofen suspension feed showed a slightly improved compaction behaviour (increased tensile strength/decreased out-of-die porosity), which in turn also led to a slightly prolonged disintegration time and dissolution of ibuprofen compacts. However, dissimilarities were found not crucial for process and product development. Hence, ibuprofen suspension feed in twin-screw wet granulation is comparable to traditional ibuprofen dry blend feed and can therefore be used to link chemical and pharmaceutical continuous manufacturing.

However, when API suspension feed is investigated in twin-screw wet granulation for stand-alone process development, deviations in the granulation behaviour may be obtained due to the use of a suspending or wetting agent. The suspending or wetting agent may be needed to improve the wetting and to stabilise the suspension. For sodium pyrophosphate and polysorbate 80, it was shown that the use of a suspending or wetting agent in the formulation can affect the dissolved fraction of solid components in the granulation liquid significantly. Thereby, variation may be introduced in the granulation process. The higher the dissolved fraction of solid components was found in the granulation liquid, the less liquid was needed to induce particle agglomeration.

3.3 In-barrel-drying

3.3.1 Background and objectives

In this chapter, it was studied how to unify drying and twin-screw wet granulation with API suspension feed. It was investigated if drying efforts could be limited by already utilising the TSG for drying of wet granules. It was hypothesised, that by heating certain parts of the equipment with unusual and drastic conditions, wet granulation and (pre-) drying could be combined inside the barrels, from now on referred to as in-barrel-drying.

Therefore, the objectives were to investigate:

- the feasibility of in-barrel-drying in a TSG. A process is evaluated to achieve robust in-barrel-drying.
- critical factors and their appropriate ranges in in-barrel-drying to receive (pre-) dried granules. A screening DOE is used.
- the identified ranges and combinations further to improve modelling and the predictive power. An optimisation DOE is used.
- a merged process of API suspension feed and in-barrel-drying in twin-screw wet granulation. It is studied, if in-barrel-drying could be used to overcome extensive drying efforts after the granulation or even eliminate it.
- granule (granule size distribution, flowability, morphology) and compact properties (tensile strength, out-of-die porosity, disintegration time) from twin-screw wet granulation with API suspension feed and in-barrel-drying and to compare it against the traditional processes twin-screw wet granulation with API dry blend feed and fluidised-bed drying.

3.3.2 Evaluation of the in-barrel-drying process setup

In order to assess the feasibility of in-barrel-drying in twin-screw wet granulation, a robust process had to be developed. As in any other drying processes, one crucial aspect of in-barrel-drying is the successful discharge of moisture. This removal of the vaporised liquid poses challenge, due to the high resulting gas volume. It will significantly trigger the drying rate of the process. Another process that can be operated in a TSG is hot melt extrusion. For some of such processes, water is evaporated to decrease the moisture content of polymers. Thereby process fluctuations are reduced in the machine torque and/or in the pressure at the die (135). The lower variation hence results in an increased product quality. For venting in hot melt extrusion, degassing vent ports are used (Figure 33). Thus, their application was also tested for the in-barrel-drying. The difference is the much higher gas volume in the wet granulation case.



Figure 33: (a) Degassing vent ports, installed on the upper barrel in the zone of evaporation. (b) Bottom-view of a degassing vent port.

In a set of experiments, the application of degassing vent ports was tested to discharge evaporated granulation liquid during in-barrel-drying (details on the used methodology are listed in sections 2.2.1.2 (screening of API suspensions and preparation of the granulation liquid), 2.2.1.3 (twin-screw wet granulation and in investigating in-barrel-drying)). There to, a 35 % w/w lumefantrine suspension was tested in a setup using three barrel zones as evaporation zone, which were operated at a temperature of 200 °C. Degassing vent ports were installed in all three barrel zones of the evaporation zone. The suspension was processed at various liquid mass flow rates, in order to assess different drying requirements. It was observed, that at high liquid mass flow rates above 800 g/h, the material was conveyed successfully along all degassing vent ports. However, the processed mass of water per unit of time was probably too high, since the material was obtained still as a suspension. For a lower liquid mass flow rate of 350 g/h, the material was successfully conveyed along the first degassing vent port, but accumulated in the second port. Less than 20 seconds thereafter, material accumulation was also observed for the third and last degassing vent port. Both venting ports got clogged. A sufficient discharge of moisture failed therefore. At a liquid mass flow rate of 200 g/h, the first degassing vent port got clogged immediately. Less than 20 seconds thereafter, the second port got clogged and another few seconds later

Results and Discussion

the third port got clogged (Figure 34). It is hypothesised, that the accumulation of material in the degassing vent ports can be attributed to the material properties in the process. When the material was found relatively dry or still suspended in the liquid (material behaved liquid-like), it was conveyed along the degassing vent ports successfully. However, when the material behaved solid-like, but was still containing a high level of moisture, it behaved cohesively and accumulated in the ports. Such behaviour was already observed for the paste formation in twin-screw wet granulation and has been used to assess the upper L/S ratio boundary for the granulation window (section 3.1.3). No robust process was achieved for in-barrel-drying using degassing vent ports.



Figure 34: Material accumulation in the degassing vent ports. Over time ports got clogged and evaporation of water failed.

The previous described hypothesis was supported by similar observations that were made, when MCC was processed as solid and water was added as granulation liquid in in-barrel-drying. At an L/S ratio of 3.6 and a barrel temperature of 150 °C in the evaporation zone, the material was conveyed successfully along the first degassing vent port (material was suspended and behaved liquid-like), but got then accumulated in the second and immediately thereafter in the third degassing vent port (material behaved solid-like and contained a high level of moisture). For an L/S ratio of 0.6, the material was conveyed successfully along all three degassing vent ports (material contained low level of moisture).

Subsequently, two hypotheses were formed and investigated to resolve the material accumulation and to ensure the discharge of evaporated water in in-barrel-drying. First, it was hypothesised that a suboptimal material transport provided opportunity for the material to interact with the barrel surface and to accumulate in the port. Second, it was hypothesised that the design of the degassing vent port triggered the material accumulation.

To investigate the first hypothesis, screw elements were exchanged in the venting zone. Common CEs were exchanged by either long helix CEs or wide throat elements (Figure 35). Both screw elements are specifically designed to optimise material transport, for example in the zone of solid feeding. Since wide

Results and Discussion

throat screw elements are not available for the lab-scale TSG Pharma 11 mm, the test of these screw elements was conducted on a TSG Pharma 16 mm. For both modifications of the screw design it was found, that material still accumulated in the degassing vent port and was clogging it finally. The evaporation of water and thereby the in-barrel-drying failed.



Figure 35: (a) Conveying screw elements with a small pitch size (right-hand side) and long helix conveying screw elements with a larger pitch size (left-hand side). (b) Wide throat elements.

The second hypothesis was tested by evaluating two alternatives for the degassing vent port. First, it was evaluated if material agglomeration could be prevented by disassembling the port in the barrel zone completely and run the equipment with an open port (Figure 36a). It was assumed that thereby the pressure was decreased, which could have pushed material into the degassing vent port (larger opening, less pressure of evaporating vapour). Second, it was evaluated if material agglomeration could be prevented by using a liquid nozzle adapter port (Figure 36b and c). The port was assembled without nozzle and provided only a narrow opening for degassing. It was assumed that by the smaller opening and the positioning of the opening, the material flow could be better directed along the evaporation zone

(improved material transport). For both tested options, it was found that material still accumulated in the opening of the port. Thereby no robust processing of in-barrel-drying was obtained.

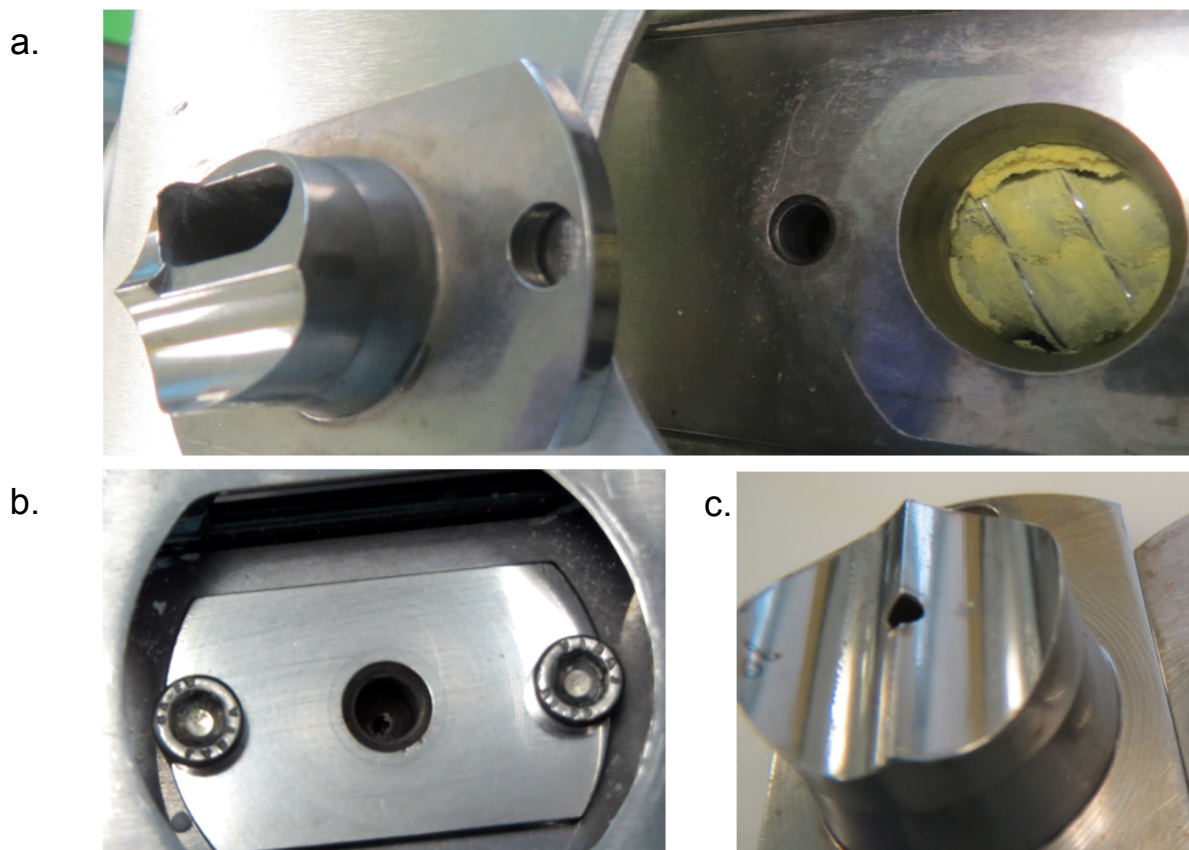


Figure 36: (a) Disassembling of a degassing vent port. The equipment was run with an open port. (b) Top-view of a liquid nozzle adapter port without a nozzle attached to it. (c) Bottom-view of a liquid nozzle adapter port.

In a final attempt, it was studied if in-barrel-drying could be operated successfully, having all ports closed in the barrel zones. For degassing of the evaporated water the natural opening at the TSG exit was used. Indeed, it was found that all water vapour could be discharged from the system via the natural opening at the TSG exit. Thereby water was evaporated sufficiently and the product LOD of the material was reduced. For example, for the 35 % w/w lumefantrine suspension that has been processed, the product LOD was reduced from 65 % w/w to 14 % w/w (liquid mass flow rate was 350 g/h; evaporation zone temperature was 200 °C). Although such process setup may have a limited degassing efficiency (relatively small single opening at the TSG exit) and thereby may diminish the drying rate, a robust in-barrel-drying was observed (Figure 37).



Figure 37: The in-barrel-drying process for lumefantrine. Water was evaporated via the opening at the TSG exit.

3.3.3 Characterising the in-barrel-drying process

Parts of this section are submitted for publication in the research article “Continuous single-step wet granulation with integrated in-barrel-drying.”

In order to characterise the in-barrel-drying, critical factors and their appropriate ranges to receive (pre-) dried granules were studied for a lumefantrine formulation (blend feed) by using DOE (Table 3). Details on the used methodology are listed in the sections 2.2.1.3 (twin-screw wet granulation and in investigating in-barrel-drying), 2.2.2.1 (particle size distribution of powders and granules) and 2.2.2.12 (design of experiments). First, a screening DOE was selected. A broad knowledge space was targeted (i.e. relatively wide factor ranges were chosen) (Table 6).

Results and Discussion

Table 6: Factor settings scaled for the range from -1 to +1 and obtained process responses for the screening DOE. TMMF= total material mass flow rate [g/h]; L/S ratio= liquid-to-solid mass flow ratio; ScSp= screw speed [rpm]; Temp. Pre= temperature in the pre-heating zones [°C]; Temp. Eva= temperature in the evaporation zones [°C]; CP= centre point.

Factors						Responses				
Exp.	TMMF [g/h]	L/S ratio	ScSp [rpm]	Temp. Pre [°C]	Temp. Eva [°C]	Product LOD [% w/w]	Evapor. mass H ₂ O [g/h]	X ₅₀ [µm]	Product temp. [°C]	Drying efficiency [%]
Range	240 - 500	0.6 - 1.0	50 - 350	20 - 100	160 - 200	3.2 - 35.4	59 - 198	167 - 467	58 - 89	45 - 97
1	500	1.0	350	20	160	35.4	121	423	59	45
2	240	0.6	350	20	160	19.1	59	308	62	61
3	240	1.0	50	20	160	27.5	78	467	58	62
4	500	0.6	50	20	160	23.9	98	253	63	48
5	370	0.8	200	60	160	29.6	84	413	64	47
6	240	1.0	350	100	160	24.1	85	274	63	68
7	500	1.0	50	100	160	30.5	148	167	70	56
8	500	0.6	350	100	160	22.4	106	350	66	52
9	240	0.6	50	100	160	12.2	73	333	63	77
10	370	0.8	200	20	180	24.9	102	445	68	58
11 _{CP}	370	0.8	200	60	180	24.4	104	317	67	63
12 _{CP}	370	0.8	200	60	180	25.4	101	283	66	58
13 _{CP}	370	0.8	200	60	180	25.7	99	385	63	57
14	240	0.8	200	60	180	20.9	75	394	63	67
15	500	0.8	200	60	180	28.2	122	456	66	51
16	370	0.6	200	60	180	17.7	95	352	64	64
17	370	1.0	200	60	180	28.1	118	383	64	61
18	370	0.8	50	60	180	19.6	120	393	59	70
19	370	0.8	350	60	180	23.9	106	418	62	61
20	370	0.8	200	100	180	22.6	110	445	64	64
21	240	0.6	50	20	200	3.2	88	325	89	95
22	500	1.0	50	20	200	20.5	198	372	65	74
23	500	0.6	350	20	200	20.0	118	348	72	58
24	240	1.0	350	20	200	22.3	89	397	60	71
25	370	0.8	200	60	200	20.7	116	412	64	67
26	500	0.6	50	100	200	7.5	170	273	85	91
27	240	1.0	50	100	200	4.9	117	297	84	97
28	240	0.6	350	100	200	6.2	84	169	88	93
29	500	1.0	350	100	200	24.4	176	308	64	71

Results and Discussion

All process responses were shown sensitive to the investigated factor ranges. After model refinement, models were obtained that were descriptive, predictive, significant and reproducible for all process responses (Table 7). Models of the product LOD, evaporated mass of water and drying efficiency showed a high descriptive and predictive power, whereas models of product temperature and granule size x_{50} were shown valid and applicable, at least for indicating trends, but with less descriptive and predictive power. For the product temperature, this could be attributed to the applied measurement method (e.g. the product temperature decreased rapidly after the material exited the granulator). For the model of the granule size x_{50} , the lower descriptive and predictive power could be a result of a lower reproducibility. The increased experimental variation thereby could be explained by the uncommon high temperatures in the granulator. For example, higher pre-heating zone temperatures could have influenced the evaporation of at least some of the granulation liquid and thereby impacted the particle agglomeration (i.e. increasing evaporation of the binder water and thereby less particle agglomeration). More variability could have been introduced. Further, the model of the granule size x_{50} could have been impacted by mechanical and/or other stress (caused by the rapid heating and water evaporation) during in-barrel-drying. Granule breakage during the drying may have diminished initial differences in the wet granule size between the process settings, impacting modelling and the model quality. The obtained bimodal particle size distribution could be an indication for this, although it is commonly reported for granules received from twin-screw wet granulation processes (granule size distributions of individual experiments are attached in the appendix; Figure). However, for all process responses, statistically significant models were implemented successfully to analyse the effects of investigated factors.

Table 7: Summary of model fit for the screening DOE after model refinement.

Process response	Goodness of fit (R^2)	Goodness of prediction (Q^2)	Model validity	Reproducibility
Quality parameter	>0.50	>0.50	>0.25	>0.50
Product LOD	0.99	0.97	0.70	0.99
Evapor. mass H ₂ O	0.99	0.96	0.67	0.99
Drying efficiency	0.98	0.95	0.95	0.95
Granule size x_{50}	0.76	0.54	0.84	0.75
Product temp.	0.81	0.60	0.57	0.94

In the following paragraphs, the critical factor terms were evaluated for all five process responses. First, the drying operation of the in-barrel-drying was described by the responses product LOD, evaporated mass of water and drying efficiency. Second, the product temperature as a potentially critical process response for the product quality was evaluated in detail. Third, the granule size x_{50} was studied to describe the granulation operation of the in-barrel-drying. Finally, the results of product LOD and granule

Results and Discussion

size x_{50} were evaluated in combination, since both are considered crucial for successful drying and granule formation.

The process responses product LOD, evaporated mass of water and drying efficiency were analysed together. All three responses are highly correlated with each other. However, they all emphasise different aspects of the in-barrel-drying. The evaporated mass of water stresses the drying performance in absolute numbers per unit of time. The drying efficiency evaluates the previously described drying performance in relation to the highest possible amount of water to evaporate. Finally, the product LOD focusses on the residual amount of water in the product, and is of relevance for further processing.

For all three process responses, main effects of all investigated factors were observed (Figure 38). For the product LOD and the drying efficiency, the strongest main effect was the evaporation zone temperature. For the evaporated mass of water, only the total material mass flow rate showed a stronger effect than the evaporation zone temperature. It was found, that with increasing evaporation zone temperature, the evaporated mass of water increased. Subsequently, the drying efficiency increased and the product LOD decreased. This by itself is not surprising, since a higher barrel zone temperature increases the temperature difference between material and barrel, and thereby increases the heat-transfer and consequently water evaporation (136). A similar effect was observed for the pre-heating zone temperature, but less pronounced because of lower selected temperature ranges (limited water evaporation was targeted in those zones). Moreover, it was observed that by increasing the L/S ratio, the evaporated mass of water was increased, but the drying efficiency was decreased and the product LOD was increased. By increasing the L/S ratio, the processed mass of water is increased. Since the liquid density is higher than the density of a bulk powder and since the powder material is typically densified by increasing amounts of liquid, it is assumed that overall the material density in the TSG was increased with increasing L/S ratios. Thereby the contact surface between material and barrel was increased. Consequently, the heat-transfer was improved and the evaporated mass of water was increasing. However, by increasing the L/S ratio, more water was introduced than the process can manage for water evaporation (higher energy requirements for the evaporation of all the water). Hence, the drying efficiency was decreasing and the product LOD was increasing. A comparable effect was observed for the total material mass flow rate. Increasing values for the total material mass flow rate resulted in an increase of the evaporated mass of water, a decrease of the drying efficiency and an increase of the product LOD. By changing the total material mass flow rate, the TSG fill-level was impacted, which in turn affected the contact surface between material and barrel (heat-transfer) and the material volume that has to be heated (energy requirements for heating and evaporating water) simultaneously. If the TSG is imagined as two tube channels, typically a more favourable ratio between the material contact surface with the barrel and the material volume in the TSG would be obtained at low TSG fill-level (e.g. at low total material mass flow rates) (impact of heating and mixing by the two screws is not considered). With increasing the total material mass flow rate, the overall heat-transfer was increased and more water was evaporated

Results and Discussion

(evaporated mass of water was increasing). But simultaneously, more water was introduced to the in-barrel-drying process than it can manage for water evaporation. Additionally, a less favourable ratio between the material contact surface with the barrel and the material volume in the TSG was obtained. Consequently, the drying efficiency was decreasing and the product LOD was increasing. The effect of the screw speed is rather complex, since it impacts the previous described TSG fill-level and the residence time (drying time) of the material in the process at the same time. For example, by increasing the screw speed, the TSG fill-level and the residence time of the material in the TSG were decreased. Although it is assumed that by decreasing the TSG fill-level a more favourable ratio between the material contact surface with the barrel and the material volume would be obtained, the overall heat-transfer is decreasing. Moreover, the decreasing material residence time emphasises the decrease in heat-transfer (less time for heating and evaporating water) (101). As a result, the evaporated mass of water decreases with increasing screw speed, which in turn led to a decreasing drying efficiency and an increasing product LOD.

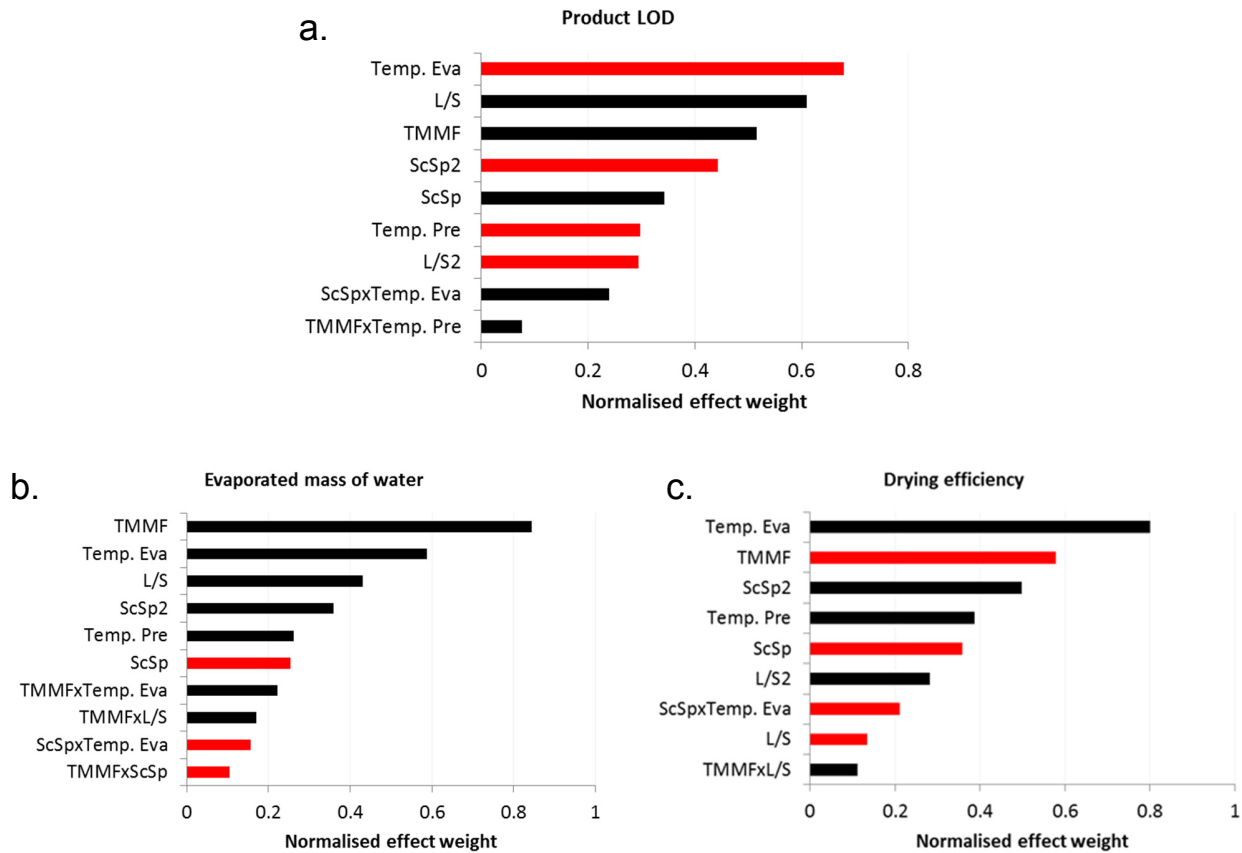


Figure 38: (a) Pareto plot of significant effects on the process response product LOD. A minus (red bar) / plus (black bar) main effect of a factor thereby represents a decrease/increase in the process response, when the factor is increased from its low level to its high level, while the other factors remain constant on their centre level.; a x b= interaction effect between factor a and b.; a²= square effect of factor a.; TMMF= total material mass flow rate; L/S= liquid-to-solid mass flow ratio; ScSp= screw speed; Temp. Pre= temperature in the pre-heating zone; Temp. Eva= temperature in the evaporation zone. (b) Pareto plot of significant effects on the process response evaporated mass of water. (c) Pareto plot of significant effects on the process response drying efficiency.

Moreover, one interaction effect was found significant for all three process responses related to water evaporation. The interaction effect was shown between the screw speed and the evaporation zone temperature. The effect of increasing evaporation zone temperature to increase the evaporated mass of water and the drying efficiency, as well as to decrease the product LOD, was found emphasised at low screw speed, compared to high screw speed (Figure 39). This effect can be attributed to an additive positive effect on the heat-transfer by an increased residence time/TSG fill-level (decreasing screw speed) and a higher temperature difference between material and barrel (increasing evaporation zone temperature). Consequently, a higher mass of water was evaporated, the drying efficiency was increased and the product LOD was decreased. At high screw speed on the other hand, the residence time was

Results and Discussion

shorter and the TSG fill-level was lower. Thereby, the overall increase in the heat-transfer was lower. Thus, a lower increase in the evaporated mass of water was obtained, which in turn led to a lower increase in the drying efficiency and to a lower decrease of the product LOD.

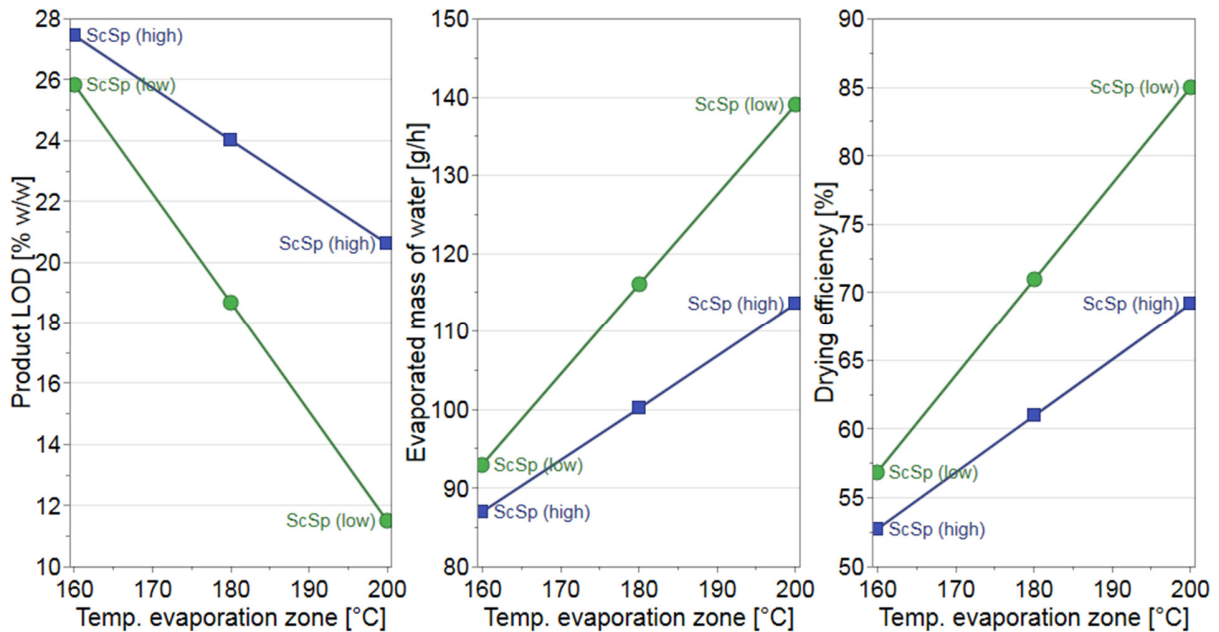


Figure 39: Interaction effect between the screw speed (ScSp) and the evaporation zone temperature for the process responses product LOD, evaporated mass of water and drying efficiency.

Another interaction effect was found significant only for the responses evaporated mass of water and drying efficiency. The interaction effect was obtained between the total material mass flow rate and the L/S ratio. The effect of increasing total material mass flow rate to increase the evaporated mass of water is emphasised at high L/S ratios, compared to low L/S ratios. Thereby, the decrease in the drying efficiency was lower. This effect can be attributed to an additive positive effect on the heat-transfer. By increasing the total material mass flow rate, also the TSG fill-level is increased. Moreover, it is hypothesised that the material density in the TSG is higher at high L/S ratios, compared to low L/S ratios. Both result in an increased heat-transfer and thereby in an increased evaporated mass of water. The drying efficiency is decreasing less. At low L/S ratio, the material density in the TSG is hypothesised to be lower. The heat-transfer is increasing less, as well as the evaporated mass of water. The decrease in the drying efficiency is higher. This interaction effect was not significant for the product LOD. Probably, the change in the evaporated mass of water was too low in relation to the processed mass of solids (which results in minor changes in the product LOD).

Results and Discussion

Furthermore, interaction effects were observed for either one of the process responses product LOD or evaporated mass of water. For the product LOD, an interaction effect was found between the total material mass flow rate and the pre-heating zone temperature. The effect of increasing pre-heating zone temperature to decrease the product LOD was more pronounced at low total material mass flow rate, than at high total material mass flow rate. At low total material mass flow rate, lower amounts of water are processed that need to be heated before evaporation and a more favourable ratio between the material contact surface with the barrel and the material volume in the TSG is obtained. Additionally, the heat-transfer is emphasised at higher pre-heating zone temperature. Hence, the described interaction effect is an additive effect of an increased heat-transfer (higher pre-heating zone temperature), lower energy requirements for heating water before evaporation and a more favourable ratio between the material contact surface with the barrel and the material volume in the TSG (lower total material mass flow rate). Thus, more water is evaporated and the product LOD is decreasing. At high total material mass flow rate, higher amounts of water require more energy for heating before water evaporation and the ratio between material contact surface with the barrel and the material volume in the TSG is less favourable. Thereby the increase in heat-transfer by increasing pre-heating zone temperature was of less effect. A similar interaction effect was observed for the evaporated mass of water. But instead of the pre-heating zone temperature, this effect was found between the evaporation zone temperature and the total material mass flow rate. A last interaction effect was found for the evaporated mass of water between the factors total material mass flow rate and the screw speed. The effect of increasing total material mass flow rate to increase the evaporated mass of water was emphasised at low screw speed, compared to high screw speed. This effect was attributed to an additive positive effect on the heat-transfer by an increased contact surface between material and barrel (increasing TSG fill-level by increasing total material mass flow rate/decreasing screw speed) and an increasing residence time (decreasing screw speed). At high screw speed, the residence time was shorter and the TSG fill-level lower. Therefore the increase in heat-transfer was lower.

Finally, a square term of the screw speed was found significant for all three process responses, whereas another square term of the L/S ratio was found significant only for the product LOD and the drying efficiency. It was shown, that with increasing screw speed the evaporated mass of water and the drying efficiency initially decreased rapidly (for the product LOD: increased), before the gradient of the function constantly increased (for product LOD: decreased). For the screw speed, the square effect could be attributed to the simultaneous effect on the residence time and the TSG fill-level. With increasing screw speed, the material is conveyed faster. The residence time (drying time) and the TSG fill-level are decreasing. Although thereby the overall heat-transfer was decreased, a lower material volume had to be heated and a more favourable ratio of the material contact surface with the barrel and the material volume in the TSG was obtained (lower TSG fill-level). At higher screw speed, the overall decrease in the evaporated mass of water and the drying efficiency, and the overall increase in the product LOD (= described main effects) are increasingly compensated by a lower material volume that had to be heated

Results and Discussion

and a more favourable ratio of the material contact surface with the barrel and the material volume in the TSG (= square effect). For increasing L/S ratios, it was observed that the drying efficiency initially decreased rapidly (for the product LOD: increased), before the gradient of the function constantly increased (for product LOD: decreased) (Figure 40). Increasing values for the L/S ratio, lead to an increase in the processed mass of water and hence to an increase in the required energy to heat water before evaporation. Simultaneously, it is hypothesised that the density of the material in the TSG increases with increasing L/S ratios. Thereby, the contact surface between material and barrel increases and the heat-transfer is emphasised. The evaporated mass of water increases. However, with increasing L/S ratio, more water is introduced than the process can manage for water evaporation. The drying efficiency decreases and the product LOD increases rapidly. At higher L/S ratio, the overall decrease in the drying efficiency and the overall increase in the product LOD (= described main effect) are increasingly compensated by an emphasised heat-transfer and water evaporation (= square effect). The negative gradient of the drying efficiency and the positive gradient of the product LOD as function of the L/S ratio were decreasing.

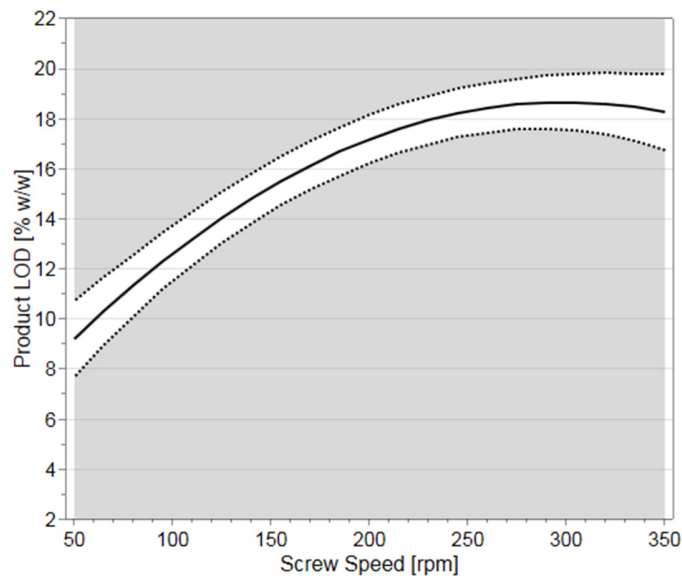


Figure 40: Square effect of the screw speed on the product LOD, visualised by a prediction plot. (process settings: total material mass flow rate= 370 g/h; L/S ratio= 0.8; Screw speed= 50 - 350 rpm; pre-heating zone temperature= 100 °C and evaporation zone temperature= 200 °C).

The next process response was the product temperature. For this response, main terms were shown from the pre-heating zone temperature, the evaporation zone temperature, the L/S ratio and the screw speed (Figure 41). With increasing the temperatures in the barrel zones, the product temperature was increasing. This finding is not a surprise, since increasing barrel zone temperatures enhance the heat-transfer (higher temperature difference between material and barrel). Furthermore, it was observed that

Results and Discussion

increasing the L/S ratio led to a decrease in the product temperature. Also this observation is line with the expectations. Increasing L/S ratios lead to increasing processed amounts of water. Thus, more energy is consumed by heating water and water evaporation. Less energy is provided to heat the product. Finally, it was shown that increasing the screw speed decreases the product temperature. This effect is associated with the impact of the screw speed on the material residence time in the TSG and the TSG fill-level. Increasing screw speed decreases the drying time, as well as the TSG fill-level (lower contact surface between material and barrel). Both results in a decrease of the heat-transfer.

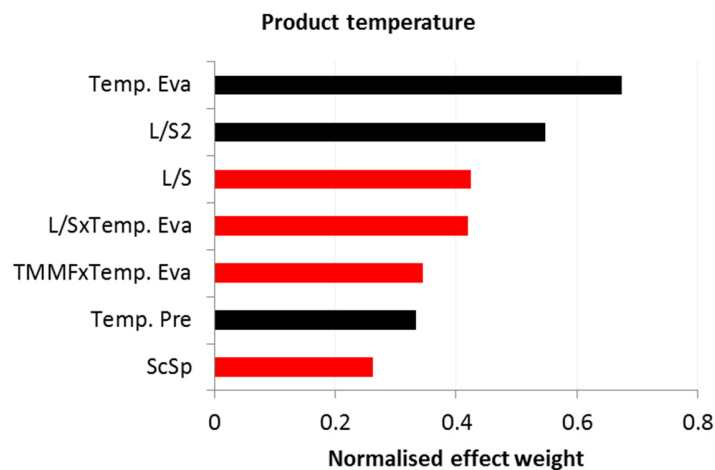


Figure 41: Pareto plot of significant effects on the process response product temperature. A minus (red bar) / plus (black bar) main effect of a factor thereby represents a decrease/increase in the process response, when the factor is increased from its low level to its high level, while the other factors remain constant on their centre level.; a x b= interaction effect between factor a and b.; a²= square effect of factor a.; TMMF= total material mass flow rate; L/S= liquid-to-solid mass flow ratio; ScSp= screw speed; Temp. Pre= temperature in the pre-heating zone; Temp. Eva= temperature in the evaporation zone.

Two interaction terms were found, namely between the evaporation zone temperature and either the L/S ratio or the total material mass flow rate. The effect of increasing evaporation zone temperature to increase the product temperature is emphasised at low L/S ratios (compared to high L/S ratios) or at low total material mass flow rate (compared to high total material mass flow rate) respectively. As already described for the main effect of the L/S ratio on the product temperature: the more water is processed, the more energy is consumed for heating and evaporating water, and the less the product is heated. In this case, less water is processed. Thus, the interaction effects are an additive effect of a higher heat-transfer (higher evaporation zone temperature) and less energy consumption by heating and evaporating water. Consequently, the product is increasingly heated and the product temperature increases. At high L/S ratios or total material mass flow rate, more energy is consumed for heating and evaporating water. Thereby, the product is heated less and the product temperature increases less.

Results and Discussion

Finally, one square term was observed from the L/S ratio. With increasing L/S ratio, the product temperature was initially decreasing rapidly, before the negative gradient was decreasing at higher L/S ratios. As described in the sections before, with increasing L/S ratio multiple conditions change simultaneously. With increasing L/S ratio, the processed mass of water increases and in addition it is hypothesised that the material density increases and thereby the contact surface between material and barrel (increasing heat-transfer). Initially, with increasing L/S ratio, increasing amounts of energy were consumed for heating and evaporating increasing amounts of water. As a consequence, the product was heated less and the product temperature was decreasing (= main effect). At higher L/S ratios, the heat-transfer was increasingly emphasised and the product temperature was decreasing less (= square effect).

For the granule size x_{50} , main effects were observed for the factors L/S ratio and pre-heating zone temperature (Figure 42). The L/S ratio is one of the most crucial process parameter for inducing particle agglomeration in twin-screw wet granulation (55). Therefore, it is obvious that increasing L/S ratios increased the granule size x_{50} . However, the pre-heating zone temperature triggers the evaporation, at least of some of the water, leading to a lower L/S ratio in the process and hence decreases the granule size x_{50} .

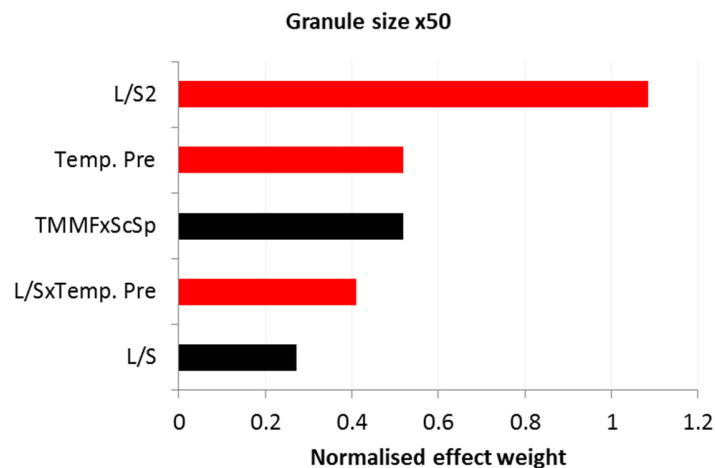


Figure 42: Pareto plot of significant effects on the process response granule size x_{50} . A minus (red bar) / plus (black bar) main effect of a factor thereby represents a decrease/increase in the process response, when the factor is increased from its low level to its high level, while the other factors remain constant on their centre level.; a x b= interaction effect between factor a and b.; a²= square effect of factor a.; TMMF= total material mass flow rate; L/S= liquid-to-solid mass flow ratio; ScSp= screw speed; Temp. Pre= temperature in the pre-heating zone.

Furthermore, two interaction effects were found: one between the total material mass flow rate and the screw speed, another one between the L/S ratio and the pre-heating zone temperature. At increasing total material mass flow rate combined with a high screw speed, the granule size x_{50} was increasing

Results and Discussion

(Figure 43). However, at increasing total material mass flow rate combined with a low screw speed, the granule size x_{50} was decreasing. The TSG fill-level increases with increasing the total material mass flow rate. At low screw speed, the TSG fill-level increases further. According to literature, the fraction of coarse particles should increase at increasing TSG fill-level (96). Granules would therefore be expected even coarser at low screw speed than at process settings with high screw speed. However, it could be that granules initially became coarser, before they were milled more intensively in the zone of distributive flow elements at the screw end and broke apart into smaller, polydisperse granules. Milling effects of distributive flow elements have been described in literature (94). This could have then led to an overall decrease in the granule size x_{50} at low screw speed. Moreover, breakage of initially coarser wet granules could have been emphasised additionally by a high stress during drying (e.g. mechanical stress, stress from very high temperatures and rapid water evaporation). The effect of increasing pre-heating zone temperature to decrease the granule size x_{50} was emphasised at high L/S ratios, compared to low L/S ratios. As described previously, increasing the pre-heating zone temperature leads to the evaporation of at least some of the water and hence decreases the L/S ratio (and particle agglomeration). Since intensive particle agglomeration can be observed especially at higher L/S ratios, the effect of increasing pre-heating zone temperatures is higher at high L/S ratio.

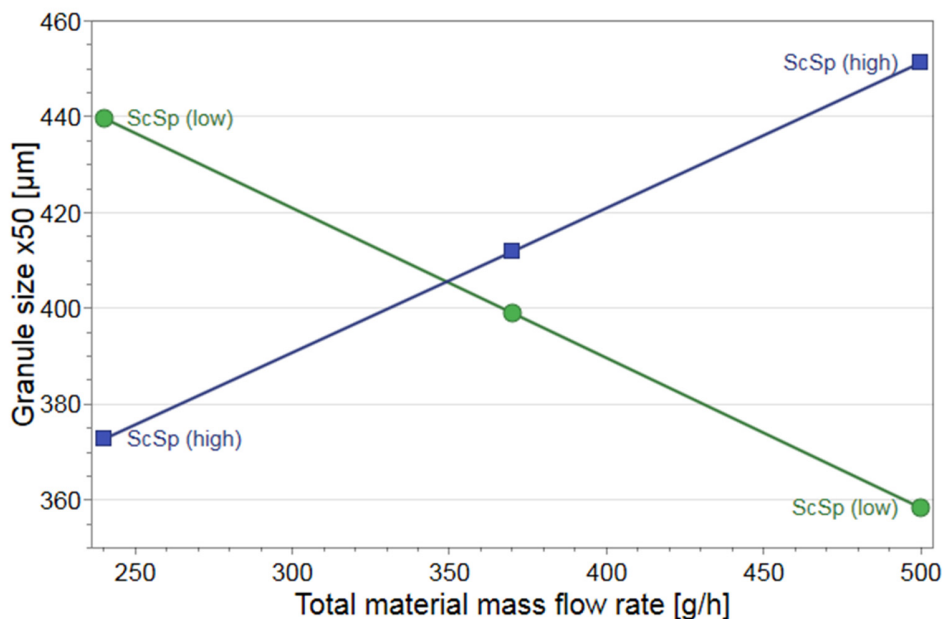


Figure 43: Interaction effect between the total material mass flow rate and the screw speed (ScSp) on the process response granule size x_{50} .

Finally, a square effect was observed for the L/S ratio. With increasing L/S ratio it was found, that the granules size x_{50} was constantly increasing up to a certain L/S ratio. At higher L/S ratios, the granule size x_{50} was decreasing. As described in the previous section, one explanation could be that the granule size

Results and Discussion

was constantly increasing with increasing L/S ratios, but above certain L/S ratios milling was emphasised in the zone of distributive flow elements at the screw end. By milling, granules may have broken apart into smaller, polydisperse granules. Thereby, the granule size x_{50} was decreasing again above particular L/S ratios.

Most of above described effects on the granule size x_{50} can be visualised in a single contour plot (Figure 44). The main effect of the L/S ratio to increase the granule size x_{50} is shown in vertical direction, whereas the main effect of the pre-heating zone temperature to decrease the granule size x_{50} is displayed in horizontal direction. The main effect of the pre-heating zone temperature is emphasised especially at higher L/S ratios (e.g. at an L/S ratio of 0.8), which reflects the interaction effect between L/S ratio and pre-heating zone temperature. The square effect of the L/S ratio on the granule size x_{50} is reflected in the curvature and is emphasised at higher L/S ratios.

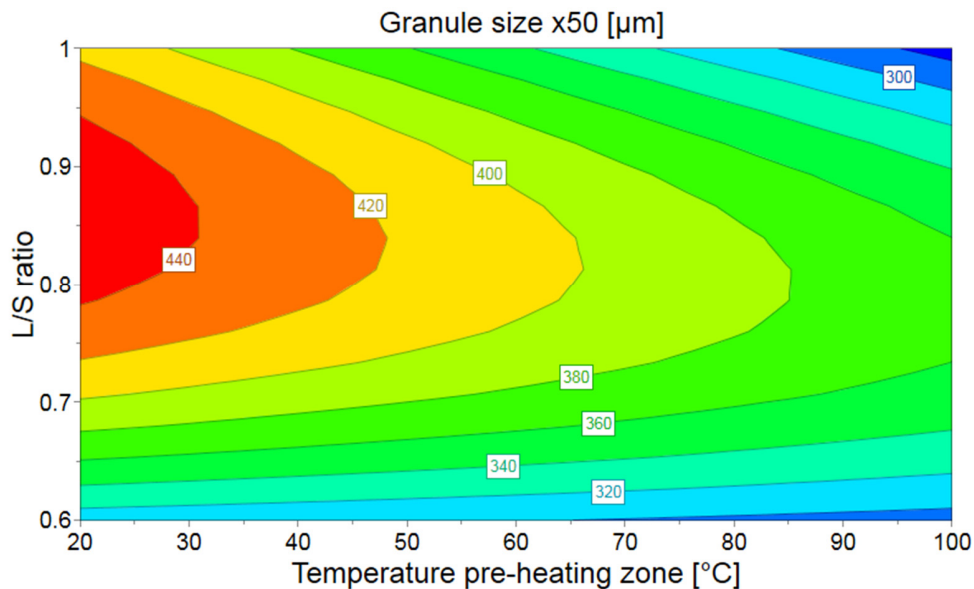


Figure 44: Contour plot of the granule size x_{50} for the factor settings L/S ratio 0.6 - 1.0, pre-heating zone temperature 20 - 100 °C, total material mass flow rate 370 g/h, screw speed 200 rpm and evaporation zone temperature 180 °C.

Combining the two aims of achieving particle agglomeration and a low product LOD simultaneously raised challenges. On the one hand, certain water amounts are required to initiate particle agglomeration (137). On the other hand, increasing amounts of water may decrease the drying efficiency and hence increase the resulting product LOD. The described situation was reflected in the pareto plots of the two process responses product LOD and granule size x_{50} (Figure 38a and Figure 42). Most main and square effects, which were beneficial for increasing the granule size x_{50} , simultaneously increased the product

Results and Discussion

LOD (main effects of the L/S ratio and the pre-heating zone temperature, square effect of the L/S ratio). Only the evaporation zone temperature was shown to be beneficial to achieve dry granules, while still ensuring particle agglomeration. This indicates that after granules were formed in a first compartment of the TSG (pre-heating zone), the temperature in the evaporation zone was not anymore of relevance for their size. This makes the evaporation zone temperature one of the key parameter for in-barrel-drying. Another beneficial range for achieving wet granulation combined with drying was indicated at low total material mass flow rate, L/S ratio and screw speed. However, this would limit the material throughput of the entire manufacturing line.

A crucial process boundary in in-barrel-drying, as in any other drying operation, is the product temperature in relation to the material heat-stability. The product temperature was comparable at drying efficiencies from 40 to 80 % (Figure 45). When drying was even more efficient, the product temperature increased rapidly. This effect could be explained by the two phases of every drying process, the heat-transfer-limited and the mass-transfer-limited phase (64). In the initial phase of a drying process, heat-transfer limitations are predominant. The material is heated less, since energy is consumed by water evaporation. In the following mass-transfer-limited phase, remaining water has to diffuse to the particle surface first, before it can evaporate. Since thereby less energy is consumed by water evaporation, the material is heated increasingly. The product temperature increases rapidly. It has to be kept in mind, that the assessed product temperature might be not equal to the highest product temperature in the investigated process, since granules rapidly cooled down when exiting the TSG. However, high product temperatures could trigger material degradation and hence impact the product quality. An in-line control is therefore recommended. However, the duration of the high temperature for each particle is extremely short (typically a few seconds), so the risk of degradation is minimal.

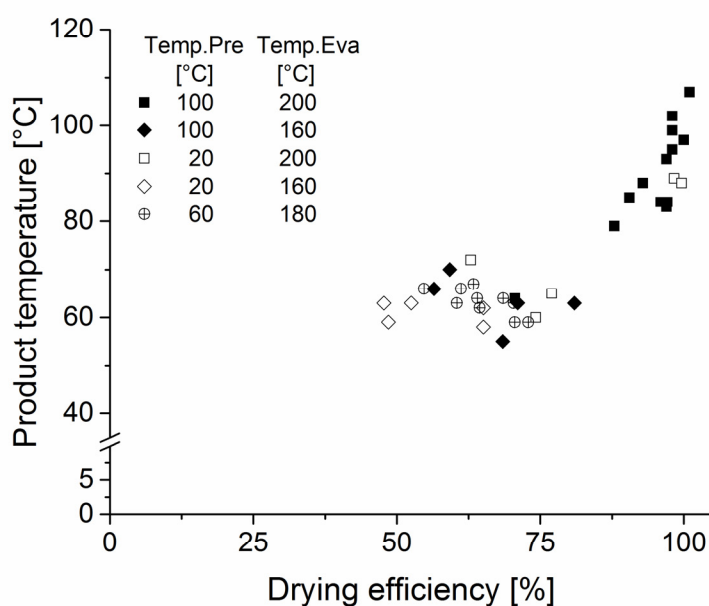


Figure 45: Product temperatures as a function of the drying efficiency. Temp. Pre= pre-heating zone temperature; Temp. Eva= evaporation zone temperature. (individual experiments)

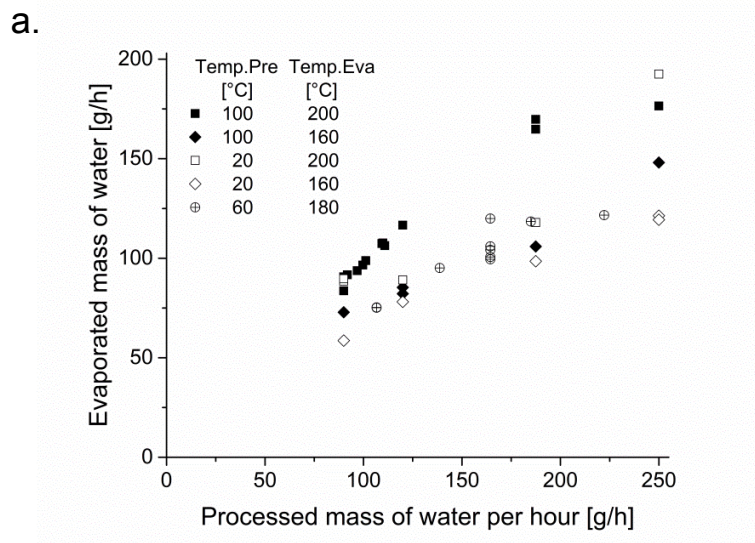
Another fact that has to be highlighted for the interpretation of effects is the confounding of factors that describe the material mass throughput and its composition. The material mass throughput and its composition can be described by the total material mass flow rate, the L/S ratio, the liquid mass flow rate or the solid mass flow rate. However, any two of these factors are enough to describe throughput and composition. Independent from the combination of factors chosen, the factors are confounded in the TSG fill-level, the residence time distribution and/or the liquid mass flow rate. Among other parameters, in a contact dryer the heat-transfer is obviously depending on the contact surface between material and barrel (i.e. the heat-transfer is influenced by the TSG fill-level). Since the liquid, solid and total material mass flow rates are highly confounded in the TSG fill-level, the total material mass flow rate was chosen together with the L/S ratio to describe the material mass throughput and its composition.

Since the L/S ratio and the total material mass flow rate are confounded in the liquid mass flow rate, for example, the drying process as function of the processed mass of water was investigated in more detail. A strong correlation was found for the evaporated mass of water as function of the processed mass of water (Figure 46a). It was demonstrated, that the more water was processed, the more water was evaporated (screw speed may have changed simultaneously, but had minor effect on this correlation). For example at a temperature profile of 100 °C in the pre-heating zone and 200 °C in the evaporation zone, the evaporated mass of water increased from 84 - 91 g/h to 176 g/h at a processed mass of water of 90 g/h and 250 g/h respectively. This observation can be attributed to an increased contact surface

Results and Discussion

between material and barrel with increasing processed amounts of water. The heat-transfer increases and thereby the evaporated mass of water. But with increasing the processed mass of water, the ratio of the material contact surface with the barrel and the material volume in the TSG becomes less favourable. Only a fraction of the processed mass of water can be evaporated.

Furthermore, it was observed that with increasing barrel zone temperature, the evaporated mass of water increased (Figure 46a). Moreover, the described small effect of the screw speed on the correlation between the processed and the evaporated mass of water was highlighted especially towards relatively low screw speeds (Figure 46b). For example, at a processed mass of water of 164 g/h, 60 °C pre-heating zone temperature and 180 °C evaporation zone temperature, a comparable mass of water was evaporated for the screw speed 200 rpm (99; 101; 104 g/h) and 350 rpm (105 g/h). However, at 50 rpm screw speed, the evaporated mass of water was increased to 119 g/h (experiments 11 - 13 and 18 - 19). Those findings correspond to the effects that were observed for the product LOD (screening DOE). With increasing temperature and decreasing screw speed, the product LOD was decreasing (increasing evaporated mass of water).



b.

Figure 46: (a) The evaporated mass of water as function of the processed mass of water per hour for various temperature profiles. The screw speed may change simultaneously, but has only a small effect on the observed correlation. Temp. Pre= pre-heating zone temperature [°C]; Temp. Eva= evaporation zone temperature [°C]. (individual experimental points); (b) Effect of the screw speed on the evaporated mass of water. The temperature profile and the processed mass of water were kept constant at 60 °C (pre-heating zone temperature), 180 °C (evaporation zone temperature) and 164 g/h (processed mass of water). (individual experimental points)

Results and Discussion

A favourable process range, for which completely dried granules were achieved, was found at high barrel zone temperatures and low total material mass flow rate, L/S ratio and screw speed (Figure 47a). For example, in experiment number 21 the powder blend (LOD= 2.2 % w/w, x_{10} = 13 μm , x_{50} = 68 μm , x_{90} = 167 μm ; (\bar{x} , n=3)) was granulated together with 38 % w/w of water. After in-barrel-drying, the powder blend was found granulated (granule size distribution at x_{10} = 79 μm , x_{50} = 325 μm , x_{90} = 1044 μm) and dried (product LOD= 3.2 % w/w) (Figure 47b). Thereby, a drying unit operation downstream the manufacturing line could possibly be omitted and the material could be tableted straight away.

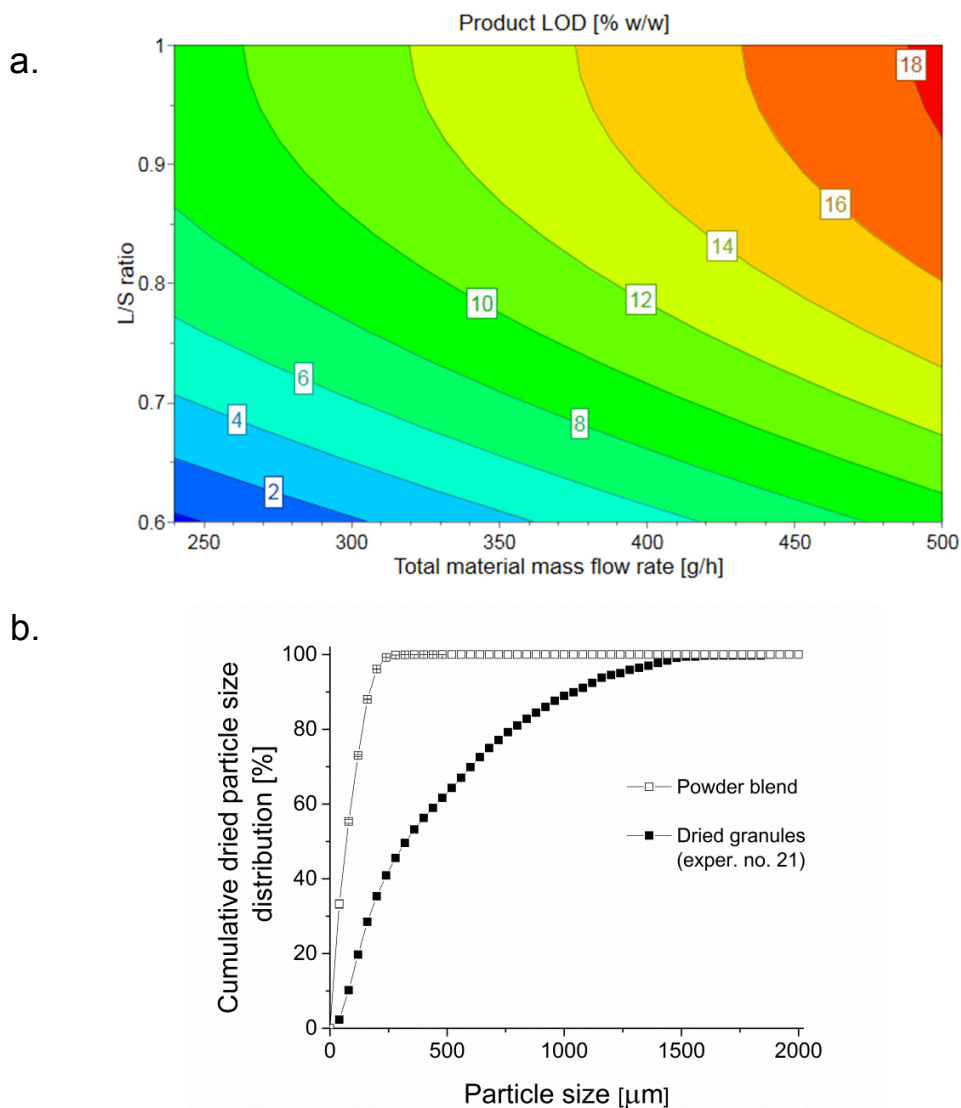


Figure 47: (a) Contour plot of the product LOD for the factor settings total material mass flow rate 240 - 500 g/h, L/S ratio 0.6 - 1.0, screw speed 80 rpm, temperature in the pre-heating zone 100 °C and temperature in the evaporation zone 200 °C. (b) Cumulative dried particle size distribution for initial powder blend ($\bar{x} \pm s$; n= 3) and for the granulated and dried material after in-barrel-drying (experiment no. 21; n= 1).

A design space was predicted for product LOD values between 1 and 4 % w/w. It was assumed, that such material could be used directly for tableting, since its LOD is comparable to the LOD value of the original powder blend. The design space for desirable LOD values was relatively narrow (Figure 48). One explanation for this finding is the constraint between drying efficiency and product temperature. Towards high drying efficiencies, the product temperature increased rapidly (Figure 45). Thereby, the lower boundary depends among other things on the heat-stability of the material. Another explanation for the finding of a narrow design space, is the predominant correlation between the evaporated and the processed mass of water (Figure 46a). For a specific parameter setting and formulation, the processed mass of water must match up with the amount of water that the equipment can evaporate. Tolerances are small. However, the design space can be varied by changing for example the barrel zone temperatures. Another influential parameter is the screw speed. By decreasing the screw speed, the residence time is increased for the material in the process. Thereby the heat-transfer is increased, which in turn increases water evaporation. The big advantage of this parameter is that it can be changed instantaneously. Thereby, the screw speed could be used to “fine-tune” and to keep control over the in-barrel-drying process.

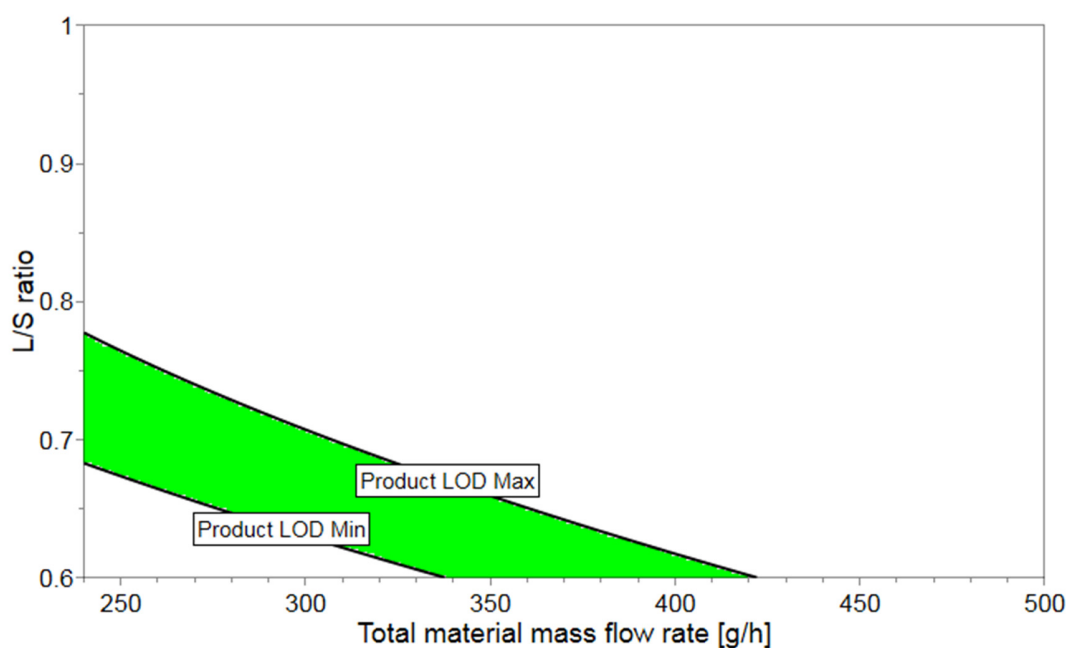


Figure 48: Design space predicted for a targeted product LOD between 1 to 4 % w/w. The factor settings were: total material mass flow rate 240 - 500 g/h, L/S ratio 0.6 - 1.0, screw speed 50 rpm, pre-heating zone temperature 100 °C and evaporation zone temperature 200 °C.

Results and Discussion

In a next step, the model of the product LOD that was obtained from the screening DOE was verified for its predictive power by using the optimizer function of the DOE software MODDE. Factor settings were predicted at a confidence interval of 95 % for three targeted product LOD values within the evaluated design space for dried granules (Figure 49). Although the model suggested a high descriptive and predictive power ($R^2= 0.99$; $Q^2= 0.97$), two predictions did not match up with the experimental observation. Possible explanations for this deviation could be the relatively low number of performed experiments, the broad knowledge space compared to the narrow design space for dried granules and/or the selection of the model design. The central composite face-centred design may be less susceptible to experimental error (all star-points are within the investigated domain). However, such process design provides the operator with lower predictive power at the edges of the domain (in this case the range of interest) and with a basic modelling of quadratic effects only, due to 3 factor levels. Therefore, the learnings of this screening DOE were taken for a follow-up optimisation DOE.

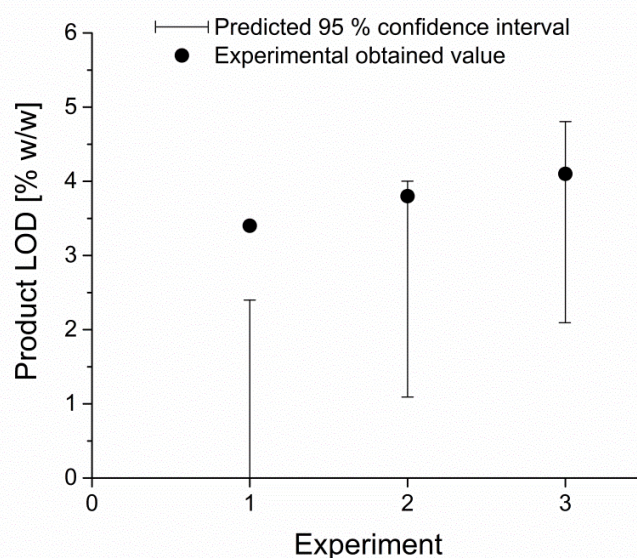


Figure 49: Use of the model of the product LOD, that was obtained from the screening DOE. Predictions for three targeted LOD values at a confidence level of 95 % are shown together with the product LOD value, obtained during experiments. All experiments: pre-heating zone temperature 100 °C, evaporation zone temperature 200 °C; Experiment 1: total material mass flow rate 287 g/h, L/S ratio 0.62, screw speed 57 rpm; Experiment 2: total material mass flow rate 250 g/h, L/S ratio 0.68, screw speed 60 rpm; Experiment 3: total material mass flow rate 253 g/h, L/S ratio 0.62, screw speed 110 rpm.

For the optimisation DOE, the factor ranges have been adapted according to the learnings from the first screening DOE (Table 8). The range of the evaporation zone temperature was narrowed and shifted to higher values, extending even the previously investigated knowledge space. The factor range of the pre-

Results and Discussion

heating zone temperature was narrowed to the upper edge of the previously investigated factor range. The factor ranges of the L/S ratio and the screw speed were narrowed to the lower edge of their previously investigated ranges. Since thereby less water was processed (lower L/S ratios) at an increasing material residence time (lower screw speed), higher total material mass flow rates could be targeted. By narrowing the factor ranges, the model resolution was increased. One additional experiment was added to the edge of the domain for extreme conditions (lowest total material mass flow rate, L/S ratio and screw speed combined with highest barrel zone temperatures), to further increase the model resolution in the range of interest. The model design was changed to a central composite circumscribed design, including now 5 factor levels.

Results and Discussion

Table 8: Factor settings scaled for the range from -1 to +1 and obtained process responses for the optimisation DOE. TMMF= total material mass flow rate [g/h]; L/S ratio= liquid-to-solid mass flow ratio; ScSp= screw speed [rpm]; Temp. Pre= temperature in the pre-heating zones [°C]; Temp. Eva= temperature in the evaporation zones [°C]; CP= centre point.

Factors						Responses				
Exp.	TMMF [g/h]	L/S ratio	ScSp [rpm]	Temp. Pre [°C]	Temp. Eva [°C]	Product LOD [% w/w]	Evapor. mass H ₂ O [g/h]	x ₅₀ [µm]	Product temp. [°C]	Drying efficiency [%]
Range	360 - 560	0.6 - 0.8	50 - 100	60 - 100	205 - 215	2.1 - 22.9	118 - 201	212 - 538	80 - 117	66 - 100
1	460	0.7	75	80	200	14.0	152	270	82	80
2	360	0.6	100	60	205	8.8	118	397	91	88
3	360	0.8	50	60	205	10.7	141	495	84	88
4	560	0.6	50	60	205	12.4	169	331	85	80
5	560	0.8	100	60	205	22.9	165	538	83	66
6	360	0.6	50	100	205	3.1	133	225	102	98
7	360	0.8	100	100	205	12.4	136	410	85	85
8	560	0.6	100	100	205	12.6	168	344	84	80
9	560	0.8	50	100	205	15.3	201	349	84	81
10	460	0.7	75	50	210	13.9	152	479	83	81
11	310	0.7	75	80	210	6.7	119	341	99	93
12	460	0.5	75	80	210	4.4	146	212	95	95
13	460	0.7	40	80	210	7.6	173	253	82	91
14 _{CP}	460	0.7	75	80	210	12.5	157	496	84	83
15 _{CP}	460	0.7	75	80	210	12.2	158	334	83	84
16 _{CP}	460	0.7	75	80	210	11.0	163	448	85	86
17 _{CP}	460	0.7	75	80	210	11.4	161	347	85	85
18	460	0.7	110	80	210	13.4	154	302	82	81
19	460	0.9	75	80	210	16.1	177	318	80	81
20	610	0.7	75	80	210	14.1	201	255	82	80
21	460	0.7	75	110	210	10.2	165	451	84	87
22	360	0.6	50	60	215	2.7	134	332	108	99
23	360	0.8	100	60	215	11.6	139	430	87	87
24	560	0.6	100	60	215	11.1	175	333	86	83
25	560	0.8	50	60	215	15.1	201	328	81	81
26	360	0.6	50	100	215	2.1	135	314	117	100
27	360	0.6	100	100	215	6.5	125	435	102	92
28	360	0.8	50	100	215	5.6	153	438	89	95
29	560	0.6	50	100	215	5.4	198	260	92	94
30	560	0.8	100	100	215	17.7	190	433	86	76
31	460	0.7	75	80	220	10.3	165	384	87	87

Results and Discussion

After model refinement, models were obtained for the product LOD, the evaporated mass of water, the drying efficiency and the product temperature that were obtained significant with a high R^2 and Q^2 , as well as a high reproducibility (Table 9). In contrast, the model that was obtained for the granule size x_{50} did not fulfil the criteria of a good model due to relatively high variation in the replicates at the centre points. It is assumed, that partial water evaporation in the pre-heating zone and higher values of pre-heating zone temperatures introduced increasing variation in the particle agglomeration (reduced reproducibility of the granule size x_{50}). A comparable observation was made already for the screening DOE. However, potential variation in the water evaporation after the pre-heating zone was diminished after the evaporation zone. Thereby, a good model quality was obtained for the other process responses. Therefore, the focus was put on the drying operation of the in-barrel-drying.

Table 9: Summary of model fit for the optimisation DOE after model refinement.

Process response	Goodness of fit (R^2)	Goodness of prediction (Q^2)	Model validity	Reproducibility
Quality parameter	>0.50	>0.50	>0.25	>0.50
Product LOD	0.96	0.94	0.71	0.98
Evapor. mass H ₂ O	0.99	0.97	0.78	0.99
Drying efficiency	0.98	0.96	0.87	0.97
Granule size x_{50}	0.58	0.40	0.95	0.15
Product temp.	0.96	0.88	0.36	0.99

Again, the process responses product LOD, evaporated mass of water and drying efficiency were analysed all together (Figure 50). For all three responses the same main effects were found significant as in the screening DOE. However, the ranking of the effects was different. The most significant change was observed for the total material mass flow rate and the evaporation zone temperature. For example, the effect weight of the total material mass flow rate on the evaporated mass of water was 0.8 in the screening DOE, whereas in the optimisation DOE it was increased to 1.1 (increase of 38 %). However, the effect weight of the evaporation zone temperature on the evaporated mass of water dropped down by 67 % from 0.6 in the screening DOE to 0.2 in the optimisation DOE. Those changes can be attributed to the factor ranges that were adapted for the optimisation DOE. Whereas the factor range of the evaporation zone temperature was narrowed significantly from 160 - 200 °C for the screening DOE to 205 - 215 °C for the optimisation DOE, the span of the range of the total material mass flow rate was comparable (240 - 500 g/h for the screening DOE and 360 - 560 g/h for the optimisation DOE).

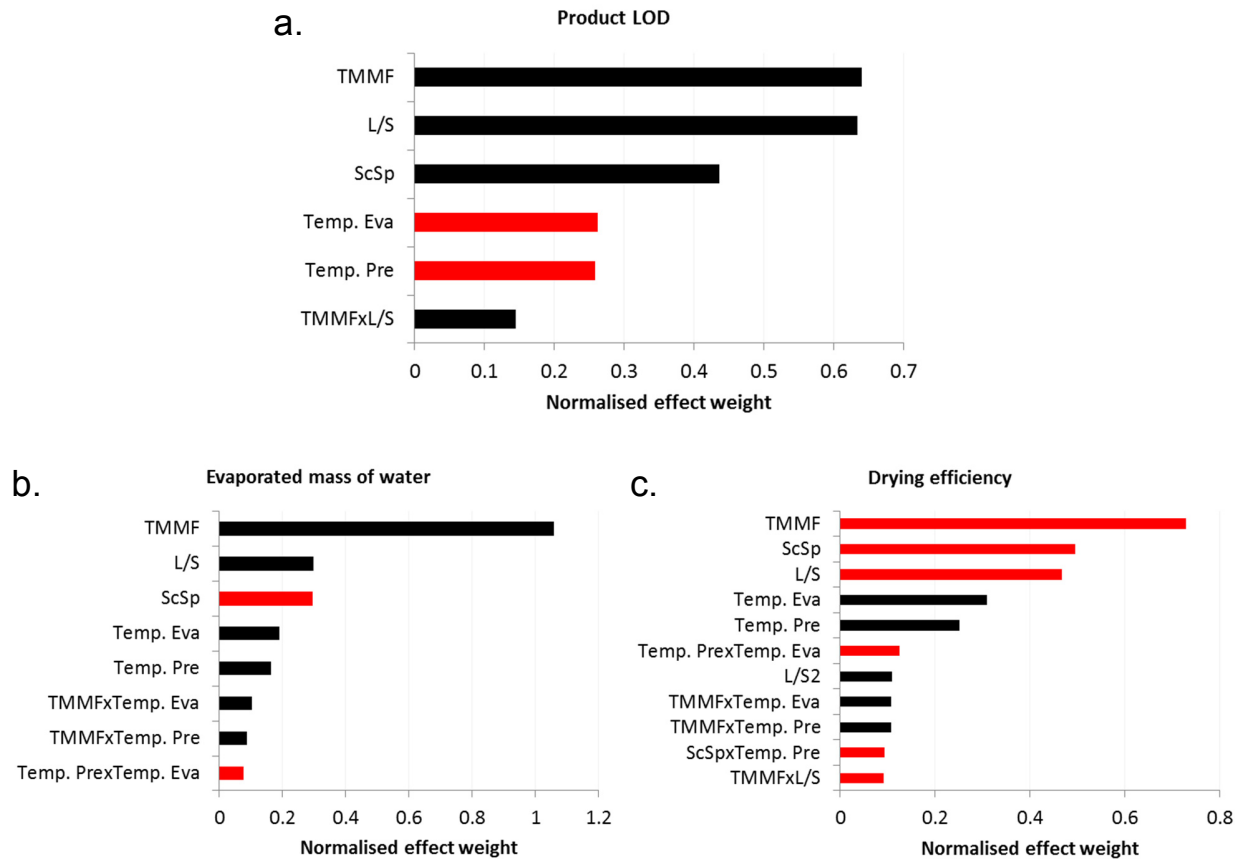


Figure 50: (a) Pareto plot of significant effects on the process response product LOD. A minus (red bar) / plus (black bar) main effect of a factor thereby represents a decrease/increase in the process response, when the factor is increased from its low level to its high level, while the other factors remain constant on their centre level.; a x b= interaction effect between factor a and b.; a²= square effect of factor a.; TMMF= total material mass flow rate; L/S= liquid-to-solid mass flow ratio; ScSp= screw speed; Temp. Pre= temperature in the pre-heating zone; Temp. Eva= temperature in the evaporation zone. (b) Pareto plot of significant effects on the process response evaporated mass of water. (c) Pareto plot of significant effects on the process response drying efficiency.

Alteration was observed in the significance of the interaction effects for the single process responses. In general, comparable interaction effects have been observed as in the screening DOE. It could be, that the interaction effect was now shown significant for another of the three process responses than in the screening DOE. However, two interaction effects were found, which have not been described before. Both were found significant for the drying efficiency. The interaction effects were shown between the pre-heating zone temperature and either the screw speed or the evaporation zone temperature. The effect of increasing pre-heating zone temperature to increase the drying efficiency was emphasised at low screw speed, compared to high screw speed. This effect is similar to the previously described interaction effect between the evaporation zone temperature and the screw speed (for the screening DOE and the process

Results and Discussion

responses product LOD, evaporated mass of water and drying efficiency). The interaction effect is attributed to an additive positive effect on the heat-transfer. At low screw speed, the heat-transfer is emphasised by an increased material residence time and an increased TSG fill-level. Simultaneously, at high pre-heating zone temperature, the heat-transfer is emphasised by an increased temperature difference between material and barrel. All enhanced the water evaporation and increased the drying efficiency. At high screw speed, the increase in heat-transfer was lower due to a shorter material residence time and a lower TSG fill-level (lower increase in drying efficiency). Furthermore, the effect of increasing pre-heating zone temperature to increase the drying efficiency was emphasised at high evaporation zone temperature, compared to low evaporation zone temperature. This effect obviously can be explained by an additive positive effect of high barrel zone temperatures on the heat-transfer (higher temperature difference between material and barrel).

Moreover, the significance of square terms was diminished for all three process responses. Whereas in the screening DOE square effects were found for every single process response, only the drying efficiency showed a significant square effect for the L/S ratio in the optimisation DOE. The alteration in the interaction effects, as well as the diminished significance of square terms is assumed to be caused by the change of factor ranges for the optimisation DOE. However, the results of the screening and the optimisation DOE are comparable overall.

Again, the model that was obtained for the product LOD was verified for its predictive power by using the optimizer function of the DOE software MODDE. Factor settings were predicted at a confidence interval of 95 % for three product LOD values within the design space for dried granules (Figure 51). The predictions were found to match up with the product LOD that was obtained during the experiments. Thereby the predictive power of the product LOD model from the optimisation DOE was confirmed. The model was then used to predict the process settings for the following investigation of in-barrel-drying and twin-screw wet granulation with API suspension feed.

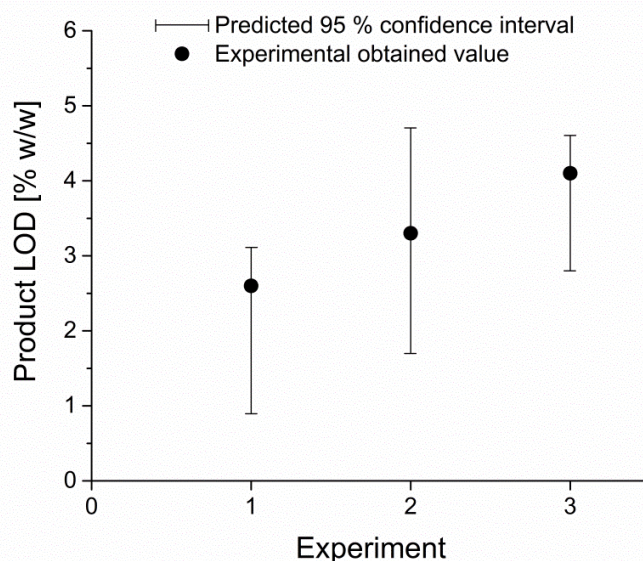


Figure 51: Use of the model of the product LOD that was obtained from the optimisation DOE. Predictions for three targeted LOD values at a confidence level of 95 % are shown together with the product LOD value, obtained during experiments. All experiments: pre-heating zone temperature 100 °C, evaporation zone temperature 215 °C; Experiment 1: total material mass flow rate 381 g/h, L/S ratio 0.62, screw speed 47 rpm; Experiment 2: total material mass flow rate 383 g/h, L/S ratio 0.50, screw speed 97 rpm; Experiment 3: total material mass flow rate 392 g/h, L/S ratio 0.65, screw speed 55 rpm.

3.3.4 Application of in-barrel-drying for API suspension feed

Parts of this section are submitted for publication in the research article “Continuous single-step wet granulation with integrated in-barrel-drying.”.

In the final part of this study, in-barrel-drying was investigated for twin-screw wet granulation with API suspension feed and compared against the traditional API blend feed for a lumefantrine formulation (Table 3). It was evaluated, if the previously characterised in-barrel-drying process could indeed be used for reducing or even eliminating separate drying after twin-screw wet granulation with API suspension feed. Subsequently, in-barrel-drying was compared against traditional fluidised-bed drying to evaluate the impact of the combined wet granulation and drying process on the product quality in more detail. Details on the used methodology are listed in the sections 2.2.1.2 (screening of API suspensions and preparation of the granulation liquid), 2.2.1.3 (twin-screw wet granulation and in investigating in-barrel-drying), 2.2.1.4 (fluidised-bed drying), 2.2.1.5 (compaction), 2.2.2.1 (particle size distribution of powders and granules), 2.2.2.2 (helium density of granules), 2.2.2.3 (bulk and tapped density), 2.2.2.4 (scanning electron

Results and Discussion

microscopy), 2.2.2.5 (compact porosity), 2.2.2.6 (tensile strength), 2.2.2.7 (friability) and 2.2.2.8 (disintegration time). Granule and compact properties were evaluated.

Indeed, it was found that in-barrel-drying can be used for twin-screw wet granulation with API suspension feed in a single-step operation. As expected, granules obtained completely dried for the investigated settings for both processes, API blend and API suspension feed. Traditionally, a drying operation is required (e.g. fluidised-bed drying). For the comparison with fluidised-bed drying, it has to be highlighted that the settings for the screw speed in twin-screw wet granulation were slightly different and that the fluidised-bed drying process was not optimised for this formulation. However, it was found that a drying step could be omitted completely by using in-barrel-drying.

The granule properties were compared for API suspension feed versus blend feed and for in-barrel-drying versus fluidised-bed drying. The descriptors of the granule size distribution of the in-barrel-drying and API blend feed were found at $x_{10}= 83 \pm 5 \mu\text{m}$, $x_{50}= 296 \pm 34 \mu\text{m}$ and $x_{90}= 1143 \pm 31 \mu\text{m}$, whereas for the in-barrel-drying and API suspension feed the descriptors were found at $x_{10}= 98 \pm 8 \mu\text{m}$, $x_{50}= 404 \pm 87 \mu\text{m}$ and $x_{90}= 1211 \pm 23 \mu\text{m}$ ($\bar{x} \pm s$; $n=3$) (Figure 52a). The descriptors of the fluidised-bed drying and API suspension feed were found at $x_{10}= 38 \pm 0 \mu\text{m}$, $x_{50}= 85 \pm 6 \mu\text{m}$ and $x_{90}= 494 \pm 110 \mu\text{m}$ ($\bar{x} \pm s$; $n=3$) (Figure 52a). Thereby, the in-barrel-drying processes of API suspension and API blend feed resulted in a comparable granule size distribution. However, granules from fluidised-bed drying were found with a significant higher fraction of fines, compared to the in-barrel-drying. One explanation could be a higher mechanical stress on the granules during fluidised-bed drying (as it was observed for the investigation on API suspension feed in twin-screw wet granulation for an ibuprofen formulation (section 3.2.2)). Another explanation could be the significant difference in the process temperatures in twin-screw wet granulation. In literature it has been described, that the solubility of solids in the granulation liquid is of significant impact for the particle agglomeration (130-132). The higher the solid solubility, the coarser the granules were observed for a similar amount of granulation liquid. For the setup with fluidised-bed drying, twin-screw wet granulation was run at barrel zone temperatures of 20 °C, whereas for the in-barrel-drying setup the temperature was set to 100 °C in the pre-heating and granulation zone. At this high temperature, the dissolution of solids in the granulation liquid was probably increased. This could have emphasised particle agglomeration in in-barrel-drying, compared to the setup with fluidised-bed drying. For API suspension and API blend feed in in-barrel-drying, the process conditions were similar. Therefore, comparable amounts of solids were dissolved and comparable particle agglomeration behaviour was found.

The bulk and tapped density for granules from the in-barrel-drying and API blend feed was found at $0.37 \pm 0.01 \text{ g/ml}$ and $0.42 \pm 0.01 \text{ g/ml}$, and for granules from the in-barrel-drying and API suspension feed it was found at $0.36 \pm 0.01 \text{ g/ml}$ and $0.42 \pm 0.01 \text{ g/ml}$, respectively ($\bar{x} \pm s$; $n=3$). Furthermore, for granules from fluidised-bed drying and API suspension feed, the bulk density was found at $0.49 \pm 0.01 \text{ g/ml}$ and the tapped density was found at $0.55 \pm 0.01 \text{ g/ml}$ ($\bar{x} \pm s$; $n=3$). Thereby the bulk and tapped density of the

Results and Discussion

API suspension and API blend feed were comparable, whereas for fluidised-bed drying higher densities were found compared to the in-barrel-drying. This can be attributed to the finer particle size of granules from fluidised-bed drying, which allows a denser packing with less air entrapment. For API suspension and API blend feed, the particle size distribution was comparable, which resulted in a comparable packing of particles and hence in comparable bulk and tapped densities. This can also be visualised by SEM images (Figure 52b to d). Whereas granules from fluidised-bed drying were relatively small in size, granules from in-barrel-drying were obtained coarser. However, good flowability has been found for granules from all three processes (Hausner ratio of 1.13 and 1.15 for API blend feed compared to API suspension feed, and 1.14 and 1.15 for fluidised-bed drying compared to in-barrel-drying).

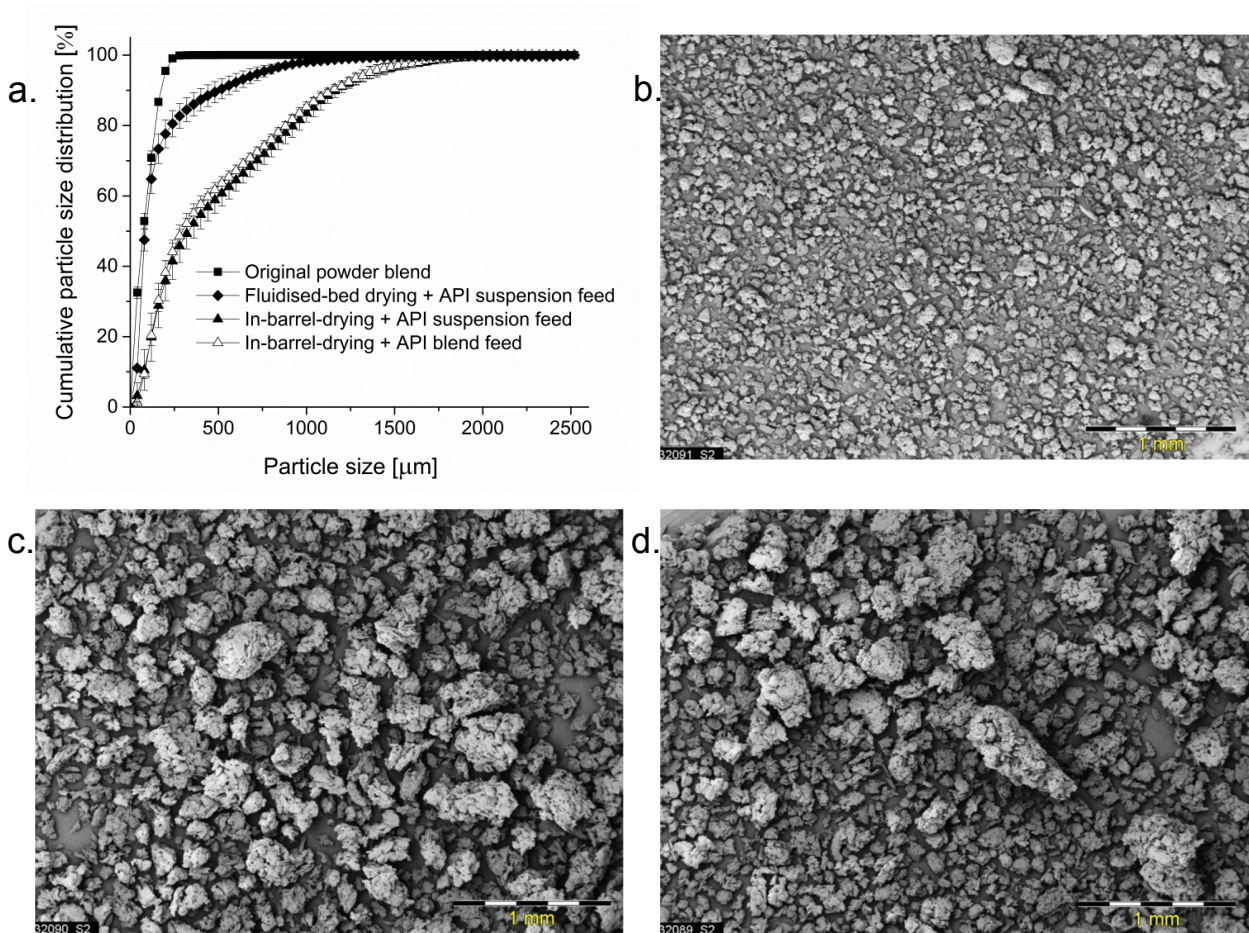


Figure 52: (a) Particle size distributions of the original powder blend, granules from API blend feed compared to API suspension feed in in-barrel-drying and granules from in-barrel-drying compared to fluidised-bed drying for the API suspension feed. ($\bar{x} \pm s$; $n=3$). (b) SEM image of granules from API suspension feed and fluidised-bed drying. (c) SEM image of granules from API suspension feed and in-barrel-drying. (d) SEM image of granules from API blend feed and in-barrel-drying.

Following, the properties of compacts from all three processes were compared. For compacts of granules from the API suspension feed compared to the API blend feed, the tensile strength was comparable at all

Results and Discussion

applied compaction pressures (Figure 53a). For compacts of granules from fluidised-bed drying compared to the in-barrel-drying, the tensile strength was also comparable for compaction pressures above 150 MPa. However, the tensile strength of compacts from fluidised-bed drying was higher than for compacts from the in-barrel-drying for compaction pressures below and equal to 150 MPa. The higher tensile strength of compacts from fluidised-bed drying can be explained by the finer granule size. Thereby, a denser powder packing (higher tapped density) enabled increasing particle-particle bonds, which in turn enhanced the tensile strength of subsequent produced compacts (138). For the API suspension feed and API blend feed, the granule size and the powder packing was comparable (comparable tapped density). Hence, a comparable tensile strength of the compacts was observed. The data from the out-of-die porosity supports this argumentation (Figure 53b). Compacts of granules from fluidised-bed drying were denser with less air entrapment (lower out-of-die porosity), than compacts of granules from in-barrel-drying (for compaction pressures up to 150 MPa). From compaction pressures of 200 MPa or higher, the out-of-die porosity was comparable for compacts of both processes, which indicates that the maximum densification of this formulation was reached. This explains why the tensile strength was comparable for compacts of both processes for compaction pressures of 200 MPa or higher. For compacts of granules from API suspension feed and API blend feed, the out-of-die porosity was comparable at any compaction pressure, which agrees with the data of the comparable tensile strength. The friability of compacts from all processes was found below 0.4 % w/w, indicating good mechanical stability. Another critical compact property is the disintegration time (Figure 53c). The disintegration time of compacts from API blend feed and API suspension feed was comparable, whereas the disintegration time of compacts from fluidised-bed drying was found three times shorter than for compacts from in-barrel-drying (API blend feed with in-barrel-drying: 11:39 ± 2:53 minutes:seconds versus API suspension feed with in-barrel-drying: 8:51 ± 4:18 minutes:seconds versus API suspension feed with fluidised-bed drying: 3:41 ± 0:24 minutes:seconds; $\bar{x} \pm s$; n= 6; compaction pressure 100 MPa). It is assumed, that the high temperatures during in-barrel-drying could have affected the functionality of the disintegrant sodium carboxymethylcellulose negatively. Thereby, the disintegration time, as well as its variability increased for the in-barrel-drying, compared to the fluidised-bed drying. This argumentation is supported by the comparable data of API suspension and API blend feed with in-barrel-drying. However, material from all processes resulted overall in an acceptable product quality.

Results and Discussion

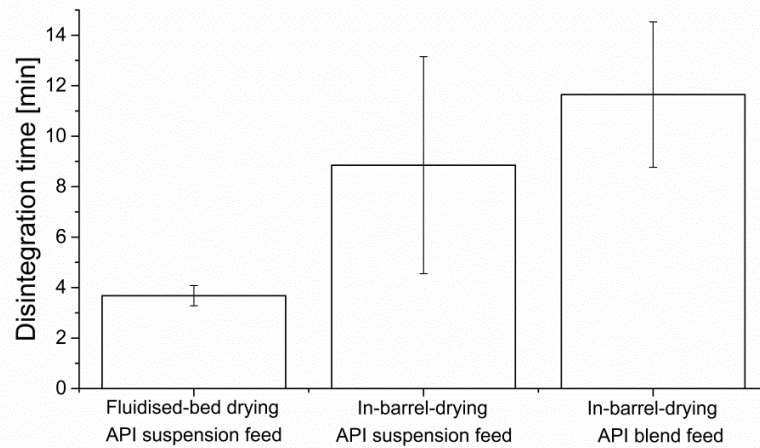
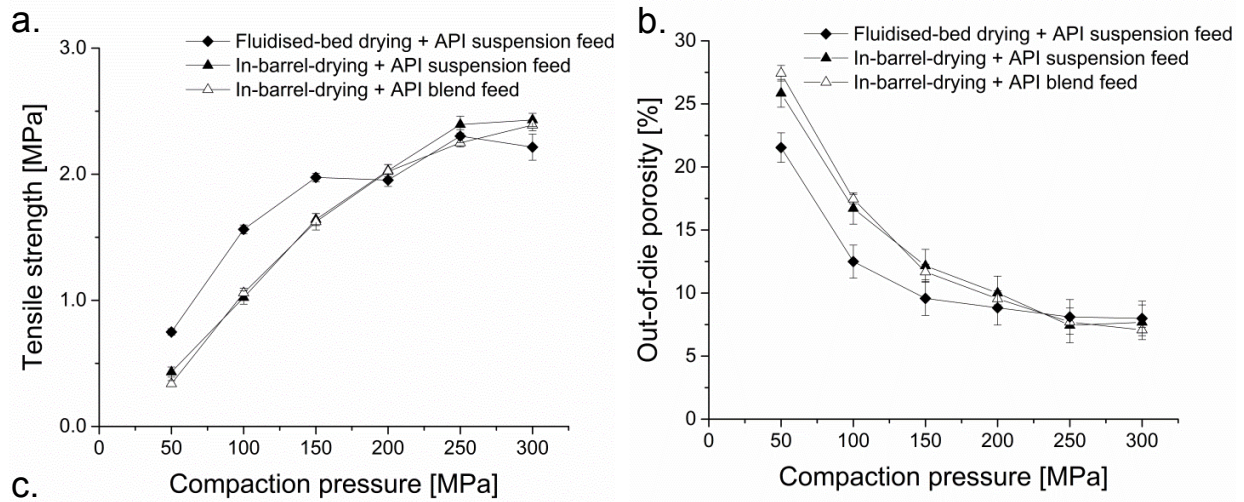


Figure 53: (a) Comparison of the tensile strength for API blend feed versus API suspension feed and in-barrel-drying versus fluidised-bed drying. ($\bar{x} \pm s$; $n=10$); (b) Comparison of the out-of-die porosity for API blend feed versus API suspension feed and in-barrel-drying versus fluidised-bed drying. ($\bar{x} \pm s$; $n=10$); (c) Comparison of the disintegration time for API blend feed versus API suspension feed and in-barrel-drying versus fluidised-bed drying. ($\bar{x} \pm s$; $n=6$; compacts manufactured at a compaction pressure of 100 MPa)

3.3.5 Summary

In this chapter, it was demonstrated that the process operations wet granulation and drying can be combined in a TSG. It was shown, that in a first compartment of the TSG, the material can be granulated and pre-heated. In a following second compartment, the material can then be heated further under drastic conditions such that water is evaporated in a single-step granulation and drying. The water vapour can be discharged via the opening at the TSG exit. Additional degassing vent ports were not required, which avoided the observed challenge of material accumulation and clogging of those ports. In-barrel-drying was demonstrated feasible and yielded in completely dried and granulated material at specific process settings. Thereby, a subsequent drying step after twin-screw wet granulation could be omitted in the manufacturing line. For the in-barrel-drying, the evaporation zone temperature and the liquid mass flow rate were identified as key parameters. The evaporation zone temperature was shown to increase the drying capability without affecting the particle agglomeration. Moreover, it was found that the evaporated mass of water increased with an increasing mass of water in the process. However, if completely dried material is targeted, the processed mass of water has to be well balanced with the drying capability of the equipment at specific process settings. Another critical aspect could be the heat-stability of the processed material. The product temperature was shown to increase rapidly towards higher drying efficiencies. However, it was found that the in-barrel-drying process can be fine-tuned effectively and controlled by using the screw speed. The screw speed can be adapted instantaneously and gives control over the material residence time and the TSG fill-level. Increasing the screw speed decreases the material residence time and the TSG fill-level, which in turn decreases the heat-transfer. The drying efficiency is decreasing (increasing product LOD), as well as the product temperature. Decreasing the screw speed consequently increases the material residence time and the TSG fill-level. The heat-transfer is emphasised, which increases the drying efficiency (decreasing product LOD) and the product temperature.

Furthermore, it was shown that in-barrel-drying can be used together with API suspension feed in twin-screw wet granulation. The product quality of granules and manufactured compacts from in-barrel-drying were comparable for API suspension and API blend feed. However, the in-barrel-drying showed significant differences when compared to traditional fluidised-bed drying. Compared to fluidised-bed drying, the in-barrel-drying resulted for example in coarser granules, lower bulk and tapped density, lower tensile strength at low compaction pressures and in a prolonged disintegration time. However, an acceptable product quality was obtained for all processes. Therefore the in-barrel-drying can be used to overcome extensive drying efforts after twin-screw wet granulation with API suspension feed. Using such process setup, even two drying processes, before and after twin-screw wet granulation, could be omitted in the manufacturing line.

4 Summary and Outlook

This thesis focusses on enabling continuous manufacturing of pharmaceuticals/drug products by investigating twin-screw wet granulation as link between chemical and pharmaceutical manufacturing. It was assumed, that an API suspension that is received from chemical continuous manufacturing could be processed directly in twin-screw wet granulation. The suspending liquid would thereby be used directly as granulation liquid. Hence, the API suspension feed represents the interface between chemical and pharmaceutical manufacturing in a possible configuration of an end-to-end continuous manufacturing process.

In a first chapter of this thesis, process prerequisites were evaluated to enable the API suspension feed in twin-screw wet granulation. Since in such a process setup the dosing of API and granulation liquid are linked, typically high amounts of liquid could end up and challenge the granulation. To ensure appropriate granulation behaviour at the expected (high) L/S ratio, a suitable model formulation had to be selected. Therefore, a quantitative method was developed to assess L/S ratio boundaries in twin-screw wet granulation for a formulation-specific granulation window. It was demonstrated, that the upper L/S ratio boundary of the granulation window was indicated by a change in gradient of the wet granule mass flow variation as a function of the L/S ratio. Furthermore, the lower L/S ratio boundary of the granulation window was indicated by a change in gradient of the dried granule size x_{50} as a function of the L/S ratio. The formulation composition was shown to be essential for the range of applicable L/S ratios in twin-screw wet granulation. Finally, an MCC-Na-CMC based formulation was selected.

In a second chapter of this thesis, the ibuprofen suspension feed in twin-screw wet granulation was studied in detail (proof of concept). Various ibuprofen suspensions were successfully processed. It was shown, that the granulation behaviour of the ibuprofen suspension feed is comparable to the traditional ibuprofen dry blend feed. For comparable granule batches, the compressibility and resulting compact properties were investigated. The compressibility of granules from both processes is comparable. However, minor differences were found in the compact properties. For compacts of granules from the ibuprofen suspension feed, the tensile strength was found to be slightly higher and the out-of-die porosity was shown to be lower than for compacts of granules from ibuprofen blend feed. As a consequence, the disintegration time was slightly prolonged for compacts from the ibuprofen suspension feed, which in turn prolonged the dissolution of ibuprofen. However, these minor differences were considered as not crucial for process and product development. Hence, ibuprofen suspension feed and blend feed were comparable. Therefore, API suspension feed could be used to link chemical and pharmaceutical continuous manufacturing. Moreover, by using the API suspension feed, a typical drying step after API crystallisation and washing may be omitted, since the suspending liquid is used directly as granulation liquid.

Summary and Outlook

In a third and final chapter of this thesis, it was investigated how to eliminate a separate drying step after twin-screw wet granulation with API suspension feed. Therefore, it was investigated if the TSG could be utilised for drying the wet material directly after granulation. A segmented temperature control was used to establish two temperature compartments. One compartment was set at low temperature to granulate and to pre-heat the material. Another compartment was set at high temperature to evaporate the granulation liquid rapidly.

The in-barrel-drying was demonstrated to be feasible and yielded completely dried and granulated material at specific process settings. In these cases, a downstream drying process could be omitted. Degassing of the granulation liquid can be performed via the opening at the TSG exit. Additional degassing vent ports were not required. The evaporation zone temperature was shown to increase the drying capability of the equipment without impacting the particle agglomeration. Furthermore, the evaporated mass of water was increasing by increasing the mass of water in the process. However, if completely dried material is targeted, the processed mass of water has to be well balanced with the drying capability of the equipment at the specific process settings. Hence, the evaporation zone temperature and the liquid mass flow rate were identified as key parameters to balance the evaporation capacity of the process and the material throughput. Another critical aspect could be the heat-stability of the processed materials. Towards high drying efficiencies, the product temperature increased rapidly. There is a risk of material degradation and it needs to be evaluated compound-specific. The application of in-barrel-drying therefore may be restricted to thermostable materials. The screw speed was demonstrated as a valuable process parameter to fine-tune the process. Instantaneously, the screw speed can be increased (or decreased) to control the in-barrel-drying. Thereby the drying time/fill-level in the TSG is decreased (increased). The drying efficiency decreases (increases), as well as the product temperature.

For the API suspension feed, in-barrel-drying also yielded dried and granulated material at specific settings. In the following, the process was compared against API blend feed and against traditional fluidised-bed drying. For the comparison against API blend feed, no significant differences have been observed. However, compared to fluidised-bed drying, the in-barrel-drying resulted in a coarser mean granule size and lower bulk and tapped density. Compacts resulted in a lower tensile strength at low compaction pressures and a significantly prolonged disintegration time, compared to compacts from fluidised-bed drying. However, an acceptable product quality was observed for all process setups. Therefore, in-barrel-drying was demonstrated as a feasible single-step process option in combination with twin-screw wet granulation with API suspension feed. When combining the API suspension feed and in-barrel-drying concepts, both separate drying steps in an end-to-end integrated process chain can be omitted.

The API suspension feed and in-barrel-drying in twin-screw wet granulation provide a valuable toolset to realise end-to-end continuous manufacturing for a wet granulation operation. Moreover, at specific

Summary and Outlook

settings two drying steps could be omitted in the manufacturing line, making the continuous process more efficient and reducing the overall thermal stress of the product in the process chain. Therefore, API suspension feed and in-barrel-drying in twin-screw wet granulation constitute one step forward in making pharmaceutical manufacturing more cost efficient and thereby sustainable for future. However, further work is needed to make the proposed process techniques a reality. For example, for the in-barrel-drying a detailed investigation on the material stability would be of great interest. Moreover, the discharge of moisture for in-barrel-drying in a closed continuous manufacturing line needs to be addressed. After that, it would be of great interest to investigate the process stability of proposed techniques over long manufacturing times in an end-to-end continuous manufacturing setup.

5 Zusammenfassung und Ausblick

Die vorliegende Arbeit beschäftigt sich mit der kontinuierlichen Herstellung von Arzneimitteln. Im Einzelnen fokussiert diese Arbeit den Prozessschritt der kontinuierlichen Nassgranulierung im Doppelschneckengranulator und untersucht wie dieser Prozessschritt dazu genutzt werden kann, um chemische und pharmazeutische kontinuierliche Produktionslinien miteinander zu koppeln. Es wurde näher untersucht, ob dieses ambitionierte Ziel durch eine direkte Dosierung einer Wirkstoffsuspension in den Doppelschneckengranulator erreicht werden kann. Die Wirkstoffsuspension resultiert dabei aus vorhergehenden kontinuierlichen chemischen Prozessschritten. Direkt in der Nassgranulierung verarbeitet, könnte das Suspensionsmedium als Granulierflüssigkeit genutzt werden. Die Dosierung der Wirkstoffsuspension in den Doppelschneckengranulator stellt die Schnittstelle von chemischer und pharmazeutischer Produktion in einem vollständig kontinuierlichen Produktionsprozess für Arzneimittel dar.

In einem ersten Teil dieser Arbeit wurden Prozessvoraussetzungen untersucht, um eine Nassgranulierung mit einer Wirkstoffsuspension im Doppelschneckengranulator zu ermöglichen. Es wurde gezeigt, dass durch die Wirkstoffdosierung als Suspension ungewöhnlich hohe Mengen an Granulierflüssigkeit in der Nassgranulierung verarbeitet werden müssen, da Wirkstoff- und Flüssigkeitsdosierung aneinander gekoppelt sind. Das Verhältnis, in welchem Flüssigkeit und Feststoff (L/S Verhältnis) in der Doppelschneckengranulierung verarbeitet wird, ist für das Granulierverhalten im Doppelschneckengranulator von entscheidender Bedeutung. Um das erwünschte Granulierverhalten bei einem spezifischen L/S Verhältnis zu erzielen, musste eine geeignete Modelformulierung entwickelt werden. Dazu wurde eine quantitative Methode erarbeitet und genutzt, die es erlaubt, formulierungsspezifisch eine untere und eine obere Prozessgrenze für die Granulierung, abhängig vom L/S Verhältnis zu definieren. Die obere Prozessgrenze wurde dabei von einer unmittelbaren Veränderung der Kurvensteigung indiziert, welche sich aus der Auftragung von der Variabilität in dem Massendurchsatz des nassen Granulatmaterials als Funktion des L/S Verhältnisses ergibt. Die untere Prozessgrenze wurde von einer unmittelbaren Veränderung der Kurvensteigung indiziert, welche sich aus der Auftragung von der mittleren Korngröße der getrockneten Granulate als Funktion des L/S Verhältnisses ergibt. Die Zusammensetzung der Formulierung war ausschlaggebend dafür, welche L/S Verhältnisse in der Doppelschneckengranulierung prozessiert werden konnten. Schlussendlich wurde eine Formulierung basierend auf MCC und Na-CMC ausgewählt.

In einem zweiten Teil dieser Arbeit wurde die Doppelschneckengranulierung mit einer Suspensions-Wirkstoffdosierung im Einzelnen erforscht. Dazu wurden zahlreiche Ibuprofen-Wirkstoffsuspensionen erfolgreich verarbeitet. Es konnte gezeigt werden, dass die Dosierung von Ibuprofen als Wirkstoffsuspension mit der üblichen Verarbeitung von Ibuprofen als Pulvermischung vergleichbar ist. Für

Zusammenfassung und Ausblick

vergleichbare Granulatchargen beider Prozesse wurde die Kompressibilität näher untersucht. Weiterhin wurden die resultierenden Tabletteneigenschaften miteinander verglichen. Die Kompressibilität von Granulaten aus beiden Prozessen ist vergleichbar. Geringfügige Unterschiede wurden allerdings bei den Tabletteneigenschaften festgestellt. Tabletten, die aus Granulaten von der Ibuprofen-Wirkstoffdosierung als Suspension hergestellt worden sind, zeigten sowohl eine geringfügig höhere Druckfestigkeit als auch eine leicht niedrigere Tablettenporosität im Vergleich zu Tabletten, die aus Granulaten von der Ibuprofen-Wirkstoffdosierung als Pulvermischung hergestellt worden sind. Folglich wurde eine leicht erhöhte Zerfalls- und Freisetzungszeit für Ibuprofen-Tabletten gefunden, welche aus Granulaten von der Ibuprofen-Wirkstoffdosierung als Suspension hergestellt worden sind. Für Prozess- und Produktentwicklung sind die gefundenen geringfügigen Unterschiede allerdings nicht kritisch. Daher ist die Dosierung von Ibuprofen als Suspension vergleichbar mit der Dosierung von Ibuprofen als Pulvermischung. Folglich kann die Dosierung einer Ibuprofen-Wirkstoffsuspension dazu genutzt werden, chemische und pharmazeutische kontinuierliche Produktionslinien miteinander zu koppeln. Dabei könnte durch die Wirkstoffdosierung als Suspension sogar ein Trocknungsprozess eingespart werden, welcher üblicherweise nach der Kristallisation und Aufarbeitung des Wirkstoffes etabliert ist. Anstatt die Suspensionsflüssigkeit dem Material komplett zu entziehen, wird diese eingeeengt (z.B. bis eine hochkonzentrierte prozessierbare Wirkstoffsuspension von 50 % w/w resultiert) und als Granulierflüssigkeit weiterverarbeitet.

In einem dritten und letzten Teil dieser Arbeit wurde untersucht, wie Trocknungsschritte nach der Doppelschneckengranulierung, welche durch die Wirkstoffdosierung als Suspension signifikant verlängert werden können, verkürzt oder gar eliminiert werden können. Es wurde erforscht, ob ein Trocknungsschritt in den Doppelschneckengranulator integriert werden könnte. Der Doppelschneckengranulator konnte durch seine segmentierte Temperaturregelung in zwei Temperaturzonen eingeteilt werden. Innerhalb einer ersten Temperaturzone wurde das Material bei geringerer Temperatur granuliert und vortemperiert. In einer anschließenden zweiten Temperaturzone wurde das Material dann bei ungewöhnlich hoher Temperatur schlagartig erhitzt, um die Granulierflüssigkeit innerhalb der sehr kurzen Verweilzeit abzutrocknen.

Dieses Funktionsprinzip des sogenannten 'in-barrel-drying' konnte erfolgreich nachgewiesen werden. Mit dem 'in-barrel-drying' konnte vollständig getrocknetes Granulat hergestellt werden. Dadurch wurde gezeigt, dass unter bestimmten Prozessbedingungen ein üblicherweise anschließender Trocknungsprozess eingespart werden kann. Der entstandene Wasserdampf konnte durch die natürlich vorhandene Öffnung am Ende des Doppelschneckengranulators entlüftet werden. Zusätzliche Belüftungsschächte waren nicht erforderlich. Es konnte gezeigt werden, dass durch eine Temperaturerhöhung in der Verdampfungszone die Trocknungskapazität des 'in-barrel-drying'-Prozesses erhöht wurde. Das Granulierverhalten wurde dadurch nicht beeinflusst. Weiterhin konnte gezeigt werden, dass mehr Flüssigkeit abgetrocknet wurde, je mehr Flüssigkeit prozessiert worden ist. Allerdings, sobald

Zusammenfassung und Ausblick

vollständig getrocknetes Granulat mit dem Prozess erzielt werden soll, muss die prozessierte Wassermenge limitiert werden. Die Trocknungskapazität (hauptsächlich gesteuert über die Temperatur in der Verdampfungszone) und die prozessierte Wassermenge (definiert durch Materialdurchsatz und L/S Verhältnis) müssen sehr genau aufeinander abgestimmt sein. Beide Parameter, die Temperatur in der Verdampfungszone und die prozessierte Wassermenge, sind daher Schlüsselparameter für den 'in-barrel-drying'-Prozess. Ein weiterer wichtiger Aspekt ist die Hitzeempfindlichkeit des prozessierten Materials. Sobald ein sehr hoher Trocknungsgrad erreicht wurde, ist die Produkttemperatur zügig angestiegen. Dies kann zu potentiellen Qualitätseinbußen führen. Auch deshalb müssen die Prozessbedingungen sehr genau abgestimmt werden, und das Formulierungs- und Wirkstoff-spezifisch. Weiterhin konnte die Schneckendrehzahl als wichtiger Prozessparameter zur Feinjustierung des 'in-barrel-drying'-Prozesses herausgearbeitet werden. Die Schneckendrehzahl kann in kürzester Zeit angesteuert werden. Dadurch kann bei einer Erhöhung/Senkung der Schneckendrehzahl die Verweilzeit (Trocknungszeit) verkürzt/verlängert werden und der Füllgrad des Doppelschneckengranulators gesenkt/erhöht werden. Folglich sinkt/erhöht sich der Wärmeaustausch und damit der Trocknungsgrad, als auch die Produkttemperatur.

Ausserdem konnte gezeigt werden, dass 'in-barrel-drying' auch bei der Doppelschneckengranulierung mit der Wirkstoffdosierung als Suspension Anwendung finden kann. Unter bestimmten Prozessbedingungen konnten vollständig getrocknete Granulate hergestellt werden. Im Folgenden wurde dieser Prozess mit den üblichen Verfahrenstechniken in der Doppelschneckengranulierung und Trocknung verglichen. Zum einen wurde der Prozess mit der Wirkstoffdosierung als Pulvermischung in 'in-barrel-drying' verglichen. Dabei konnten keine signifikanten Unterschiede bei den hergestellten Granulaten und Tabletten festgestellt werden. Zum anderen wurde der Prozess mit einer konventionellen Doppelschneckengranulierung mit anschliessender Wirbelschichttrocknung verglichen. Es wurde festgestellt, dass Granulate von dem 'in-barrel-drying'-Prozess deutlich gröbere mittlere Korngrößen und niedrigere Schütt- und Stampfdichte aufwiesen als Granulate von der konventionellen Doppelschneckengranulierung mit anschliessender Wirbelschichttrocknung. Nach der Verpressung der Granulate, wurde eine vergleichsweise erhöhte Druckfestigkeit bei niedrigen Pressdrücken für Tabletten vom 'in-barrel-drying' festgestellt. Ausserdem wurde eine signifikant verlängerte Zerfallszeit ermittelt. Trotz dieser Unterschiede, wurde eine akzeptable Produktqualität mit allen Prozessen erreicht. Folglich können durch 'in-barrel-drying' lange Trocknungszeiten nach der Doppelschneckengranulierung mit Wirkstoffdosierung als Suspension verkürzt, oder gar komplett eliminiert werden.

Sowohl die Wirkstoffdosierung als Suspension, als auch das 'in-barrel-drying' stellen innovative Verfahrenstechniken in der Doppelschneckengranulierung dar, und können eine vollständig kontinuierliche Herstellung von Arzneimitteln ermöglichen. Es konnte gezeigt werden, dass unter Anwendung dieser beiden Verfahrenstechniken, für bestimmte Prozessbedingungen zwei Trocknungsprozesse eingespart werden können. Dadurch kann die kontinuierliche Herstellung von

Zusammenfassung und Ausblick

Arzneimitteln noch effizienter konzipiert werden. Infolgedessen können Arzneimittel bei niedrigeren Kosten nachhaltiger produziert werden. Dennoch sind weitere Untersuchungen erforderlich, bevor die erarbeiteten Verfahrenstechniken in einer Produktionslinie realisiert werden können. Zum Beispiel, für das 'in-barrel-drying' sind detaillierte Untersuchungen zur Materialstabilität für eine Vielzahl von Wirkstoffen von grossem Interesse. Weiterhin müssen Lösungsansätze erarbeitet werden, wie die Granulierflüssigkeit in einem kontinuierlichen Produktionsprozess abgedampft werden kann, welcher üblicherweise geschlossen gefahren wird. Nicht zuletzt ist die Prozessstabilität ausschlaggebend. Diese muss für beide Verfahrenstechniken über einen längeren Zeitraum nachgewiesen werden.

6 References

1. Rantanen J, Khinast J. The future of pharmaceutical manufacturing sciences. *Journal of Pharmaceutical Sciences*. 2015;104(11):3612-38.
2. Lee SL, O'Connor TF, Yang X, Cruz CN, Chatterjee S, Madurawe RD, et al.. Modernizing Pharmaceutical Manufacturing: from Batch to Continuous Production. *Journal of Pharmaceutical Innovation*. 2015;10(3):191-9.
3. Yu L. Continuous manufacturing has a strong impact on drug quality. *FDA Voice*. <https://blogs.fda.gov/fdavoices/index.php/2016/04/continuous-manufacturing-has-a-strong-impact-on-drug-quality>. 2016; last accessed: 04.03.2018.
4. Panzitta M, Ponti M, Bruno G, Cois G, D'Arpino A, Minghetti P, et al.. The strategic relevance of manufacturing technology: An overall quality concept to promote innovation preventing drug shortage. *International Journal of Pharmaceutics*. 2017;516(1–2):144-57.
5. Konstantinov KB, Cooney CL. White Paper on continuous bioprocessing. 2014 Continuous Manufacturing Symposium. *Journal of Pharmaceutical Sciences*. 2015;104(3):813-20.
6. O'Connor TF, Lawrence XY, Lee SL. Emerging technology: A key enabler for modernizing pharmaceutical manufacturing and advancing product quality. *International Journal of Pharmaceutics*. 2016;509(1):492-8.
7. Jiménez-González C, Poehlauer P, Broxterman QB, Yang B-S, Am Ende D, Baird J, et al.. Key green engineering research areas for sustainable manufacturing: A perspective from pharmaceutical and fine chemicals manufacturers. *Organic Process Research & Development*. 2011;15(4):900-11.
8. Fonteyne M, Verduyck J, De Leersnyder F, Van Snick B, Vervaet C, Remon JP, et al.. Process Analytical Technology for continuous manufacturing of solid-dosage forms. *Trends in Analytical Chemistry*. 2015;67:159-66.
9. FDA's Woodcock: What to expect in the next 25 years of medicine. http://www.fiercepharma.com/pharma/fda-s-woodcock-what-to-expect-next-25-years-of-medicine?utm_campaign=Emailshareutm_medium%3DEmailandutm_source%3Dforward#ixzz1bz8ToOFb. 2011; last accessed: 04.03.2018.
10. Chatterjee S, FDA perspective on continuous manufacturing. IFPAC Annual Meeting, Baltimore, MD. 2012.
11. Badman C, Trout BL. Achieving Continuous Manufacturing. 2014 Continuous Manufacturing Symposium. *Journal of Pharmaceutical Sciences*. 2015;104(3):779-80.
12. Baxendale IR, Braatz RD, Hodnett BK, Jensen KF, Johnson MD, Sharratt P, et al.. Achieving continuous manufacturing: technologies and approaches for synthesis, workup, and isolation of drug substance. 2014 Continuous Manufacturing Symposium. *Journal of Pharmaceutical Sciences*. 2015;104(3):781-91.

References

13. Byrn S, Futran M, Thomas H, Jayjock E, Maron N, Meyer RF, et al.. Achieving continuous manufacturing for final dosage formation: challenges and how to meet them. 2014 Continuous Manufacturing Symposium. *Journal of Pharmaceutical Sciences*. 2015;104(3):792-802.
14. Allison G, Cain YT, Cooney C, Garcia T, Bizjak TG, Holte O, et al.. Regulatory and quality considerations for continuous manufacturing. 2014 Continuous Manufacturing Symposium. *Journal of Pharmaceutical Sciences*. 2015;104(3):803-12.
15. Page T, Dubina H, Fillipi G, Guidat R, Patnaik S, Poehlauer P, et al.. Equipment and analytical companies meeting continuous challenges. 2014 Continuous Manufacturing Symposium. *Journal of Pharmaceutical Sciences*. 2015;104(3):821-31.
16. Myerson AS, Krumme M, Nasr M, Thomas H, Braatz RD. Control systems engineering in continuous pharmaceutical manufacturing. 2014 Continuous Manufacturing Symposium. *Journal of Pharmaceutical Sciences*. 2015;104(3):832-9.
17. Srai JS, Badman C, Krumme M, Futran M, Johnston C. Future supply chains enabled by continuous processing - opportunities and challenges. 2014 Continuous Manufacturing Symposium. *Journal of Pharmaceutical Sciences*. 2015;104(3):840-9.
18. Nepveux K, Sherlock J-P, Futran M, Thien M, Krumme M. How development and manufacturing will need to be structured - heads of development/manufacturing. 2014 Continuous Manufacturing Symposium. *Journal of Pharmaceutical Sciences*. 2015;104(3):850-64.
19. Nasr M, Krumme M, Matsuda Y, Trout BL, Badman C, Mascia S, et al.. Regulatory perspectives on continuous pharmaceutical manufacturing: moving from theory to practice. 2016 Continuous Manufacturing Symposium. *Journal of Pharmaceutical Sciences*. 2017;106(11), 3199-3206.
20. Vervaet C, Remon JP. Continuous granulation in the pharmaceutical industry. *Chemical Engineering Science*. 2005;60(14):3949-57.
21. Plumb K. Continuous processing in the pharmaceutical industry: changing the mind set. *Chemical Engineering Research and Design*. 2005;83(6):730-8.
22. Pellek A, Van Arnum P. Continuous processing: Moving with or against the manufacturing flow. *Pharmaceutical Technology*. 2008;9(32):52-8.
23. Ierapetritou M, Muzzio F, Reklaitis G. Perspectives on the continuous manufacturing of powder-based pharmaceutical processes. *AIChE Journal*. 2016;62(6):1846-62.
24. Poehlauer P, Manley J, Broxterman R, Gregertsen Br, Ridemark M. Continuous processing in the manufacture of active pharmaceutical ingredients and finished dosage forms: an industry perspective. *Organic Process Research & Development*. 2012;16(10):1586-90.
25. Nepveux K, Pavlou F, Whitfield S, Schoeters K, Weiler A. Continuous processing: is the pharma industry finally coming round to the idea?. *Pharmaceutical Technology Europe*. 2010; 22(9).
26. Singh R, Boukouvala F, Jayjock E, Ramachandran R, Ierapetritou M, Muzzio F. Flexible multipurpose continuous processing of pharmaceutical tablet manufacturing process. *GMP News, European Compliance Academic (ECA)*. 2012.

References

27. Vervaet C, Remon JP. Continuous granulation. Handbook of Pharmaceutical Granulation Technology, 3rd ed.: CRC Press; 2009. p. 308-22.
28. Shah N. Pharmaceutical supply chains: key issues and strategies for optimisation. Computers & Chemical Engineering. 2004;28(6-7):929-41.
29. Kommanaboyina B, Rhodes CT. Trends in stability testing, with emphasis on stability during distribution and storage. Drug Development and Industrial Pharmacy. 1999;25(7):857-68.
30. Mascia S, Heider PL, Zhang H, Lakerveld R, Benyahia B, Barton PI, et al.. End-to-end continuous manufacturing of pharmaceuticals: integrated synthesis, purification, and final dosage formation. Angewandte Chemie (International Edition). 2013;52(47):12359-63.
31. Gutmann B, Cantillo D, Kappe CO. Continuous-flow technology - a tool for the safe manufacturing of active pharmaceutical ingredients. Angewandte Chemie (International Edition). 2015;54(23):6688-728.
32. Hessel V. Novel process windows - gate to maximizing process intensification via flow chemistry. Chemical Engineering & Technology. 2009;32(11):1655-81.
33. Buchholz S. Future manufacturing approaches in the chemical and pharmaceutical industry. Chemical Engineering and Processing: Process Intensification. 2010;49(10):993-5.
34. Poehlauer P, Colberg J, Fisher E, Jansen M, Johnson MD, Koenig SG, et al.. Pharmaceutical roundtable study demonstrates the value of continuous manufacturing in the design of greener processes. Organic Process Research & Development. 2013;17(12):1472-8.
35. Gursch J, Hohl R, Toschkoff G, Dujmovic D, Brozio J, Krumme M, et al.. Continuous processing of active pharmaceutical ingredients suspensions via dynamic cross-flow filtration. Journal of Pharmaceutical Sciences. 2015;104(10):3481-9.
36. Yazdanpanah N, Ferguson ST, Myerson AS, Trout BL. Novel technique for filtration avoidance in continuous crystallization. Crystal Growth & Design. 2015;16(1):285-96.
37. McGlone T, Briggs NEB, Clark CA, Brown CJ, Sefcik J, Florence AJ. Oscillatory Flow Reactors (OFRs) for continuous manufacturing and crystallization. Organic Process Research & Development. 2015;19(9):1186-202.
38. Zhang H, Lakerveld R, Heider PL, Tao M, Su M, Testa CJ, et al.. Application of continuous crystallization in an integrated continuous pharmaceutical pilot plant. Crystal Growth & Design. 2014;14(5):2148-57.
39. Acevedo D, Peña R, Yang Y, Barton A, Firth P, Nagy ZK. Evaluation of mixed suspension mixed product removal crystallization processes coupled with a continuous filtration system. Chemical Engineering and Processing: Process Intensification. 2016;108:212-9.
40. Li J, Lai TC, Trout BL, Myerson AS. Continuous Crystallization of Cyclosporine: Effect of operating conditions on yield and purity. Crystal Growth & Design. 2017;17(3):1000-7.

References

41. U.S. Department of Health and Human Services - Food and Drug Administration. Guidance for industry - PAT - a framework for innovative pharmaceutical development, manufacturing, and quality assurance. <https://www.fda.gov/downloads/drugs/guidances/ucm070305.pdf>. 2004; last accessed: 04.03.2018.
42. International Council for Harmonisation of Technical Requirements for Pharmaceuticals for Human Use (ICH), Pharmaceutical Development Q8. http://www.ich.org/fileadmin/Public_Web_Site/ICH_Products/Guidelines/Quality/Q8_R1/Step4/Q8_R2_Guideline.pdf. 2009; last accessed: 04.03.2018.
43. Malet-Sanz L, Susanne F. Continuous Flow Synthesis. A pharma perspective. *Journal of Medicinal Chemistry*. 2012;55(9):4062-98.
44. Niedergassel B, Leker J. Open innovation: chances and challenges for the pharmaceutical industry. *Future Medicinal Chemistry*. 2009;1(7):1197-200.
45. Engisch W, Muzzio F. Using Residence Time Distributions (RTDs) to address the traceability of raw materials in continuous pharmaceutical manufacturing. *Journal of Pharmaceutical Innovation*. 2016;11(1):64-81.
46. Woodcock J. Modernizing pharmaceutical manufacturing - continuous manufacturing as a key enabler. 2014 Continuous Manufacturing Symposium. 2014.
47. Teżyk M, Milanowski B, Ernst A, Lulek J. Recent progress in continuous and semi-continuous processing of solid oral dosage forms: a review. *Drug Development and Industrial Pharmacy*. 2016;42(8):1195-214.
48. Mortier STFC, Gernaey KV, De Beer T, Nopens I. Analysing drying unit performance in a continuous pharmaceutical manufacturing line by means of mass – Energy balances. *European Journal of Pharmaceutics and Biopharmaceutics*. 2014;86(3):532-43.
49. U.S. Department of Health and Human Services - Food and Drug Administration. Guidance for Industry: SUPAC: Manufacturing Equipment Addendum. <http://academy.gmp-compliance.org/guidemgr/files/UCM346049.pdf>. 2014; last accessed: 04.03.2018.
50. Sacher S, Khinast JG. An overview of pharmaceutical manufacturing for solid dosage forms. process simulation and data modeling in solid oral drug development and manufacture. 2016; Humana Press, New York, pp. 311-383.
51. El-Hagrasy AS, D'Amico F, Drennen JK. A Process Analytical Technology approach to near-infrared process control of pharmaceutical powder blending. Part I: D-optimal design for characterization of powder mixing and preliminary spectral data evaluation. *Journal of Pharmaceutical Sciences*. 2006;95(2):392-406.
52. Deveswaran R, Bharath S, Basavaraj B, Abraham S, Furtado S, Madhavan V. Concepts and techniques of pharmaceutical powder mixing process: a current update. *Research Journal of Pharmacy and Technology*. 2009;2(2):245-9.
53. Pernenkil L, Cooney CL. A review on the continuous blending of powders. *Chemical Engineering Science*. 2006;61(2):720-42.

References

54. Berthiaux H, Marikh K, Gatumel C. Continuous mixing of powder mixtures with pharmaceutical process constraints. *Chemical Engineering and Processing: Process Intensification*. 2008;47(12):2315-22.
55. Iveson SM, Litster JD, Hapgood K, Ennis BJ. Nucleation, growth and breakage phenomena in agitated wet granulation processes: a review. *Powder Technology*. 2001;117(1–2):3-39.
56. Saleh K, Vialatte L, Guigon P. Wet granulation in a batch high shear mixer. *Chemical Engineering Science*. 2005;60(14):3763-75.
57. Agrawal R, Naveen Y. Pharmaceutical processing - a review on wet granulation technology. *International Journal of Pharmaceutical Frontier Research*. 2011;1(1):65-83.
58. Hansuld EM, Briens L. A review of monitoring methods for pharmaceutical wet granulation. *International Journal of Pharmaceutics*. 2014;472(1–2):192-201.
59. Rana AS, Hari Kumar S. Manufacturing defects of tablets - a review. *Journal of Drug Delivery and Therapeutics*. 2013;3(6):200-6.
60. Amidon GE, Houghton ME. The effect of moisture on the mechanical and powder flow properties of microcrystalline cellulose. *Pharmaceutical Research*. 1995;12(6):923-9.
61. Benyahia B, Lakerveld R, Barton PI. A plant-wide dynamic model of a continuous pharmaceutical process. *Industrial & Engineering Chemistry Research*. 2012;51(47):15393-412.
62. Mortier STFC, De Beer T, Gernaey KV, Remon JP, Vervaet C, Nopens I. Mechanistic modelling of fluidized bed drying processes of wet porous granules: a review. *European Journal of Pharmaceutics and Biopharmaceutics*. 2011;79(2):205-25.
63. Wang HG, Dyakowski T, Senior P, Raghavan RS, Yang WQ. Modelling of batch fluidised bed drying of pharmaceutical granules. *Chemical Engineering Science*. 2007;62(5):1524-35.
64. Airaksinen S, Karjalainen M, Räsänen E, Rantanen J, Yliruusi J. Comparison of the effects of two drying methods on polymorphism of theophylline. *International Journal of Pharmaceutics*. 2004;276(1–2):129-41.
65. Aghbashlo M, Sotudeh-Gharebagh R, Zarghami R, Mujumdar AS, Mostoufi N. Measurement techniques to monitor and control fluidization quality in fluidized bed dryers: a Review. *Drying Technology*. 2014;32(9):1005-51.
66. Peinado A, Hammond J, Scott A. Development, validation and transfer of a Near Infrared method to determine in-line the end point of a fluidised drying process for commercial production batches of an approved oral solid dose pharmaceutical product. *Journal of Pharmaceutical and Biomedical Analysis*. 2011;54(1):13-20.
67. Khadka P, Ro J, Kim H, Kim I, Kim JT, Kim H, et al.. Pharmaceutical particle technologies: an approach to improve drug solubility, dissolution and bioavailability. *Asian Journal of Pharmaceutical Sciences*. 2014;9(6):304-16.
68. Loh ZH, Samanta AK, Sia Heng PW. Overview of milling techniques for improving the solubility of poorly water-soluble drugs. *Asian Journal of Pharmaceutical Sciences*. 2015;10(4):255-74.

References

69. Nakach M, Authelin J-R, Chamayou A, Dodds J. Comparison of various milling technologies for grinding pharmaceutical powders. *International Journal of Mineral Processing*. 2004;74:173-81.
70. Silva AFT, Burggraeve A, Denon Q, Van der Meeren P, Sandler N, Van Den Kerkhof T, et al.. Particle sizing measurements in pharmaceutical applications: Comparison of in-process methods versus off-line methods. *European Journal of Pharmaceutics and Biopharmaceutics*. 2013;85(3, Part B):1006-18.
71. Luypaert J, Massart DL, Vander Heyden Y. Near-infrared spectroscopy applications in pharmaceutical analysis. *Talanta*. 2007;72(3):865-83.
72. Sastry SV, Nyshadham JR, Fix JA. Recent technological advances in oral drug delivery – a review. *Pharmaceutical Science & Technology Today*. 2000;3(4):138-45.
73. Wu CY, Hancock BC, Mills A, Bentham AC, Best SM, Elliott JA. Numerical and experimental investigation of capping mechanisms during pharmaceutical tablet compaction. *Powder Technology*. 2008;181(2):121-9.
74. Yu LX. *Pharmaceutical Quality by Design: product and process development, understanding, and control*. *Pharmaceutical Research*. 2008;25(4):781-91.
75. De Beer T, Burggraeve A, Fonteyne M, Saerens L, Remon JP, Vervaet C. Near infrared and Raman spectroscopy for the in-process monitoring of pharmaceutical production processes. *International Journal of Pharmaceutics*. 2011;417(1–2):32-47.
76. Blanco M, Alcalá M. Content uniformity and tablet hardness testing of intact pharmaceutical tablets by near infrared spectroscopy: a contribution to process analytical technologies. *Analytica Chimica Acta*. 2006;557(1–2):353-9.
77. Chao P-C. *EASY FLOW Kontinuierliche Feuchtgranulation am Beispiel von Calciumcarbonat*. Ph.D. Thesis. University of Bonn. 2013.
78. Freeman T, Birkmire A, Armstrong B. A QbD approach to continuous tablet manufacture. *Procedia Engineering*. 2015;102:443-9.
79. Vanhoorne V, Vanbillemont B, Vercruyse J, De Leersnyder F, Gomes P, Beer TD, et al.. Development of a controlled release formulation by continuous twin screw granulation: Influence of process and formulation parameters. *International Journal of Pharmaceutics*. 2016;505(1–2):61-8.
80. GEA. *Successful Tableting Supplement*. https://www.gea.com/en/binaries/Successful%20Tableting%20Supplement_tcm11-31710.pdf. 2016; last accessed: 04.03.2018
81. Sinka I, Motazedian F, Cocks A, Pitt K. The effect of processing parameters on pharmaceutical tablet properties. *Powder Technology*. 2009;189(2):276-84.
82. Mehrotra A, Chaudhuri B, Faqih A, Tomassone MS, Muzzio FJ. A modeling approach for understanding effects of powder flow properties on tablet weight variability. *Powder Technology*. 2009;188(3):295-300.
83. Geipel-Kern A. *Pharmaceutical manufacture gets a makeover*. https://www.glatt.com/fileadmin/user_upload/26_Glatt-Pharma.pdf. 2015; last accessed: 04.03.2018.

References

84. Pharmaceutical Technology Editors. FDA Approves Tablet Production on Janssen Continuous Manufacturing Line. <http://www.pharmtech.com/fda-approves-tablet-production-janssen-continuous-manufacturing-line>. 2016; last accessed: 04.03.2018.
85. Porta R, Benaglia M, Puglisi A. Flow chemistry: recent developments in the synthesis of pharmaceutical products. *Organic Process Research & Development*. 2016;20(1):2-25.
86. Adamo A, Beingsner RL, Behnam M, Chen J, Jamison TF, Jensen KF, et al.. On-demand continuous-flow production of pharmaceuticals in a compact, reconfigurable system. *Science*. 2016;352(6281):61-7.
87. Quon JL, Zhang H, Alvarez A, Evans J, Myerson AS, Trout BL. Continuous crystallization of aliskiren hemifumarate. *Crystal Growth & Design*. 2012;12(6):3036-44.
88. Novartis, MIT. Novartis-MIT Center for continuous manufacturing. <https://novartis-mit.mit.edu/>. 2013; last accessed: 04.03.2018.
89. Meier R, Thommes M, Rasenack N, Moll KP, Krumme M, Kleinebudde P. Granule size distributions after twin-screw granulation – do not forget the feeding systems. *European Journal of Pharmaceutics and Biopharmaceutics*. 2016;106:59-69.
90. El Hagrasy AS, Hennenkamp JR, Burke MD, Cartwright JJ, Litster JD. Twin screw wet granulation: influence of formulation parameters on granule properties and growth behavior. *Powder Technology*. 2013;238:108-15.
91. Seem TC, Rowson NA, Ingram A, Huang Z, Yu S, de Matas M, et al.. Twin screw granulation - a literature review. *Powder Technology*. 2015;276:89-102.
92. Thompson MR. Twin screw granulation - review of current progress. *Drug Development and Industrial Pharmacy*. 2015;41(8):1223-31.
93. Barrasso D, El Hagrasy A, Litster JD, Ramachandran R. Multi-dimensional population balance model development and validation for a twin screw granulation process. *Powder Technology*. 2015;270:612-21.
94. Sayin R, El Hagrasy AS, Litster JD. Distributive mixing elements: towards improved granule attributes from a twin screw granulation process. *Chemical Engineering Science*. 2015;125:165-75.
95. Sayin R, Martinez-Marcos L, Osorio JG, Cruise P, Jones I, Halbert GW, et al.. Investigation of an 11 mm diameter twin screw granulator: screw element performance and in-line monitoring via image analysis. *International Journal of Pharmaceutics*. 2015;496(1):24-32.
96. Meier R, Moll K-P, Krumme M, Kleinebudde P. Impact of fill-level in twin-screw granulation on critical quality attributes of granules and tablets. *European Journal of Pharmaceutics and Biopharmaceutics*. 2017;115:102-12.
97. Vercruyse J, Córdoba Díaz D, Peeters E, Fonteyne M, Delaet U, Van Assche I, et al.. Continuous twin screw granulation: influence of process variables on granule and tablet quality. *European Journal of Pharmaceutics and Biopharmaceutics*. 2012;82(1):205-11.

References

98. Lee KT, Ingram A, Rowson NA. Twin screw wet granulation: the study of a continuous twin screw granulator using Positron Emission Particle Tracking (PEPT) technique. *European Journal of Pharmaceutics and Biopharmaceutics*. 2012;81(3):666-73.
99. Kumar A, Alakarjula M, Vanhoorne V, Toiviainen M, De Leersnyder F, Vercruyssen J, et al.. Linking granulation performance with residence time and granulation liquid distributions in twin-screw granulation: an experimental investigation. *European Journal of Pharmaceutical Sciences*. 2016;90:25-37.
100. Dhenge RM, Fyles RS, Cartwright JJ, Doughty DG, Hounslow MJ, Salman AD. Twin screw wet granulation: granule properties. *Chemical Engineering Journal*. 2010;164(2):322-9.
101. Kumar A, Vercruyssen J, Toiviainen M, Panouillot P-E, Juuti M, Vanhoorne V, et al.. Mixing and transport during pharmaceutical twin-screw wet granulation: experimental analysis via chemical imaging. *European Journal of Pharmaceutics and Biopharmaceutics*. 2014;87(2):279-89.
102. Dhenge RM, Cartwright JJ, Hounslow MJ, Salman AD. Twin screw wet granulation: effects of properties of granulation liquid. *Powder Technology*. 2012;229:126-36.
103. Liu Y, Thompson M, O'Donnell K, Grasman N. Effect of temperature on the wetting behavior of hydroxypropyl methylcellulose in a twin-screw granulator. *Powder Technology*. 2016;302:63-74.
104. Fonteyne M, Vercruyssen J, Diaz DC, Gildemyn D, Vervaet C, Remon JP, et al.. Real-time assessment of critical quality attributes of a continuous granulation process. *Pharmaceutical Development and Technology*. 2013;18(1):85-97.
105. Dhenge RM, Washino K, Cartwright JJ, Hounslow MJ, Salman AD. Twin screw granulation using conveying screws: effects of viscosity of granulation liquids and flow of powders. *Powder Technology*. 2013;238:77-90.
106. Waje SS, Thorat BN, Mujumdar AS. Screw conveyor dryer: process and equipment design. *Drying Technology*. 2007;25(1):241-7.
107. Osman HB. Granular flow and heat transfer in a screw conveyor heater: a discrete element modeling study. Master thesis. University of Singapore. 2012.
108. Waje S, Patel A, Thorat B, Mujumdar A. Study of residence time distribution in a pilot-scale screw conveyor dryer. *Drying Technology*. 2007;25(1):249-59.
109. Meena AK, Desai D, Serajuddin AT. Development and optimization of a wet granulation process at elevated temperature for a poorly compactible drug using twin screw extruder for continuous manufacturing. *Journal of Pharmaceutical Sciences*. 2017;106(2):589-600.
110. Shah AC, Mlodozieniec AR. Mechanism of surface lubrication: influence of duration of lubricant-exipient mixing on processing characteristics of powders and properties of compressed tablets. *Journal of Pharmaceutical Sciences*. 1977;66(10):1377-82.
111. Council of Europe. *European pharmacopoeia*, 9th ed.. Council of Europe. Strasbourg. 2017.
112. Fell JT, Newton JM. Determination of tablet strength by the diametral-compression test. *Journal of Pharmaceutical Sciences*. 1970;59(5):688-91.

References

113. United States Pharmacopeia and National Formulary (USP 39-NF 34 S2). Rockville, MD. United States Pharmacopeial Convention. 2016.
114. Iveson SM, Wauters PAL, Forrest S, Litster JD, Meesters GMH, Scarlett B. Growth regime map for liquid-bound granules: further development and experimental validation. *Powder Technology*. 2001;117(1-2):83-97.
115. Miwa A, Yajima T, Itai S. Prediction of suitable amount of water addition for wet granulation. *International Journal of Pharmaceutics*. 2000;195(1-2):81-92.
116. Chandel S, Singh SN, Seshadri V. Comparative study on the performance characteristics of centrifugal and progressive cavity slurry pumps with high concentration fly ash slurries. *Particulate Science and Technology*. 2011;29(4):378-96.
117. Thin KC, Khaing MM, Aye KM. Design and performance analysis of centrifugal pump. *World Academy of Science, Engineering and Technology*. 2008;46:422-9.
118. Chaurette J. Pump and pump system glossary. http://www.pumpfundamentals.com/pump_glossary.htm. 2010; last accessed: 04.03.2018.
119. Netzsch. NEMO® Progressing Cavity Pump in FSIP® design. <https://pumps.netzsch.com/en/products-accessories/nemo-progressing-cavity-pumps/nemo-progressing-cavity-pump-in-fsip-design/>. 2017; last accessed: 04.03.2018.
120. Walker CI, Goulas A. Performance characteristics of centrifugal pumps when handling non-Newtonian homogeneous slurries. *Proceedings of the Institution of Mechanical Engineers, Part A: Power and Process Engineering*. 1984;198(1):41-9.
121. Kawatra SK, Bakshi AK. On-line viscometry in particulate processing. *Mineral Processing and Extractive Metallurgy Review*. 1995;14(3-4):249-73.
122. Watanabe H, Yao M-L, Osaki K, Shikata T, Niwa H, Morishima Y. Nonlinear rheology of concentrated spherical silica suspensions: 3. Concentration dependence. *Rheologica Acta*. 1999;38(1):2-13.
123. Khodakov G. On suspension rheology. *Theoretical Foundations of Chemical Engineering*. 2004;38(4):430-9.
124. Gandhi BK, Singh SN, Seshadri V. Performance characteristics of centrifugal slurry pumps. *Journal of Fluids Engineering*. 2001;123;2:271-280.
125. Voigt R. *Pharmazeutische Technologie*, 11th ed.. Deutscher Apotheker Verlag Stuttgart. Stuttgart. 2010.
126. Shaw LR, Irwin WJ, Grattan TJ, Conway BR. The effect of selected water-soluble excipients on the dissolution of paracetamol and ibuprofen. *Drug Development and Industrial Pharmacy*. 2005;31(6):515-25.
127. Kalyon DM, Aktaş S. Factors affecting the rheology and processability of highly filled suspensions. *Annual Review of Chemical and Biomolecular Engineering*. 2014;5:229-54.

References

128. Nieuwmeyer FJS, Damen M, Gerich A, Rusmini F, van der Voort Maarschalk K, Vromans H. Granule characterization during fluid bed drying by development of a near infrared method to determine water content and median granule size. *Pharmaceutical Research*. 2007;24(10):1854-61.
129. Goldszal A, Bousquet J. Wet agglomeration of powders: from physics toward process optimization. *Powder Technology*. 2001;117(3):221-31.
130. Faure A, York P, Rowe RC. Process control and scale-up of pharmaceutical wet granulation processes: a review. *European Journal of Pharmaceutics and Biopharmaceutics*. 2001;52(3):269-77.
131. Lustig-Gustafsson C, Johal HK, Podczeck F, Newton J. The influence of water content and drug solubility on the formulation of pellets by extrusion and spheronisation. *European Journal of Pharmaceutical Sciences*. 1999;8(2):147-52.
132. Yu S, Reynolds GK, Huang Z, de Matas M, Salman AD. Granulation of increasingly hydrophobic formulations using a twin screw granulator. *International Journal of Pharmaceutics*. 2014;475(1):82-96.
133. Rashchi F, Finch J. Polyphosphates: a review their chemistry and application with particular reference to mineral processing. *Minerals Engineering*. 2000;13(10-11):1019-35.
134. Seton L, Roberts M, Ur-Rehman F. Compaction of recrystallised ibuprofen. *Chemical Engineering Journal*. 2010;164(2-3):449-52.
135. Alshahrani SM, Morott JT, Alshetaili AS, Tiwari RV, Majumdar S, Repka MA. Influence of degassing on hot-melt extrusion process. *European Journal of Pharmaceutical Sciences*. 2015;80:43-52.
136. Guo Z, Li D, Wang B. A novel concept for convective heat transfer enhancement. *International Journal of Heat and Mass Transfer*. 1998;41(14):2221-5.
137. El Hagrasy A, Hennenkamp J, Burke M, Cartwright J, Litster J. Twin screw wet granulation: influence of formulation parameters on granule properties and growth behavior. *Powder Technology*. 2013;238:108-15.
138. Sun C, Grant DJW. Effects of initial particle size on the tableting properties of l-lysine monohydrochloride dihydrate powder. *International Journal of Pharmaceutics*. 2001;215(1-2):221-8.

7 Danksagung

Ein ganz herzlicher Dank gilt meinem Doktorvater Prof. Dr. Dr. h.c. Peter Kleinebudde. Danke, dass Sie die Betreuung dieses Projektes übernommen und mir damit die Industriepromotion ermöglicht haben. Diese Arbeit hat mich nicht nur wissenschaftlich voran gebracht, sondern vor allem auch persönlich. Danke für die herzliche Aufnahme in Ihren tollen Arbeitskreis. Auch wenn ich als externer Doktorand eher selten vor Ort war, habe ich mich stets involviert und wohlfühlt bei einem erneuten Wiedersehen. Danke auch dafür, dass Sie die Reisestrapazen auf sich genommen haben, um an unseren regelmässigen Projekttreffen in Basel teilzunehmen. Es waren stets interessante Diskussionen, die bei der Präsentation und der kritischen Bewertung der erzielten Ergebnisse entstanden. Dadurch konnten neue Ansätze erarbeitet werden, die schlussendlich zu einem erfolgreichen Abschluss dieser Arbeit beigetragen haben. Auch abseits der Projekttreffen hatten Sie ein offenes Ohr und standen jederzeit bei Fragen zur Verfügung. Nicht zuletzt haben Sie dies beim zügigen und kritischen Korrekturlesen der Manuskripte und der Dissertation unter Beweis gestellt. Kurzum, vielen Dank für Ihre unermüdliche Unterstützung.

Vielen Dank an meinen Mentor Prof. Dr. Jörg Breitzkreutz für die Übernahme des Koreferats und den interessanten Diskussionen beim Doktorandenseminar.

Ein grosser Dank gebührt meinem Mentor bei Novartis, Dr. Hans de Waard. Herzlichsten Dank für deinen beharrlichen Einsatz! Deine Tür stand immer offen für jegliche Art von Fragen. Du hast es jederzeit verstanden mich zu fordern und zu fördern. Auch wenn es einige Höhen und Tiefen gab - im Mittel ging es stetig bergauf! Dabei hast du mir immer Rückhalt gegeben und dafür danke ich dir von Herzen. Danke auch für deine Zeit, die du in das Korrekturlesen von den zahlreichen (internen und externen) Präsentationen, Manuskripten und dieser Arbeit gesteckt hast.

Danke an meine Manager bei Novartis, an Dr. Klaus-Peter Moll und Dr. Markus Krumme. Durch euch konnte dieses interessante und fordernde Projekt überhaupt erst initiiert werden. Bei jeglicher Art von Fragen konnte ich mich immer an euch wenden und erhielt Unterstützung. Danke für euren kritischen und kreativen Beitrag während der Projekttreffen und beim Korrekturlesen der Manuskripte und dieser Arbeit.

In diesem Zuge möchte ich mich bei all meinen Kolleginnen und Kollegen in der Continuous Manufacturing Unit und der Novel Oral Products Unit für die Unterstützung und die Freundschaft bedanken. Insbesondere möchte ich mich bedanken bei

- Julien Taillemite. Danke, dass du mich an deinem grossen Wissens- und Erfahrungsschatz rund um die praktische Arbeit im Labor hast teilhaben lassen. Ich konnte mir so einige Tipps und Tricks bei dir abschauen.

Danksagung

- Frantz Elbaz. Danke, dass du mir bei jeglicher Art von Fragen rund um das Thema design of experiments zur Seite gestanden hast. „Klack, Klack, Klack“.
- Dr. Sarah Gold. Danke für deinen kritischen Input beim Korrekturlesen der Manuskripte.
- Rik Beernink und Joris Reijneker (ehemalige Trainees) für die direkte und indirekte Unterstützung dieser Arbeit und das ein oder andere Bier nach der Arbeit.

Weiterhin möchte ich mich ganz allgemein bei der Novartis AG bedanken für die Finanzierung des Projektes, sowie für die Möglichkeit in einem internationalen und innovativen Umfeld (wie auf dem Campus in Basel) zu arbeiten.

Vielen Dank an meine „Tischnachbarin“ Victoria Pauli für die vielen fachlichen, wie auch privaten Gespräche. Du warst für jeden Spass zu haben und hast diese Zeit soviel angenehmer gemacht. Danke auch für das Anti-Stress-Programm montags beim Badminton.

Im gleichen Zuge vielen Dank auch an Chloe Lang. Danke für die schöne Zeit, im Labor (beim Troubleshooting), als auch abseits der Arbeit.

Vielen Dank an Dr. Robin Meier für die anregenden Diskussionen während der gemeinsamen Projekttreffen, als auch für das lustige Ausklingenlassen dieser Treffen.

Vom ganzen Herzen danke ich meiner Familie: meinen Grosseltern, meinen Eltern und meinem Bruder. Ihr habt mich immer bei all meinen Vorhaben unterstützt und mir immer den Rücken freigehalten. Dadurch habt ihr mir diesen Weg erst ermöglicht. Angefangen hat es bei der Mittagsverpflegung und der kritischen Hausaufgabenkontrolle nach der Schule bei meiner lieben Oma und meinem lieben Opa. Weiter ging es mit der Ermöglichung des Pharmaziestudiums in Kiel durch meine Eltern. Auch wenn ich den Haustürschlüssel hätte abgeben können nach der erfolgreichen Bankausbildung, habt ihr mich weiter unterstützt in meinem Wunsch zu studieren. Das ist nicht selbstverständlich und ich danke euch dafür sehr. Auch wenn der Weg einige Male steinig war oder ich mal nicht weiter wusste, habt ihr mich motiviert weiterzugehen. Bleibt noch mein Bruder. Als kleiner Bruder ist es nicht immer einfach (oder ratsam) nachzueifern, aber es ist Klasse einen solchen grossen Bruder an seiner Seite zu wissen. Ich bin meiner ganzen Familie für die Unterstützung und die gemeinsame Zeit unendlich dankbar. Ich liebe euch!

Bleibt noch meine liebe Frau! Seitdem ich dich während des Studiums eingefangen und nicht mehr losgelassen habe, geniesse ich jeden einzelnen gemeinsamen Tag mit dir. Dabei bist du immer geduldig mit mir, auch wenn ich mal einen nicht so guten Tag erwischte habe. Irgendwie schaffst du es mich zu motivieren, sei es mit ein paar Worten oder mit einem bezaubernden Lächeln. Danke, dass du an meiner Seite bist bei all meinen - unseren Vorhaben. Ich freue mich auf viele spannende und glückliche Ehejahre. Ich liebe dich!

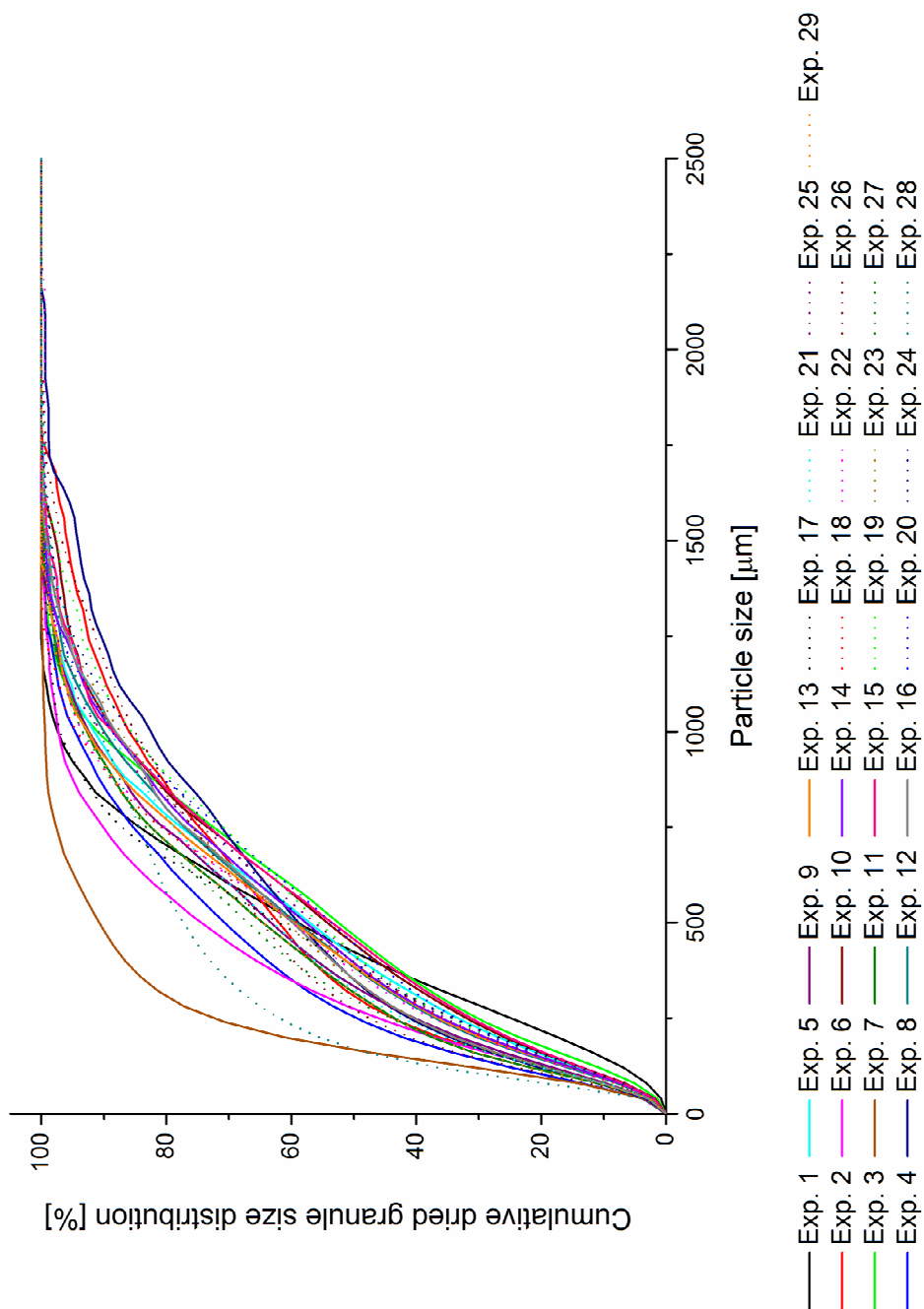


Figure 54: Particle size distribution of experiments from the screening DoE. (individual experiments)

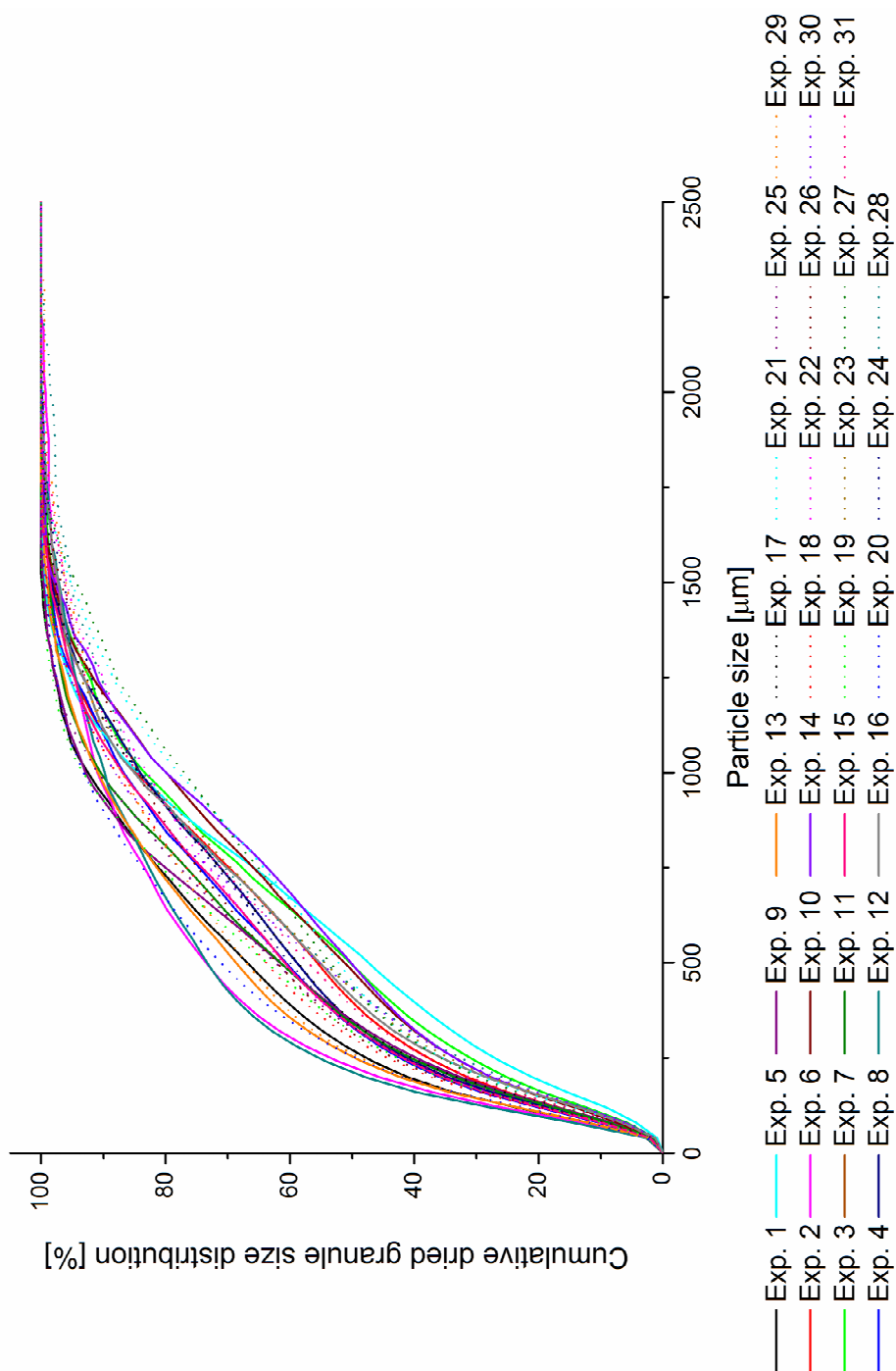


Figure 555: Particle size distribution of experiments from the optimisation DoE. (individual experiments)